UNIFORMED SERVICES UNIVERSITY, SCHOOL OF MEDICINE GRADUATE PROGRAMS
Graduate Education Office (A 1045), 4301 Jones Bridge Road, Bethesda, MD 20814

March 7, 2012

APPROVAL OF THE DOCTORAL DISSERTATION IN THE MOLECULAR AND CELL BIOLOGY GRADUATE PROGRAM

Title of Dissertation: "Regulation of CD4+ T-Cell Function by Membrane Cholesterol"

Name of Candidate: Jacqueline Surls
Doctor of Philosophy Degree
March 13, 2012

DISSERTATION AND ABSTRACT APPROVAL:

DATE

Dr. Charles Via ✓
DEPARTMENT OF PATHOLOGY
Committee Chairperson

Dr. Teodor Brumeanu 3/13/2012
DEPARTMENT OF MEDICINE
Dissertation Advisor

Dr. Sofia Casares 3/13/2012
DEPARTMENT OF MEDICINE /I.D.
Committee Member

Dr. Clifford Snapper 3/13/2012
DEPARTMENT OF PATHOLOGY
Committee Member

Dr. Andre Dubois 3/13/2012
DEPARTMENT OF MEDICINE
Committee Member

Dr. David Scott ✓3/13/2012
DEPARTMENT OF MEDICINE
Committee Member

Eleanor S. Metcalf, Ph.D., Associate Dean || www.usuhs.mil/graded || graduateprogram@usuhs.mil
Toll Free: 800-772-1747 || Commercial: 301-295-3913 / 9474 || DSN: 295-9474 || Fax: 301-295-6772

Copyright Statement

The author hereby certifies that the use of any copyrighted material in the thesis manuscript entitled:

"Regulation of CD4 T-Cell Function by Membrane Cholesterol"

is appropriately acknowledged and, beyond brief excerpts, is with the permission of the copyright owner.

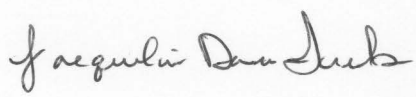

Jacqueline Dara Surls

Molecular and Cell Biology Program

Uniformed Services University

April 3, 2012

Abstract

Title of Dissertation: "**Regulation of CD4 T-Cell Function by Membrane Cholesterol"**

Author: **JACQUELINE DARA SURLS, PhD, 2012**
Uniformed Services University of the Health Sciences

Thesis directed by: **Teodor D. Brumeanu, MD, Professor**
Departments of Medicine and Molecular and Cell Biology
Uniformed Services University of the Health Sciences
4301 Jones Bridge Road, Bethesda, Maryland 20814

The CD4 T helper cells play a central role in initiating immune responses to various types of infections that have breached the immune defense. In the context of vaccination, CD4 T-cells are critical for establishing broad, long-lasting protective immunity. It is known that T-regulatory cells (T-regs) can limit CD4 T-cell responses during influenza viral infection, however less is known about the effect of T-regs in influenza vaccination. In this dissertation, I first present evidence that the size of $CD4^+Foxp3^+$ T-reg pool is an important modulatory component of the primary and memory T-cell responses to influenza vaccination. Herein, I found that immunization of BALB/c mice with a prototype of influenza A/PR/8/34 virus vaccine expanded the $CD4^+Foxp3^+$ T-reg pool and fostered the development of virus-specific $CD4^+Foxp3^+$ T-reg cells. Increasing the size of $Foxp3^+$ T-reg pool did not alter the primary PR8-specific B-cell response, but it did suppress the primary and memory PR8-specific T helper responses induced by vaccination. In contrast, the vaccination-induced T helper cell response was augmented when the pool of $CD4^+Foxp3^+$ T-regs was decreased by 50%. Thus, therapeutic 'quenching' of T-reg function prior to vaccination may enhance vaccine efficacy.

Secondly, I investigated whether enrichment of membrane cholesterol alters the functions of antigen-specific $CD4^+$ T-cells and $CD4^+Foxp3^+$ T-regs, since it is known that cholesterol-rich lipid rafts play a crucial role in T-cell signaling. Administration of squalene, a late cholesterol precursor, enriched membrane cholesterol in murine lymphocytes by 40-50%. This was paralleled by an increased number of resting CD4 T helper cells in the periphery. I also observed sensitization of the Th1 cell differentiation machinery that occurred through the redistribution of IL-2Rα, IL-4Rα, and IL-12Rβ2 subunits to lipid rafts, and increased STAT-4 and STAT-5 phosphorylation following membrane cholesterol enrichment. Antigen stimulation or CD3/CD28 polyclonal stimulation of resting CD4 T-cells enriched in membrane cholesterol followed a predominant path of Th1 differentiation, which was more vigorous in the presence of increased IL-12 secretion by APCs enriched in membrane cholesterol. Furthermore, enrichment of membrane cholesterol in antigen-specific, autoimmune Th1 cells fostered their organ-specific reactivity, as confirmed in an autoimmune diabetes mouse model. However, enrichment of membrane cholesterol in $CD4^+Foxp3^+$ T-reg cells did not alter their suppressogenic function. Together, these findings revealed a differential regulatory effect of membrane cholesterol on the function of CD4 T-cell subsets. The overall implications of this study suggest first that membrane cholesterol could be a new therapeutic target to modulate immune cell functions. Secondly, increased membrane cholesterol in various physiopathological conditions may bias the immune system toward an inflammatory T helper type 1 response. This may potentially be a disadvantage for individuals with autoimmune conditions, but an advantage for those affected by viral infections.

Regulation of CD4 T-Cell Function by Membrane Cholesterol

By

Jacqueline Dara Surls

Dissertation submitted to the Faculty of the Molecular and Cell Biology Program

Uniformed Services University of the Health Sciences in partial fulfillment of the

requirements for the degree of

Doctor of Philosophy 2012

Acknowledgements

I would like to express my gratitude to the following people:

- Dr. Teodor Brumeanu for being a good mentor, for always having time to guide me in my research, and for all our insightful scientific discussions.
- Thesis committee members: Drs. Charles Via, Sofia Casares, Andre Dubois, Clifford Snapper, and David Scott, for their helpful feedback and suggestions.
- Colleagues: Dr. Cristina Stoica-Nazarov, Margaret Kehl, Kateryna Lund, Karen Wolcott, Tom Baginski and Dr. Dennis McDaniel
- My mother and sister for all their support, encouragement, and prayers. They are my inspiration and pillars of strength.
- My husband for his love, patience, kindness, and support.
- And most importantly, my Lord and Savior Jesus Christ, for without Him none of this would have been possible for me.

Table of Contents

List of Abbreviations

Ab(s): antibody or antibodies

Ag: antigen

APC(s): antigen presenting cell(s)

Bcl-6: B cell lymphoma 6 protein, transcriptional repressor of lymphocyte differentiation

CD3: component of the T-cell receptor signaling complex

CD4: co-receptor for the T-cell receptor that recognizes peptide- major histocompatibility class II complexes

CD8: co-receptor for the T-cell receptor that recognizes peptide- major histocompatibility class I complexes

CD11c: adhesion glycoprotein expressed by dendritic cells, monocytes, macrophages, granulocytes, NK cells, and subsets of B and T cells

CD19: type 1 transmembrane glycoprotein expressed by all B cells, except plasma cells

CD22.2: expressed by mature peripheral B cells (follicular and marginal zone), B-1 cells, and plasma cells

CD25: alpha subunit of the interleukin-2 receptor

CD28: T-cell receptor co-stimulatory molecule required for naïve T-cell activation

CD44: memory T-cell surface marker in mice (high expression)

cDNA: complementary DNA, synthesized from RNA template

cMaf: transcription factor associated with T-helper type 2 cells

CTB: Cholera toxin B subunit

CLSM: confocal laser scanning microscopy

Con A: concanavalin A

DAPI: 4,6' diamidino-2-phenylindole, blue fluorescent DNA binding stain that excites at 360 nm and emits at 460 nm

DCs: dendritic cells

dTg: double transgenic

FACS: fluorescence activated cell sorting

FITC: fluorescein isothiocyanate, fluorochrome that is excited at 488 nm and emits at 520 nm

Foxp3: Fork-head box protein 3, intracellular T-regulatory cell marker

GATA3: transcription factor involved in T-cell development and T-helper type 2 cell differentiation

GM1: glycosphingolipid type 1

GFP: green fluorescent protein

HA: hemagglutinin

HAI: hemagglutination inhibition assays

HBCD: hydroxypropyl-β-cyclodextrin

HDL: high density lipids

HE: hematoxylin and eosin

HK: Hong Kong influenza virus strain

HLA: human leukocyte antigen

HMG-CoA reductase: 3-hydroxy-3-methyl-glutaryl-CoA reductase, rate-controlling enzyme of cholesterol biosynthesis

HRP: horseradish peroxidase

Ig: immunoglobulin, antibody

IL-: interleukin

i.p.: intraperitoneal

ITAM: immunoreceptor tyrosine-based activation motifs

JAK: Janus kinase

kDa: kilodalton

KO: knockout

LAT: linker of activation in T-cells

LCK: lymphocyte-specific protein tyrosine kinase

LDL: low density lipids

MBCD: methyl-β-cyclodextrin

MFI: mean fluorescence intensity

MHC: major histocompatibility complex, a set of genes located on human chromosome 6 that encodes proteins responsible for antigen processing

ORO: oil red o

PBS: phosphate buffered saline

PE: phycoerythrin, fluorochrome that is excited at 488 nm and emits at 580 nm

PI3K: phosphoinositide 3-kinase

PR8: A/PR/8/34 influenza virus strain

RAG: recombination-activating protein, required for immunoglobulin and T-cell receptor gene rearrangement

RAG2 KO, RIP-PR8/HA: recombination activating gene 2 knockout mice transgenic for hemagglutinin protein of A/PR/8/34 virus expressed in the pancreatic beta cells under the rat insulin promoter

RNA: ribonucleic acid

RORγt: transcription factor involved in differentiation of T helper 17 cells

RPM: revolutions per minute

RT: room temperature

RT-PCR: reverse transcriptase polymerase chain reaction

SDS-PAGE: sodium dodecyl polyacrylamide gel electrophoresis

Sq: squalene

STAT: signal transducers and activators of transcription

T-bet: transcription factor required for T-helper type 1 cell differentiation

TCR: T-cell receptor

TCR-PR8/HA: T- cell receptor specific for the $HA_{110-120}$ CD4 T-cell immunodominant epitope of hemagglutinin of A/PR/8/34 influenza virus

TFH: T follicular helper cells

Tg: transgenic

Th: T helper

Th1: T-helper type 1 cells

Th2: T-helper type 2 cells

Th17: T-helper 17 cells

T-reg: $CD4^{+}Foxp3^{+}$T regulatory cells

ZAP-70: T-cell receptor ζ chain associated tyrosine kinase 70 kDa

List of Additional Figures

Dissertation Introduction

The CD4 T-cells play a central role in orchestrating immune responses to various types of infections that have breached the immune defense such as influenza infection. The CD4 T helper type 1 and 2 subsets are primarily responsible for controlling and regulating the immune responses through the secretion of cytokines that stimulate, activate, and recruit other immune cells such as B cells and CD8 cytotoxic T lymphocytes to the infection site. In contrast, $CD4^+$ T-regulatory cells have shown mostly a limiting effect on anti-viral immunity and the ability to control immunopathology caused by infection. However in certain viral infections, virus-induced T-regs may promote chronic infection by limiting the efficacy of effector T-cells to clear infection [Rouse and Sehrawat et al 2010]. In mice and humans, there is evidence that the number of influenza-specific T-regulatory cells is increased in the periphery, which is paralleled by a sharp decrease in the number and function of lymphocytes shortly after virus exposure [Giamarellos-Bourboulis et al 2009]. Early reports observed reduced proliferation of virus-specific cellular immune responses following influenza infection and suggested that virus-specific CD8a T-cells contributed to this phenomenon [Hurwitz and Hackett 1985]. Recently, the suppressive mechanism of influenza-specific CD8a T-cells was shown to be associated with IL-10 secretion at the inflammation site [Sun et al 2009]. There is also evidence that $CD4^+$ T-regulatory cells can limit the delay type of hypersensitivity to intradermal influenza virus inoculation [Smith and Ziola 1986]. These studies suggest that indeed, immune suppressive mechanisms are in place during influenza infection that limits anti-viral immunity. In the context of influenza vaccination, CD4 T-cells generate a long lasting, broad memory response and facilitate a

quick recall of these responses [Gordon 1975, McKinstry et al 2011]. However, it is unknown whether the $CD4^+$ $Foxp3^+$ T-regulatory cells significantly effect the anti-viral protective immune responses induced by influenza vaccination. Identifying potential targets for down-regulating or 'quenching' T-reg function may be useful in settings where T-regs are exploited for pathogen immune evasion or possibly when a robust CD4 T-cell response is desired in response to vaccination.

A potential target for regulating T-cell function is lipid rafts membrane cholesterol. It is known that lipid rafts play a crucial role in many T-cell functions. We and others have shown that some therapeutic HMG-CoA reductase inhibitors like Lovastatin, a cholesterol lowering drug, not only reduces the amount of T-cell membrane cholesterol but also down-regulates T-cell function [Goldman et al 1996, Brumeanu et al 2006]. However, little is known about the effect of plasma membrane cholesterol enrichment on CD4 T-cell and $CD4^+$ $Foxp3^+$ T-reg function.

Un-esterified cholesterol is a major component of lipid rafts, and its content is homeostatically regulated through a fine balance between extracellular uptake from the blood circulating LDL [Ho et al 1976, Verhoeye et al 1996] and intracellular synthesis [Lehoux et al 1985]. Early studies using *in vivo* administration of radio-labeled squalene, a late cholesterol precursor, demonstrated its ability to integrate into the cholesterol biosynthetic pathway and readily generate cholesterol [Eidinoff et al 1958, Maxwell 1957]. It is ubiquitously found in the blood at very low concentrations due to its rapid turnover [Loud et al 1958], while at higher concentrations in the skin and adipose tissues [Tilvis et al 1983]. Currently, squalene is being used as an adjuvant to enhance the human immune responses to vaccination [Mbow et al 2010], but its immunomodulatory

mechanism(s) remain largely unknown. Interestingly, a number of studies show that squalene administration can limit the development of preneoplastic lesions involved in colon carcinogenesis [Murakoshi et al 1992, Rao et al 1998, Van Duuren et al 1976]. We have previously shown that exogenous squalene increases the amount of membrane cholesterol in CD4 T-cells [Nazarov- Stoica et al 2009, Brumeanu et al 2007] and may be used as an approach to study the effect of membrane cholesterol enrichment on CD4 T-cell and $CD4^+$ $Foxp3^+$ T-reg function.

Characterization of CD4+ Foxp3 T-regulatory cells

The thymus naturally-derived $CD4^+CD25^{high}Foxp3^+$ T-reg cells are 'guardians' of the immune system. These cells migrate to the periphery where they maintain immune homeostasis and restrict immune responses to both self and foreign antigens [Sakaguchi et al 2005]. Early studies helped identify the significance of 'suppressor' T-cells when normal thymectomized neonatal mice and thymectomized adult rats- (followed by X-irradiation) developed autoimmune like diseases [Nishizuka et al 1969, Kojima et al 1981, Penhale et al 1973, Penhale et al 1990, and Fowell et al 1993]. Further studies showed that adoptive transfer of isolated $CD4^+$ T cells into autoimmune prone mice prevented disease [Sakaguchi et al 1982], whereas transfer of $CD4^+$ T-cells depleted of $CD25^+$ population induced autoimmunity [Sakaguchi et al 1995]. These findings proved that two distinct populations of $CD4^+$ T-cells are capable of either inducing or suppressing autoimmunity. Subsequent attempts to characterize and identify this regulatory subset were based on their expression of specific cell markers. The most widely accepted T-reg cell surface biomarkers in mice include $CD4^+$ $CD25^{high}$ (IL-2Rα).

A variety of other cell surface markers are also expressed by T-regs such as GITR, $CD45RB^{low}$, CD62L, CD103, OX40, TNFR2, PD-1, 4-1BB, TLR-4, $CD127^{low}$ and $CTLA\text{-}4^{high}$, however they can also be expressed by non-T-reg cells [reviewed by Sakaguchi et al 2010]. Emerging biomarkers distinguishing the heterogeneous populations of T-regs include CD45RA [Seddiki et al 2006], HLA-DR [Baecher-Allan et al 2006], galectin-10 [Kubach et al 2007] and CD39 [Borsellino et al 2007]. Within the past decade, Foxp3, a fork head-winged helix transcription factor encoding for Scurfin, was identified as the master regulator for naturally derived $CD4^+$ T-regs [Fontenot et al 2003 and Hori et al 2003]. The significance of this gene was proven when mice carrying a spontaneous loss of function mutation in the Foxp3 gene (Scurfy mice) developed a fatal autoimmune disease similar to immunodysregulation polyendocrinopathy enteropathy X-linked syndrome or IPEX in humans (also known as X-linked autoimmunity-allergic dysregulation syndrome or XLAAD) [Clark et al 1999, Godfrey et al 1994, and Godfrey et al 1991]. IPEX patients develop serious conditions associated with endocrinopathy, enterophathy, and dermatitis due to defective T cell tolerance and $CD4^+$ T cell hyperactivity [Owen et al 2003]. In 2001, Foxp3 mutations were found in IPEX patients as reported by several groups [Wildin et al 2001, Levy-Lahad et al 2001, and Bennett et al 2001]. Recently, it was shown that loss of Foxp3 gene expression in mice using a Cre-lox system induced an autoreactive or "autoaggressive" memory T- cell phenotype [Zhou et al 2009].

Additional regulatory CD4 T-cell subpopulations include TGF-β producing T-helper type 3 (Th3) and IL-10 producing T-regulatory type 1 (TR1) cells which are believed to be induced in the periphery. Th3 cells are involved in mucosal immunity [Chen et al

1994]; whereas TR1 cells play an important role in autoimmune diseases and transplantation [Groux et al 1997]. Recently, it was shown in humans that TR1 cells can develop and function independently of FOXP3 [Passerini et al 2011].

Role of $CD4^+$ $Foxp3^+$ T-regulatory cells in anti-viral immune responses

T-regulatory cells which also express $CD4^+Foxp3^+$ but do not originate in the thymus are called inducible or adaptive T-regs that can be differentiated from naïve $CD4^+$ T-cells in the presence of certain cytokines like TGF-β and antigen stimulation [Chen et al 2003]. T-regs can restrict the immune responses against several viral, bacterial, and parasitic infections [Iwashiro et al 2001, Suvas et al 2004, Vahlenkamp et al 2005, Mills and McGuirk 2004 review]. In chronic HCV infection, the number of $CD4^+25^+$ $Foxp3^+$ T-reg cells is increased and depletion of this T-regulatory subset leads to enhanced HCV-specific CD4 and CD8 T-cell responses [MacDonald et al 2002, Sugimoto et al 2003, Cabrera et al 2004], although they may also have beneficial effects by limiting the migration of inflammatory T-cells from the draining lymphoid nodules to the site of infection, as suggested in the Herpes simplex virus (HSV) infection [Haas et al 2004, Lund et al 2008]. In human immunodeficiency viral infection (HIV), T-regs may induce systemic CD4 T-cell suppression even before the number of CD4 T-cell effectors declines. Data from HIV-infected patients demonstrated that $CD4^+25^+$ T-regs can suppress the virus-specific CD4 and CD8 T-cells [Aandahl et al 2004, Kinter et al 2004, Weiss et al 2004], and T-regs induced by HIV infection can inhibit infection with Cytomegalovirus virus, suggesting a broad range of suppressogenicity among the T-reg compartment [Aandahl et al 2004]. In contrast to other viral infections, the human T-cell lymphotropic virus type-1 (HTLV) preferentially infects $CD4^+Foxp3^+$ T-regs and down-

regulates their Foxp3 expression, thereby contributing to multi-organ lymphocyte infiltration [Karube et al 2004, Yamano et al 2005]. Alternative approaches like T-reg depletion showed better control of HTLV infections in depleted animals [Rouse et al 2006 review]. According to these reports, T-reg cells exhibit mostly a limiting effect on anti-viral immunity.

Mechanisms of Suppression Mediated by T-regulatory Cells

The mechanisms by which $CD4^+$ T-regs suppress immune cell functions are still under investigation. Several groups have reported the following mechanisms: secretion of inhibitory cytokines IL-10, TGF-β, and IL-35 [Kearley et al 2005, Collison et al 2009], cytolytic activity mediated by granzyme A or perforin in humans [Grossman et al 2004, Iikuni et al 2009] and granzyme B in mice [Gondek et al 2005, Thornton et al 2006], metabolic disruption through the release of adenosine nucleosides [Zarek et al 2009, Bopp et al 2007], suppression of DCs through CTLA-4 and B7 interactions [Serra et al 2003, Fallarino et al 2003], and competition of growth factors like IL-2 [Pandiyan et al 2007, Barthlott et al 2005]. Given the debate surrounding how T-regs suppress T effector cells, it is likely that T-regs have multiple redundant mechanisms of suppression and may use different mechanisms depending on their environment and location. Nevertheless, it is well documented that direct cell to cell contact is essential to regulate activation and differentiation of CD4 T-cells.

The role of T-regulatory cells on humoral immunity is less clear. It has been reported that T-regs may indirectly suppress the humoral immune response by inhibiting the secretion of stimulatory cytokines (i.e., IL-4, IL-5, and IL-6) by T helper cells, which are important for proliferation and differentiation [Lim et al 2004]. There is also suggestive

evidence that T-regs can directly suppress B-cells [Iikuni et al 2009, Zhao et al 2006, and Lim et al 2005]. In 2004, it was reported that $CD4^+CD25^+CD69^-$ T-regs are able to suppress germinal center T helper cell-dependent B-cell responses *in vitro* [Lim et al 2004], which was later shown to occur in a contact dependent manner, partially mediated by CTLA-4 and TGF-β [Lim et al 2005]. Shortly thereafter, Zhao and colleagues demonstrated that $CD4^+CD25^+$ T-regs cultured with anti-CD3 and IL-2 express high levels of granzyme B which induced B-cell apoptosis *in vitro* [Zhao et al 2006]. In a lupus mouse model (NZB/W), it was reported that mice depleted of endogenous T-cells and adoptively transferred with syngeneic T-regs ($CD4^+CD25^+$) had significantly reduced autoantibodies, which also occurred to a lesser extent without previous T-cell depletion [Iikuni et al 2009]. Iikuni and colleagues credited the reduction of autoantibodies to direct T-reg suppression of B-cells through secretion of perforin and granzymes, as determined *in vitro*. In an autoantibody dependent arthritis mouse model (K/BxN), Jang and colleagues showed that expression of the scurfy mutation (thus Foxp3 deficient) resulted in abnormal accumulation of long-lived plasma cells (PCs) in the spleen, which was paralleled by a decrease in PCs in the bone marrow [Jang et al 2011]. They attributed this result to the absence of T-regs since they were able to demonstrate *in vitro* the ability of T-regs to suppress the generation of PCs ($B220^{lo}CD138^+$) in a contact-dependent manner. Overall, these findings suggest that T-regs are capable of suppressing B-cells *in vitro* under the appropriate stimulatory conditions, which has thus far been shown to be generally mediated by granzymes and perforin in a contact dependent manner. Although the *in vivo* models discussed above demonstrate that the absence of T-regs interferes with

B-cell antibody production, it is not clear whether similar suppressive mechanisms occur *in vivo*.

Regulation of CD4 T-cell functions

Additional regulatory mechanisms of CD4 T-cell function depend on various cellular intrinsic and extrinsic factors. The differentiation of naïve CD4 T-cells into T-helper subsets is tightly regulated by 3 distinct signals delivered by antigen presenting cells (APCs), particularly dendritic cells. Antigen-presenting cells process antigens and present them as peptide fragments bound to MHC class II molecules. Naïve CD4 T-cells recognize the peptide-MHC class II complex through their T-cell receptor and CD4 co-receptor, thereby initiating the first signal required for naïve T-cell activation. The second signal stimulates survival and proliferation through the ligation of the T-cell co-stimulatory receptor CD28 to B7 molecules (B7.1/B7.2) expressed by APCs. The type of pathogen encountered by APCs determines the type of cytokines they will secrete, thus generating the third signal required to drive CD4 T-cell differentiation (**Figure I**).

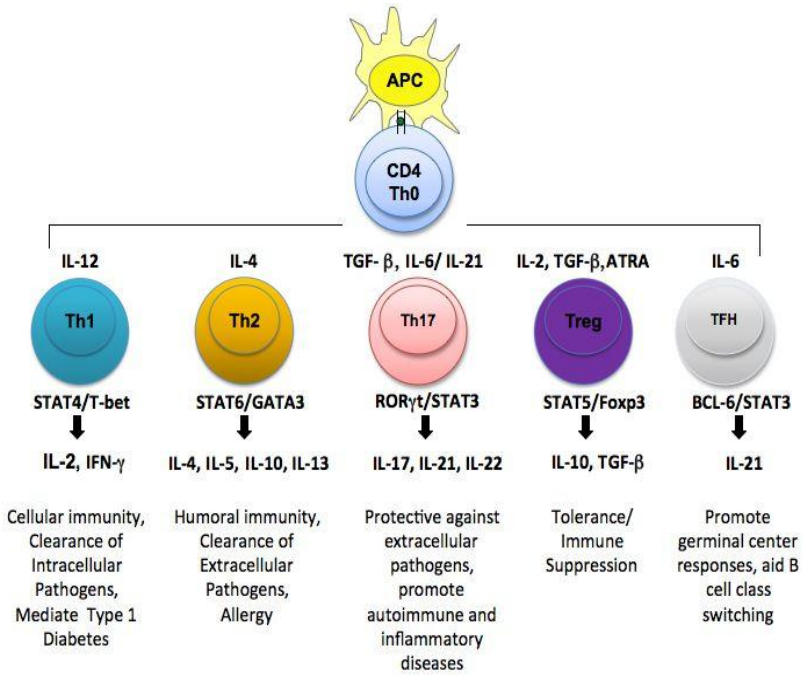

Figure I. Immunological Features and Functions of CD4 T helper subsets. Activation, proliferation, and differentiation of naïve CD4 T-cells rely on their interactions with APCs and their surrounding environment. Generally, APCs deliver signals as cytokines to drive differentiation into distinct T helper subsets that have their own signature transcription factors and cytokine profiles. *Modified and adapted from Zhou et al. Immunity 2009.*

Thus, each specialized subset has distinct immunological features and functions that help provide protective immunity. To date, five well-characterized subsets have been identified: Th1, Th2, Th17, T- follicular helper (TFH), and inducible T-regulatory (T-reg) cells. The Th1, Th2, and Th17 subsets activate their target cells; whereas inducible T-regulatory cells (T-regs) restrict immune activation and differentiation, as previously described.

Naïve CD4 T-cells differentiate into Th1 cells with the help of IL-12 cytokine secretion, primarily by dendritic cells. The IL-12Rβ2 is required for IL-12 signaling via the JAK/STAT pathway [Wu C et al 2000, Szabo et al 1997]. The IL-12Rβ2 subunit joins with the constitutively-expressed IL-12Rβ1 subunit, forming a fully functional IL-12 receptor. Binding of IL-12 to the IL-12 receptor on naïve CD4 T-cells leads to STAT4 phosphorylation and activation of the Th1 master transcription factor T-bet, which up-regulates production of IFN-γ and IL-2 while down-regulating IL-4 and IL-5 production [Sazbo et al 2000, Szabo et al 2002, Afkarian et al 2002] (**Figure II**). Conversely, IL-4 signaling leads to Th2 differentiation where the IL-4Rα subunit and common γ chain play an important role for signaling in T-cells. Binding of IL-4 to the IL-4R leads to STAT6 phosphorylation and activation of the transcription factor GATA3, which up-regulates IL-4, IL-5, IL-10 and IL-13 production [Kaplan et al 2006[a], Kaplan et al 2006[b]]. T-bet and GATA3 are antagonizing transcription factors that skew CD4 T helper differentiation towards type 1 or type 2, respectively. It was shown that GATA3 suppresses Th1

differentiation through down regulation of STAT4 in Th1 cells retrovirally-expressing GATA3 [Hwang et al 2005].

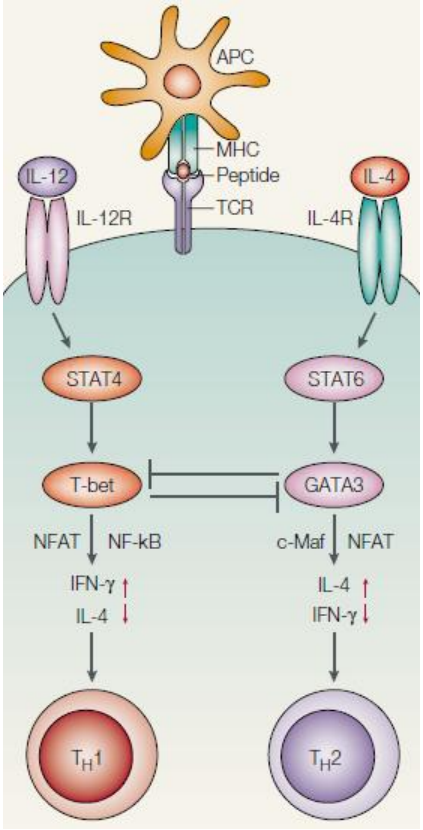

Figure II. Regulation of Th1 and Th2 cells. Th1 differentiation is initiated by IL-12 signaling, whereas Th2 differentiation is initiated by IL-4 signaling. The Th1 and Th2 transcription factors T-bet, and respectively GATA3 directly antagonize each other, skewing differentiation. *Adapted from Liew, Nature Reviews Immunology 2002*.

Alternatively, T-bet was shown to suppress Th2 differentiation by physically interfering with the binding of GATA3 to its target DNA [Usui et al 2006]. Th2 cells mediate humoral immunity, clearance of extracellular pathogens, and allergic immune responses. In contrast, Th1 cells are largely involved in cellular immunity, clearance of intracellular pathogens, and are also known to mediate some autoimmune diseases [Zhou et al 2009].

IL-2 is another important cytokine involved in T-helper cell differentiation, supporting cell growth and survival. Thus, binding of IL-2 to IL-2R promotes recruitment and phosphorylation of JAK kinases on the IL-2Rβ chain, which in turn mediates the assembly of a fully functional IL-2Rαβγ followed by STAT-5 phosphorylation, homodimerization, and translocation to the nucleus where it binds to restriction elements in the gene promoter of several genes [Cantrell and Smith 1984, Cantrell et al 1988]. Additionally, IL-2 signaling plays a major role in T-regulatory cell differentiation along with TGF-β [Sakaguchi et al 1995, Huber et al 2004]. In murine CD4 T-cells, the IL-2Rα

subunit is constitutively expressed by T-regs at a high level, as opposed to transient, low level expression by conventional CD4 T-cells [Sakaguchi et al 1995].

For Th17 cells, IL-23R, IL-1R1, and IL-8α are expressed at high levels [Mangan et al 2006, Wilson et al 2007]. Binding of IL-23 to IL-23R on CD4 T-cells leads to STAT3 phosphorylation and activation of the Th17 master transcription factor RORγt which up regulates IL-17, IL-21, and IL-22 production. Interestingly, the Th1 and Th2 signature cytokines IFN-γ and IL-4, respectively, were shown to suppress Th17 differentiation [Park et al 2005, Harrington et al 2005]. This Th1/Th2 cross-regulation occurs at the transcriptional level, such that overexpression of Th1 or Th2 associated transcription factors, T-bet or respectively c-Maf, in CD4 T-cells under IL-17 polarizing conditions inhibits IL-17 production [Ivanov et al 2005, Park et al 2005]. Suppression of Th17 cell differentiation by Th2 cells has also been demonstrated, in part, by STAT-6 mediated up-regulation of the transcription repressor Gfi-1 [Zhu et al 2009]. Suppression of Th17 differentiation by Th1 cells has been shown to be mediated by blocking of the IL-17 locus (Rorc) by T-bet, thus preventing the binding of target transcription factors [Mukasa et al 2010]. Alternatively, overexpression of RORγt inhibits STAT4 activation and T-bet upregulation in the presence of IL-12 [Mukasa et al 2010]. TGF-β not only promotes T-reg differentiation, but also Th17 cell differentiation, although the latter additionally requires IL-6 or IL-21 combination for its differentiation [Veldhoen et al 2006, Mangan et al 2006]. Th17 cells play a key role in protecting against extracellular pathogens and in promoting inflammatory and autoimmune diseases [Zhou et al 2009]. Suggestive evidence supports the role of IL-17 producing CD4 T-cells in the induction of humoral immunity since it has been shown that a deficiency or blockade in IL-17 leads to

diminished autoantibody responses in experimental autoimmune animal models like multiple sclerosis, collagen-induced arthritis, and autoimmune myocarditis [Komiyaya et al 2006, Sonderegger et al 2006, Nakae et al 2003]. The findings of Hui-Chen and colleagues have provided a clue as to how Th17 cells may promote the development of autoantibodies. In their experimental autoimmune mouse model (BXD2), the number of Th17 cells was shown to be significantly increased, which occurred in parallel with increased expression of IL-17R transcripts in splenic B-cells. It was further demonstrated that Th17 cells induced germinal center formation in vivo by preventing the migration of B-cells through enhanced expression of chemokine receptors (Rgs13 and Rgs16), thereby stabilizing the formation of autoreactive GCs [Hui-Chen et al 2008].

TFH cells have also been shown to promote germinal center responses and support B-cell class switching through multiple mechanisms (i.e., IL-4, PD-1, BAFF, IL-21, and CD40L) [reviewed by Crotty 2010]. Specifically, they induce the differentiation of GCs by promoting the expression of Bcl-6 in activated B-cells and providing cytokines for B-cell survival and differentiation. High affinity antibodies are developed as a result of these GC interactions and dysregulation of TFH function are suggested to promote autoantibody production in several autoimmune models [reviewed by Gomez-Martin et al 2011]. IL-6 and IL-21 signaling promote up regulation of the transcriptional repressor Bcl-6, driving TFH differentiation and suppressing differentiation of Th1, Th2, and Th17 subsets by blocking the binding of their master transcription factors (T-bet, GATA-3, and RORγt) to key cytokine promoters (IFN-γ, IL-4, and IL-17) [Yu et al 2009, Kusam et al 2003]. Although TFH and Th17 cells share the IL-6 and IL-21 cytokines for their differentiation, it has been reported that TGF-β differentiation skews differentiation

toward Th17 since TGF-β inhibits Bcl-6 expression [Nurieva et al 2009]. Alternatively, overexpression of Bcl-6 in Th17 cells prevents binding of RORγt to the IL-17 promoter [Yu et al 2009].

Role of cholesterol-rich lipid rafts in T-cells

The plasma membrane lipid rafts have been shown to play a significant role in regulating T-cell activation, growth, and differentiation [reviewed by Thomas et al 2004]. Lipid rafts are cholesterol- and sphingolipid- rich microdomains in the plasma membrane that constitutively express the ganglioside GM1 (**Figure III**). A unique feature of lipid rafts is that they exist in the liquid-ordered state due to the tight packing and high concentration of cholesterol and sphingolipids, as opposed to the rest of the membrane in the liquid-disordered state.

According to several studies, an estimated 30-40% of many mammalian cell membranes are lipid rafts [Gidwani et al 2001, Prior et al 2003, Simons and Toomre 2000, Stevens et al 2000]. The size of lipid rafts has been reported to range from 10 nm to as much as 300 nm [Pralle et al 2000, Zacharias et al 2002].

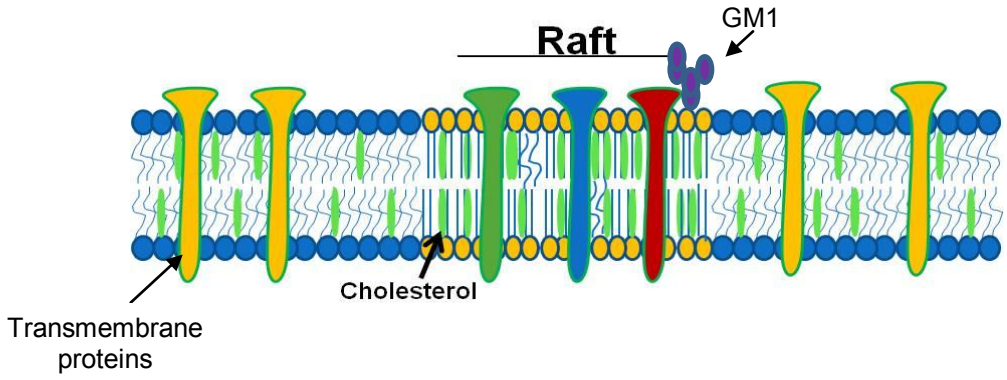

Figure III. Plasma Membrane Lipid Raft Structure. Lipid rafts are cholesterol and sphingolipid–rich microdomains that constitutively express the ganglioside GM1. The tight packing of cholesterol and sphingolipids promotes a liquid-ordered phase in the

membrane, distinguishing rafts from the rest of the membrane. Compartmentalization of receptors and signaling molecules in rafts provides a stable and efficient signaling network.

Much of our understanding regarding the role of lipid rafts in T-cell function has been gained by *in vitro* membrane cholesterol depletion studies using chemical reagents such as methyl-β-cyclodextrin (MBCD), statins, filipin, and to a much lesser extent *in vitro* cholesterol addition using hydroxypropyl-β-cyclodextrin [Nguyen et al 2004, Tani-ichi et al 2005]. According to several reports, depleting lipid rafts cholesterol *in vitro* leads to impaired T- cell function through the disassociation of major T-cell signaling proteins and kinases [Xavier et al 1998, Kabouridis et al 2000, Hillyard et al 2004, and Jury et al 2006]. Our lab and others have identified a high concentration of T-cell signaling machinery such as Src family kinases, T-cell co-receptor molecules CD4 and CD8, and CD3 ζ-chain in lipid rafts [Xavier et al 1998, Montixi et al 1998, Parolini et al 1999, Arcaro et al 2000, Thomas et al 2004].

Lipid rafts may regulate T-cell function through the partitioning of many protein receptors and signaling molecules. Studies have shown localization of individual receptor subunits in and out of lipid rafts. Specifically, the TCR/CD3 ζ-chain, IL-2Rα, and IL-4Rα subunits were found in lipid rafts, where as IL-12Rβ2 was mostly located in non-raft microdomains [Xavier et al 1998, Matko et al 2002[a], Rao et al 2004, Canda-Sanchez et al 2009]. Furthermore, their corresponding subunits for heterodimerization are generally not present in the same membrane phase, i.e., TCRαβ chains and IL-2Rβ were found in non-rafts [Montixi et al 1998, Goebel et al 2002], whereas IL-12Rβ1 was observed in rafts [Canda-Sanchez et al 2009]. Additionally, the CD28 co-stimulatory receptor resides mostly in raft microdomains during T-cell signaling [Viola et al 1999]. We previously

reported the importance of lipid rafts for maintaining CD28 signaling in T-reg precursors, thus stabilizing Foxp3 mRNA transcripts (Nazarov-Stoica et al 2008). However, the role of membrane cholesterol-rich lipid rafts on the clonal expansion and suppressogenic function of $Foxp3^+$ T-reg cells remains unknown.

The studies presented here address first, whether the $CD4^+$ $Foxp3^+$ T-regulatory cells significantly effect the anti-influenza protective immune responses induced by vaccination, and second whether antigen- specific $CD4^+$ T-cells and $Foxp3^+$ T-regulatory cell function can be altered by enriching membrane cholesterol.

Manuscript 1

Differential effect of $CD4^+Foxp3^+$ T regulatory cells on the B and T helper cell responses to influenza virus vaccination

Jacqueline Surls[1], Cristina Nazarov-Stoica[1], Margaret Kehl[1], Sofia Casares[1, 2], and Teodor-D. Brumeanu[1]*

[1]Department of Medicine, Division of Immunology, Uniformed Services University of the Health Sciences, Bethesda, MD 20814, U.S.A.

[2]Naval Medical Research Center, Infectious Diseases Directorate, Silver Spring, MD 20910, U.S.A.

*Address correspondence to T-D. Brumeanu, Uniformed Services University of the Health Sciences, Department of Medicine, Division of Immunology, #A3074, Bethesda, MD 20814. Tel. +1 301 295 3608; FAX: +1 301 295 3557.

Email address: tbrumeanu@usuhs.edu

ABSTRACT

The T-regulatory (T-reg) cells restrict the T-cell functions in various viral infections including influenza infection. However little is known about the effect of T-regs in influenza vaccination. Herein, we found that immunization of BALB/c mice with a prototype of UV-inactivated influenza A/PR/8/34 virus vaccine expanded the $CD4^+Foxp3^+$ T-reg pool and fostered the development of virus-specific $CD4^+Foxp3^+$ T-reg cells. Increasing the size of $Foxp3^+$ T-reg pool did not alter the primary PR8-specific B-cell response, but it did suppress the primary and memory PR8-specific T helper responses induced by vaccination. In contrast, the vaccination-induced T helper cell response was augmented in the absence of $CD4^+Foxp3^+$ T-reg cells. Since CD4 T helper cells contribute to anti-influenza protection, therapeutic "quenching" of T-reg function prior to vaccination may enhance the efficacy of influenza vaccination.

1. Introduction

Pandemic outbreaks of the influenza A viruses may result in numerous fatalities around the globe. Effective vaccines represent the best approach to prevent the pandemic spread, but at present the vaccine preparations using inactivated viruses provide limited protective immunity for the upper respiratory tract where the infectious process is first taking place. Therefore, deciphering the mechanisms that restrict anti-influenza protection by vaccination is a prerequisite to improving the efficacy of vaccination.

Influenza viruses are enveloped orthomyxoviruses with a segmented RNA genome of negative polarity, containing eight segments that encode ten proteins in the case of type A and B viruses, and seven segments encoding nine proteins in the case of type C virus [1]. The influenza viruses are divided into three types based on structural differences among the internal proteins, and in subtypes based on differences in the amino acid sequences and antigenicity of their hemagglutinin and neuraminidase proteins. Regardless the influenza virus strain, the hemagglutinin (HA) envelope protein plays an important role in viral entry in the cells and therefore, is a critical factor of virulence. The anti-influenza viral immunity is a complex process involving both the B and T-cell compartments of the innate and adaptive immunity. Both the CD4 and CD8 mediated anti-influenza viral responses specific for peptides derived from viral proteins are well presented by MHC class II and class I encoded gene products [2, 3] expressed on antigen presenting cells [4].

Mice and individuals infected by influenza virus have a sharp decrease in the number and function of lymphocytes concomitant with an increased number of T-regulatory (T-reg) cells shortly after exposure to the virus [5, 6]. A number of reports argue for a suppressogenic effect of T-regs on the anti-viral immune responses [7-10]. Early studies

on the mechanisms by which A/Puerto Rico/8/34 [H1N1] influenza virus limits the proliferation of virus-specific cellular immune responses suggested a role of virus-specific CD8a T-cells [11]. Recently, the suppressive mechanism of influenza-specific CD8a T-cells was attributed to IL-10 secretion at the site of inflammation [12]. There is also evidence that $CD4^+$ T-regs can limit the delay type of hypersensitivity to intradermal influenza virus inoculation [13]. A significant increase in the number of peripheral $CD4^+$ T-reg pool in individuals infected by influenza A (H1N1) virus, particularly in those with pneumonia complications, was recently reported [6].

Thymus derived $CD4^+(25^{high})$ $Foxp3^+$ T-regs maintain the T- and B-cell homeostasis and can also restrict T-cell responses to *self* and foreign antigens [14]. T-regs are critical not only for protection against autoimmunity [15], but also for protection of fetus against maternal immune responses [16], restriction of host allogeneic T-cell responses against graft transplantation [17], suppression of CTL anti-tumor activity in cancer [18], and modulation of Th2 responses in allergic diseases [19]. Recently, T-regs were shown to restrict immune responses against viral, bacterial, and parasitic infections [20-24]. Thus, in chronic Hepatitis C (HCV) viral infection the number of $CD4^+25^+$ $Foxp3^+$ T-regs is increased, whilst T-reg depletion associates with enhanced HCV-specific CD4 and CD8 T-cell responses [25-27]. In Herpes simplex viral infection, depletion of T-regs was followed by a greater migration of T inflammatory cells from the draining lymphoid nodules to the site of infection [28,29]. Data from HIV-infected patients demonstrated that $CD4^+25^+$ T-regs suppress the virus-specific CD4 and CD8 T-cells [30-32], and that HIV-induced T-regs can restrict the infectivity of Cytomegalovirus virus [30]. In contrast to other viral infections, the human T-cell lymphotropic virus type-1 preferentially infects

the $CD4^+Foxp3^+$ T-regs and down-regulates their Foxp3 expression, thereby contributing to multi-organ lymphocyte infiltration [33, 34]. However, in most cases, T-reg depletion leads to a better control of viral infections in various animal models [reviewed in 35].

Recent data suggested a restrictive effect of T-reg cells on the delay type of hypersensitivity to influenza infection [10, 13], but little is known about their effect on the anti-influenza CD4 T helper cell responses induced by vaccination. Herein, we investigated the effects of $CD4^+Foxp3^+$ T-reg cells on B and T cell responses induced by influenza virus vaccination.

2. Materials and methods

2.1. Animals

Naïve BALB/c and BALB/c, RAG2 KO mice (4-5 week-old) were obtained from Jackson Laboratory (Bar Harbor, Maine). TCR-PR8/HA transgenic (Tg) mice expressing the 14.3d T-cell receptor that recognizes the $HA_{110-120}$-CD4 T-cell immunodominant epitope of hemagglutinin protein (HA) of the A/PR/8/34 influenza virus [36] were used as source of antigen-specific T-regs and conventional HA-specific CD4 T-cells. RAG2 KO, RIP-PR8/HA Tg mice on a BALB/c background expressing the influenza HA viral protein in pancreatic β-cell islets under the rat insulin promoter [36] were used as cell recipients in adoptive transfer experiments. The TCR-PR8/HA Tg and RAG2 KO, RIP-PR8/HA Tg mice were maintained in our pathogen-free facility at USUHS according to federal and local regulations.

2.2. Immunization protocols

Naïve BALB/c mice enriched or not with syngeneic naïve T-reg cells (sorted $CD4^+CD25^+Foxp3^+$ cells from BALB/c mice), and BALB/c, RAG2 KO mice reconstituted with either total spleen cells or T-reg depleted spleen cells from naïve BALB/c mice were immunized intraperitoneally (i.p.) with a single dose of 200 μg of UV-inactivated type A/PR/8/34 (PR8) or type B HK (BHK) influenza viruses with respect to the protein content as measured by Bio-Rad assay (Bio Rad Laboratories, Hercules, CA). Both influenza viral strains were purified by centrifugation on sucrose gradient (Charles River, North Franklin, CT). T-reg enrichment of BALB/c mice was carried out 3 days before vaccination by intraperitoneal (i.p.) infusion of naïve BALB/c T-regs ($6.5x10^6$ $CD4^+CD25^+$ cells) sorted on magnetic immunobeads according to the manufacturer's instructions (Miltenyi Biotech, Auburn, CA and R&D Systems, Minneapolis, MN). Adoptive cell transfers in BALB/c, RAG2 KO mice with $74x10^6$ total spleen cells/mouse or CD25-depleted spleen cells/mouse were carried out 1 day before the i.p. vaccination with 100 μg viral proteins/mouse. On day 8 post-vaccination, spleens were collected and cells were analyzed.

2.3. Cell isolation

Single-cell suspensions of $CD4^+CD25^+$ T-reg cells were negatively-sorted to 90-95% purity from the spleen of naïve BALB/c mice on CD4 columns followed by incubation with CD25 immunobeads and enrichment with PE-labeled anti-CD25 Abs coupled to magnetic beads according to the manufacturer's instructions (Miltenyi Biotech, Auburn, CA and R&D Systems, Minneapolis, MN). Sorted $CD4^+CD25^+$ T-regs showed Foxp3

expression as determined by FACS intra-nuclear staining with anti-Foxp3 Ab (eBioscience, San Diego, CA).

2.4. Cell Proliferation assay

Single-cell suspensions of splenocytes (10^7 cells) from individual mice of each group of mice were incubated with $HA_{110-120}$ synthetic peptide (40 μg/mL) or Con A (2 μg/mL) in flat bottom 12-well plates (Corning, Lowell, MA) for 5 days at 37°C. Aliquot cultures were transferred in flat bottom 96-well plates for testing the proliferative index using Cell Titer 96® Non-Radioactive Cell Proliferation Assay according to the manufacturer's protocol (Promega, Madison, WI). The index of proliferation was determined based on the OD units (λ=490 nm) measured in a 96-well plate reader (Molecular Devices Vmax, Sunnyvale, CA).

2.5. Cytokines assay

Single-cell suspensions of splenocytes from individual mice in each group of mice were incubated at 10^6 cells/well with either $HA_{110-120}$ synthetic peptide (20 μg/10^6 cells), Con A (1 μg/10^6 cells), or UV-inactivated PR8 virus preparation (10 μg protein/10^6 cells). Cells were incubated in round bottom 96-well plates at 5% CO_2 and 37°C for 2 days for IL-2 measurements, and 3 days for IL-4, IL-10, and IFN-γ measurements. Cytokine secretion in cell culture supernatants was assessed by Multiplex mouse cytokines kits using a Luminex instrument according to the manufacturer's instructions (Luminex Corporation, Austin, TX). Cytokine concentrations were calculated based on the acquired

mean fluorescence intensity (MFI) using a 5 parameter logistics model equation (MasterplexQT software, Miraibio, San Francisco, CA).

2.6. Immunohistology of pancreas

Pancreata of mice were fixed overnight in 10% phosphate-buffered formalin and embedded in paraffin. Serial paraffin-embedded sections were stained with hematoxylin-eosin, or immunostained with 1:200 dilution of a rabbit anti-insulin antibody (Santa Cruz Biotech, Santa Cruz, CA) and revealed by a 1:5,000 dilution of goat anti-rabbit IgG-HRP conjugate (Southern Biotechnologies, Birmingham, AL).

2.7. Adoptive cell transfer experiments

Negatively-sorted $CD4^+$ splenic cells from naïve BALB/c mice enriched or not in T-regs and then immunized with PR8 or BHK virus were isolated on CD4 columns (R&D Systems, Minneapolis, MN) 42 days post-immunization, and infused alone, or co-infused i.p. with diabetogenic TCR-PR8/HA splenic cells into RAG2 KO, RIP-PR8/HA Tg mice. The blood glucose level in recipient mice was determined bi-weekly in the blood withdrawn from the tail vein using Accu-Check glucose strips (Roche, Indianapolis, IN). Mice were considered diabetic after two consecutive readings of glycemia higher than 200 mg/dL. In some experiments, BALB/c, RAG2 KO mice were infused i.p. with total spleen cells or T-reg (CD25)-depleted spleen cells from naïve BALB/c mice, and 1 day later were immunized i.p. with 100 μg of UV-inactivated PR8 virus in saline. Eight days post-immunization, the spleen cells were analyzed for cytokine secretion and Foxp3 mRNA expression.

2.8. Antibody assays

Two methods were used to measure the anti-influenza Ab response in immunized mice. First, the ELISA method was carried out on flat bottom 96-well plates coated with PR8 (5 μg/ml) in 0.1 M bicarbonate buffer (pH 9.6) overnight at 4 °C and blocked overnight at 4°C with 5% BSA in PBS. Mice sera (1/100 dilution in 1% BSA/PBS) were added to the plates for 2h at 37°C, washed, and then incubated for 2 h at room temperature either with anti-mouse IgG (H+L) antibody-Biotin conjugate (Abcam, Cambridge, MA), or with anti-mouse IgG1 (Fcγ1) antibody-Biotin conjugate (Jackson ImmunoResearch, West Grove, PA), or with anti-mouse IgG2a (Fcγa) antibody-Biotin conjugate (BD Pharmingen, San Diego, CA). Plates were washed, and bound anti-IgG Ab-Biotin conjugates were revealed by a streptavidin-HRP conjugate (Jackson ImmunoResearch) developed in 3,3′,5,5′-tetramethylbenzidine (TMB) substrate (BD Biosciences, San Jose, CA). The OD units corresponding to the antibody titers were measured at λ=450 nm in flat-bottom 96-well plates in an ELISA reader instrument (Molecular Devices Vmax, Sunnyvale, CA), and then expressed as μg/ml based on a calibration curve built with a PR8-specific IgG1 Ab (#PY102) as we previously described [37]. Secondly, the PR8 and BHK neutralizing Ab titers were measured by Hemagglutination Inhibition Assay (HAI) in 96-well plates as we previously described [37]. Briefly, sera from individual mice of each group of mice (25 μl) were pre-incubated overnight at 37°C in 1 ml of phosphate buffer (pH 7.4) containing 5 mM CaCl2, and neuraminidases from Arthrobacter ureafaciens and Colstridium perfrigens (50 mU each) (Calbiochem, Gibbstown, NJ). Serial serum dilutions were further incubated for 2h at room temperature with 1% sheep red blood cells (50 μl/sample) in saline (Innovative Research, Novi, Michigan) in the

absence of presence of 25 μl of sucrose gradient-purified PR8 or BHK virus (20 μg viral protein/ml). The HAI titers were expressed as the one above the first serum dilution showing inhibition of hemagglutination.

2.9. Flow Cytometry

Single-cell suspensions of splenocytes (10^6 cells) from different groups of mice were stained for 30 min at 4°C using various antibody-dye conjugates and their corresponding isotype controls, according to the manufacturer's instructions (BD Biosciences, San Jose, CA). The mean fluorescence intensity (MFI) was measured by FACS at the single-cell level in 100,000 cell events acquired by a LSR II Becton-Dickinson instrument coupled to the WINLIST software (Verity, Topsham, ME).

2.10. Real-Time RT-PCR

Total RNA and cDNA from $CD4^+$ splenocytes was prepared using NucleoSpin RNA II kit (BD Biosciences Clontech, Palo Alto, CA) and respectively, Qiagen One Step RT-PCR kit (Qiagen Inc., Valencia, CA). Some 500 ng RNA was used to synthesize the first cDNA strand following the manufacturer's protocol. The primers for murine Foxp3 were: (forward) 5'CAGCTGCCTACAGTGCCCCTAG3', and (reverse) 5'CATTTGCCAGCAGTGGGTAG3' [38]. Specific primers for T-bet, STAT4, STAT6, cMAF, and GATA-3 were purchased from Applied Biosystems. Measurements of gene products were carried out as previously described [39]. Quantitative RT-PCR measurements were performed on an ABI Prism 7700 with SDS 1.9.1 software (Applied

Biosystems), and the relative mRNA levels were estimated using 18s rRNA as reference (Applied Biosystems, Foster City, CA).

2.11. Biostatistics

Significance of individual differences in the mean fluorescence intensity (MFI, cell density) of Foxp3 and CD44 protein expression in T-reg and memory $CD4^+$ T-cells from different groups of mice, as well as individual variations in the virus-specific Ab and HAI titers were determined by the nonparametric Student's *t*-test. *P** values lower than 0.05 were considered significant. The intra-assay differences in cytokine secretion and the proliferation index of T-cells in triplicate cultures were expressed as mean ± standard deviation (SD) at 99% interval of confidence. The relevance of differences in survival and diabetes incidence of RAG2 KO, RIP-PR8/HA mice infused with T-cells from virus-immunized BALB/c mice, or co-infused with diabetogenic TCR-PR8/HA Tg T-cells, or infused only with diabetogenic TCR-PR8/HA Tg T-cells alone (diabetes control group) was estimated by Kaplan-Meier test.

3. Results

3.1. $Foxp3^+$ T-reg cells do not alter the B-cell responses to influenza vaccination

Reports indicated that T-reg cells exert inhibitory effects on the anti-viral immune responses. Herein, we investigated whether the size of $CD4^+$Foxp3+ T-reg pool may influence the humoral response to PR8 influenza virus by comparing the anti-PR8 viral antibody titers in naïve *vs*. T-reg-enriched, BALB/c mice immunized with a UV-inactivated A/PR/8/34 vaccine prototype. Although T-reg enrichment in BALB/c mice

($6.5x10^6$ splenic T-reg cells from naïve BALB/c mice) 3 days prior to immunization increased the size of $CD4^+Foxp3^+$ T-reg pool *in vivo* from 2.8% to 4.5%, both groups of mice showed similar kinetics of virus-specific antibody titers 14 and 42 days post-immunization (**Fig. 1**). Thus, the titers of total PR8-specific IgG, IgG1, and IgG2a antibodies were not significantly altered 14 and 42 days post-vaccination in animals supplemented with T-reg cells; p=0.25 for IgG and IgG2a, and p=0.15 for IgG1 Abs between groups of mice enriched or not in T-reg pool prior to PR8 vaccination.

The anti-influenza neutralizing antibodies specific for PR8 hemagglutinin (HA) protein are critical for virus clearance from the lungs. Thus, measuring the hemagglutination inhibition Ab titers (HAI) is a relevant test for measuring protective (neutralizing) antibodies produced during the primary B cell response induced post-vaccination or during influenza viral infection. The HAI Ab titers measured 14 days after PR8 immunization were in a 1/320 to 1/640 range, as compared with mice supplemented with T-regs prior to immunization (1/240-1/160) **(Fig. 1B)**. Forty-two days post-immunization, the HAI Ab titers were comparable, but slowly declined in both groups of mice (1/160-1/320 *vs*. 1/60-1/240). These results indicated that variations in the size of $Foxp3^+$ T-reg pool do not significantly effect the primary PR8-specific B-cell response induced by vaccination.

3.2. $Foxp3^+$ T-reg cells suppress the primary and memory T-helper cell responses to influenza vaccination

Although anti-influenza neutralizing antibodies can protect against influenza infection in the absence of T-cells, the influenza-specific CD4 T-cells were shown to partially clear

the virus from the lungs independently of antibodies. At the same time, influenza-specific CD4 T memory cells play a major role in recalling the adaptive B-cell response, and thereby shortening the time of protection by neutralizing antibodies by 4-5 days [40]. This period of time is critical, if one considers that acute influenza infection can kill mice within a week. Among the effector CD4 T-cells emerging during a primary immune response to influenza infection, a subset of cells (10-20%) survive and differentiate into long-lasting memory T-cells [41-43]. We next investigated the extent to which the size of $CD4^{+}Foxp3^{+}$ T-reg pool affects the primary, memory, and memory-effector T helper cell responses to PR8 virus. Splenocytes from individual mice enriched or not with T-regs 3 days prior to immunization were harvested 14 and 42 days post-immunization and tested for the proliferative capacity and cytokine production upon *in vitro* re-stimulation with $HA_{110\text{-}120}$ synthetic peptide (the immunodominant CD4 T-cell epitope of HA of A/PR/8/34 virus) or polyclonal stimulation with concanavalin A (Con A). To reveal significant changes in the adaptive T-cell response to vaccination in relation to small variations in the size of T-reg pool, we chose a higher dose of immunization (200 μg virus protein/mouse) than conventional doses used in BALB/c mice (50-100 μg viral protein/mouse).

Fourteen days post-immunization, the splenocytes from mice immunized with PR8 virus and stimulated *in vitro* with Con A showed a robust proliferative response, whereas those from mice supplemented with T-reg cells prior to immunization showed a reduction in proliferation by 48 to 58% (**Fig. 2A**). The residual proliferative response of spleen cells detected in the absence of stimulation was most likely due to their *in vivo* activation upon PR8 immunization, since spleen cells from naïve, non immunized BALB/c mice did

not show any residual proliferation in the absence of *in vitro* stimulation (data not shown). The secretion of Th1 and Th2 cytokines was lower in mice enriched for T-regs prior to immunization, although the IL-2 and IL-4 secretion was less affected in the HA-stimulated cells than in cells stimulated with Con A (**Fig. 2B**). The Th1 suppression was detected as a reduction in IFN-γ secretion upon *in vitro* stimulation. Consistent with the cytokine results, the expression levels of Th1 transcription factors (STAT4 and T-bet) and Th2 transcription factors (STAT6, GATA3, cMAF) in the $CD4^+$ T-cells from T-reg enriched/PR8-immunized mice were lower than in those only immunized with PR8 virus, as determined 14 days post-immunization (**Fig. 2C**). The primary Th response to PR8 vaccination was also tested in the absence of a pre-existent pool of T-reg cells using BALB/c, RAG2 KO mice reconstituted i.p. with T-reg ($CD25^+$)-depleted splenocytes ($74x10^6$ cells/mouse) isolated from naïve BALB/c mice, and then immunized 1 day later i.p. with PR8 virus in saline (100 μg viral protein/mouse). The yield of spleen cell reconstitution in RAG mice 9 days after cell infusion was 33-35% ($20\text{-}25x10^6$ cells/mouse). Eight days post-immunization, RAG mice reconstituted with T-reg-depleted splenocytes showed a significantly stronger IL-2 and IFN-γ secretion (≈17-times higher) than those reconstituted with whole spleen cells when stimulated *in vitro* for 2 days with PR8 viral proteins (**Fig. 2D**).

Forty-two days after immunization of naïve BALB/c mice with PR8 virus alone, the splenic CD4 T-cells showed a strong memory-effector Th1 and Th2 cytokine response upon *in vitro* stimulation with Con A (**Fig. 3A**), as well as an $HA_{110\text{-}120}$-memory response. The HA110-120 epitope accounts for a small fraction of HA protein antigens. FACS analysis showed also a gradual increase in the size of memory $CD4^+$ ($CD44^{high}$) T-

cell pool 14 and 42 days post-immunization in mice immunized with PR8 virus only (**Fig. 3B**). In contrast, 14 and 42 days post-immunization the splenic CD4 T-cells from T-reg enriched BALB/c mice showed a lower increase in the size of memory $CD4^{+}44^{high}$ T-cell pool post-immunization than those immunized with PR8 virus alone (27.1% *vs*. 22.5% 14 days post-immunization, and 33.6% *vs*. 24% 42 days post-immunization) **(Fig. 3B)**, and a reduction in the memory-effector Th1 and Th2 function upon *in vitro* stimulation as detected in the cytokine assays.

Furthermore, to measure the extent to which $CD4^{+}$ memory-effector T-cell function is affected *in vivo* by $Foxp3^{+}$ T-reg cells induced through PR8 vaccination, we took advantage of a murine reporter system in which the PR8/HA-specific T-effector cells induce autoimmune diabetes. In this system, adoptively transferred $HA_{110\text{-}120}$-specific CD4 T-cells (TCR-PR8/HA) into RAG2 KO mice expressing the HA of PR8/A/34 influenza virus in the pancreatic β-cells (RAG2 KO, RIP-PR8/HA Tg mice) leads to fulminate autoimmune diabetes within two weeks, as depicted by hyperglycemia and heavy infiltration of pancreatic β-islets with lymphocytes (pancreatic insulitis) (**Fig 4A**) [44]. These mice can survive up to 1 month after the hyperglycemia onset. Similarly, the RAG2 KO, RIP-PR8/HA Tg mice infused with $CD4^{+}$ memory T-cells from PR8-immunized BALB/c mice harvested 42 days post-immunization developed hyperglycemia, although with a delay of 2-15 days, and longer survival (till 2 months) after hyperglycemia onset (**Fig. 4B**). Development of diabetes was indicative for activation of PR8-induced, HA-specific T memory cells toward the effector function upon encountering the PR8 viral antigens in the pancreas of RAG2 KO, RIP-PR8/HA Tg recipient mice. A short delay in diabetes onset in this group of mice may well account for

the lag period required by HA memory T-cells to develop into effector cells, to which the PR8-induced T-reg cells may have contributed by suppression of HA-specific T memory-effector cells. The recipient mice in this group also showed pancreatic insulitis, as indicated by the hematoxylin-eosin (HE) staining of pancreatic sections 50 days after the cell transfer (**Fig. 4B**).

In contrast to this group of mice, the RAG2 KO, RIP-PR8/HA Tg mice infused with memory CD4 T-cells from BALB/c mice enriched in T-regs prior to PR8 immunization remained normoglycemic for over 70 days (**Fig. 4C**). Normoglycemia was maintained even after co-infusion of TCR-PR8/HA diabetogenic T-cells ($2x10^5$ cells /mouse). Histological analysis of the pancreas of protected (normoglycemic) mice harvested 50 and 70 days after cell transfer showed a low degree of pancreatic insulitis. When tested for the insulin secretory function of pancreatic β-cells by the glucose tolerance test, the protected mice showed a sharp decline (within an hour) from a hyperglycemic-induced status to a normoglycemic status, just as the naïve RAG2 KO, RIP-PR8/HA Tg mice did (**Fig. 5A** & **5D**). In contrast, the RAG2 KO, RIP-PR8/HA Tg recipients of CD4 memory T cells from PR8-only immunized BALB/c mice tested by the glucose tolerance test remained in a hyperglycemic state for 3h (**Fig. 5C**) as compared with those infused only with TCR-PR8/HA diabetogenic T-cells (diabetes control group) in which hyperglycemia persisted longer than 3 h after the glucose load (**Fig. 5B**). These data indicated first, that PR8 vaccination induced HA-specific memory CD4 T-cells able to develop into HA-specific T-effector cells upon encountering the PR8/HA protein antigens in the pancreas of RAG2 KO, RIP-PR8/HA Tg mice. Second, the T-reg cells induced by PR8 immunization were fully functional, as they efficiently suppressed the PR8/HA-specific

(diabetogenic) T-cells in this system. The suppressive effect of PR8-induced T-regs on TCR-PR8/HA diabetogenic T-cell function was stronger when the size of T-reg pool was enriched in BALB/c donors prior to vaccination.

These results strongly suggest that the size of $CD4^+Foxp3^+$ T-reg pool is a critical modulatory component of the adaptive (PR8 virus-specific) $CD4^+$ T-cell primary and memory responses induced by vaccination.

3.3. Influenza vaccination favors expansion of $CD4^+Foxp3^+$ T-reg cells

We next questioned whether the PR8 vaccination alters the number of T-reg cells. for this, we compared T-reg frequency during the primary and memory T helper immune responses to PR8 virus after a single high-dose immunization (200 μg viral protein/mouse) with that of T-regs in BALB/c mice enriched or not with naive BALB/c $CD4^+Foxp3^+$ T-regs prior to immunization. Data from naïve, non-immunized BALB/c mice supplemented or not with $Foxp3^+$ T-regs in the absence of immunization showed a relative constant frequency of $Foxp3^+$ cells among the $CD4^+$ T-cell pool (2.8-3.2% and 3.8-4.4% $CD4^+Foxp3^+$ cells, respectively) during a 42-day follow-up (**Fig. 6**). This indicated that in the absence of immunization the homeostatic expansion of peripheral $Foxp3^+$ T-reg cells was insignificant. However, 14 days post-immunization with PR8 virus alone, the number of $CD4^+Foxp3^+$ cells increased by ~28% and continued to increase 42 days later by ~ 100% (**Fig. 6A**), which clearly indicated an expansion of $Foxp3^+$ T-reg pool induced by PR8 immunization. The BALB/c mice enriched with T-regs prior to immunization showed a higher increase in the number of $CD4^+Foxp3^+$ T-reg cells 14 and 42 days post-immunization (~39% to ~ 73%) (**Fig. 6B**). These data clearly

indicated that the size of $CD4^+Foxp3^+$ T-reg pool was expanded after PR8 immunization proportionally to its size prior to immunization.

Alternatively, we used a subtractionist approach to measure the *in vivo* T-reg kinetics upon PR8 viral vaccination. In this system, BALB.c/RAG2 KO mice were first infused with naïve T-reg ($CD25^+$)-depleted spleen cells or total spleen cells ($74x10^6$ cells/mouse) from BALB/c mice, then immunized with PR8 virus 1 day later, and Foxp3 mRNA expression was compared 8 days post-immunization in the spleen cells by real-time RT-PCR (**Fig. 6C**). While the non-reconstituted RAG mice that were immunized with PR8 virus showed a lack of Foxp3 mRNA expression, those reconstituted with T-reg-depleted spleen cells and immunized with PR8 virus showed the presence of a small amount of Foxp3 mRNA. Also, the pre-existent Foxp3 mRNA expression in RAG mice pre-infused with total spleen cells was increased by ≈18% upon PR8 vaccination.

Together, these results indicated that PR8 vaccination expands the pool of T-reg cells, and at the same time, a fraction of T-reg cells differentiate from the naïve conventional T-cell pool following PR8 vaccination.

3.4. Influenza vaccination favors the development of PR8 (HA)-specific $Foxp3^+$ T-reg cells

Recent data from individuals vaccinated for flu showed that $CD4^+CD25^-$ T-cells can differentiate into fully functional, antigen (HA)-specific $CD4^+CD25^+$ ($Foxp3^+$) T-reg cells upon stimulation *in vitro* with influenza $HA_{306-318}$ peptide [45]. It is believed that the antigen-specific T-reg suppression of cognate T-effector cells is more powerful than nonspecific bystander suppression induced by T-regs with unrelated antigen-specificity

or naïve T-reg cells that have not experienced the antigen. To test the antigen specificity of T-reg cells induced *in vivo* by PR8 vaccination, we immunized groups of naïve or T-reg enriched BALB/c mice with the same dose of UV-inactivated BHK influenza strain, and compared the capacity of BHK- *vs*. PR8-induced T-reg cells to suppress PR8/HA-specific T-cells that induce diabetes in the BALB/c, RAG2 KO, RIP-PR8/HA transgenic mouse. The BHK virus lacks the PR8/HA antigens. Immunization of mice with BHK virus induced similar titers of HAI Abs (1/320-1/640) to those detected in PR8-immunized mice (1/160-1/320). The RAG2 KO, RIP-PR8/HA Tg mice infused only with $CD4^+$ T cells alone ($2x10^5$ cells/mouse) from BHK-immunized BALB/c mice 14 days post-immunization remained free of diabetes (data not shown), indicating that the HA-specificity of T-effector cells induced by BHK immunization is unrelated to the HA-specificity of T-effector cells induced by PR8 immunization. Also, co-infusion of $2x10^5$ TCR-PR8/HA specific (diabetogenic) T-cells together with memory $CD4^+$ T splenic cells ($2x10^5$ cells/mouse) harvested 42 days post-BHK immunization of mice enriched or not with the same number ($6.5x10^6$ cells/mouse) of naïve BALB/c T-reg cells, did not protect against diabetes. These mice developed diabetes within the same period of time (2 weeks) and showed lymphocyte infiltration of pancreatic β-islets as those infused only with $2x10^5$ TCR-PR8/HA specific (diabetogenic) T-cells (diabetes control group) (**Fig. 7**). These results showed that the BHK HA-specificity of T memory-effector cells as well as T-reg cells was unrelated to the PR8/HA-specificity. Only the PR8-induced T-reg cells were able to protect against diabetes in this mouse model for PR8/HA-induced diabetes (Fig. 4), which demonstrated that the suppressogenic effect of T-reg cells induced by PR8 vaccination was restricted to the T-effector cells specific for HA protein of PR8/A/34

influenza strain. These experiments demonstrated that a fraction of T-reg cells induced by PR8 vaccination were specific for PR8/HA antigens.

Discussion

Human HA-specific $CD4^+CD25^+Foxp3^+$ T-regs can be generated *in vitro* from naïve and memory $CD4^+CD25^-$ T-cells of individuals previously vaccinated for flu by a 10-day re-stimulation *in vitro* with dendritic cells pulsed with influenza $HA_{306-319}$ consensus peptide [45]. T-reg suppression of antigen (HA)-specific T-effector cells as well as nonspecific bystander suppression of T-effector cells specific for tetanus toxoid antigens was only achieved in the presence of $HA_{306-319}$ cognate peptide, implying that $Foxp3^+$ T-reg cells require antigen stimulation to gain both antigen-specific and nonspecific bystander suppressive functions [45]. The $CD4^+Foxp3^+$ T-regs are naturally-born in thymus by differentiation of T-cell precursors upon TCR stimulation by MHC-peptide complexes [46]. Like the human T-reg cells [45], the murine naïve $CD4^+Foxp3^-$ T-cells can up-regulate Foxp3 expression and gain suppressogenic function in periphery upon encountering antigen in the presence of TGF–β [46], or IL-2 and IL-15 [47, 48].

A body of evidence showed that T-regs can efficiently suppress autoimmunity including type 1 diabetes. Using a BALB/c, RAG2 KO, RIP-PR8/HA transgenic mouse model in which infusion of influenza PR8/HA-specific T-effector cells (from a TCR-PR8/HA Tg mouse) induces fulminate diabetes, we found that the $CD4^+CD25^+$ ($Foxp3^+$) T-regs induced in BALB/c mice through vaccination with influenza PR8 virus, abolished the diabetogenic function of PR8/HA-specific T-effector cells for as long as 70 days. A fraction of $Foxp3^+$ T-regs induced by PR8 vaccination were HA-specific, since the T-regs

induced by vaccination with BHK virus expressing a structurally different HA protein did not abolish the diabetogenic function of PR8/HA-specific T-effector cells in the RAG2 KO, RIP-PR8/HA mouse system. This clearly indicated that the PR8/HA-specific $Foxp3^+$ T-regs suppressed more efficiently their cognate T-effector cells *in vivo* than the T-reg bystander suppressors specific for BHK/HA antigens.

Vaccination of BALB/c mice with a single high-dose of a prototype UV-inactivated influenza A/PR/8/34 virus vaccine expanded the $Foxp3^+$ T-reg pool by almost 30% and 100%, 14 and respectively 42 days post-vaccination. A two-fold increase in the size of $Foxp3^+$ T-reg pool over the pre-existent pool size (before vaccination) did not alter the PR8-specific B-cell responses, but it did lower significantly the primary and memory PR8-specific T helper responses to the virus. Conversely, mice depleted of T-regs mounted a significantly higher T helper response to PR8 viral vaccination than those with a pre-existent T-reg pool. Interesting enough, a small fraction of newly-generated T-reg cells from naïve conventional T-cells was detected post-vaccination in mice depleted of T-regs, which is consistent with a number of reports indicating that T-regs may differentiate from peripheral naïve $CD4^+Foxp3^+$T-cells upon encountering antigen in a milieu of TGF–β, or IL-2 and IL-15 [46-48].

B memory cell responses specific for influenza HA viral proteins are particularly long-lived, as demonstrated by studies in elderly individuals after several decades from the virus exposure [49]. The HA-specific B memory cells are critical for clearing the virus from the lungs, as they are activated to secrete neutralizing antibodies subsequent to repeated infections with the same virus or cross reactive viruses [50]. Upon encountering viral antigens, the CD4 T-cells are activated and differentiate into antigen (virus)-specific

Th cells. A large number of these cells die by activation-induced apoptosis, whereas a smaller number enter the peripheral lymphoid organs to become memory Th cells [51]. Upon the antigen recall following a viral infection or vaccination boost, the virus-specific memory T helper cells rapidly become memory-effector cells [52, 53]. Influenza-specific T memory cells induced by vaccination or exposure to the live virus do not clear efficiently the virus in the absence of antibodies [54], but they do contribute significantly to the anti-viral protective immunity by shortening the time of recall for B memory cell activation leading to secretion of neutralizing antibodies. A delay of 4 to 5 days in virus clearance from the lungs was observed in CD4-depleted mice, which was essential for recovery from infection and survival [55]. We noticed that PR8 vaccination led to increased number of $CD4^{+}CD44^{high}$ T memory cells 14 and 42 days post-immunization following similar kinetics to those reported for memory T-cells activated upon re-infections [56-58]. In contrast to influenza-specific B-cell responses, the virus-specific Th1 and Th2 primary and memory responses were significantly suppressed by the PR8 vaccination-induced $CD4^{+}Foxp3^{+}$T-reg cells.

In summary, our findings showed that the size of $CD4^{+}Foxp3^{+}$ T-reg pool is an important modulatory component of primary and memory T-cell responses to influenza vaccination. Since the CD4 T-cells play an important role in anti-influenza viral protection through a quick recall of the adaptive B memory cell response, and T-regs are expanded as consequence of vaccination, one may explain at least in part why not all vaccinated individuals are resistant to influenza exposure. Individual variations in the size of T-reg compartment in various ethnic groups were so far correlated with susceptibility to autoimmune diseases [59]. Thus, attempts to deplete T-reg cells prior to vaccination

[60], or to abolish T-reg suppressive function by GITR blocking Ab [61, 62] or by manipulating expression of sphingosine 1-phosphate receptor type 1 ($S1P_1$) [63] may raise safety concerns due to the increased risk of autoimmunity. Early studies on influenza virus suggested that hypothetical suppressogenic epitopes expressed among immunogenic epitopes of the viral envelope are responsible for induction of antigen-specific T "suppressor" cells, and that down-modulation of such suppressogenic epitopes might help designing new vaccine preparations able to increase the resistance to infection [11]. However, it has been later demonstrated in various antigen-specific systems that the immunogenic epitopes are structurally identical to the suppressogenic ones [7] and thereby, the concept of "epitope structural identity" may greatly impact the vaccinology field by generating new influenza viruses with random mutations in HA protein. Such newly-generated (mutated) viral epitopes may outsmart antigen-drifting that occurs on a regular basis among the influenza strains, although they may lack not only suppressogenic epitopes, but also immunogenic epitopes required for induction of protective immunity. Our basic knowledge about "regulation" of T-reg cells is in infancy, but new findings suggest that the dendritic cells may be used to turn-off T-reg function through mechanisms engaging IL-6, TLRs 4, or TLR9 [64, 65]. Without a doubt, investigations on the therapeutic "quenching" of T-reg function prior to vaccination is an exciting area that may lead to the development of anti-viral vaccines endowed with better efficacy.

Acknowledgements: This work was supported by a grant from the Uniformed Services University of the Health (RO83U-07/09) to T-D.B. We thank Mrs. Karen Wolcott and Kateryna Lund from USUHS Biomedical Instrumentation Center for valuable assistance with FACS and Luminex analyses, and Dr. Constantin A Bona for critical comments on the manuscript.

References

[1] Kilbourne ED. Influenza. New York: Plenum, 1987: 234.

[2] Townsend A, Bodmer H. Antigen recognition by class I-restricted T lymphocytes. Annu Rev Immunol 1989; 7:601-24.

[3] Milligan GN, Flaherty L, Braciale VL, Braciale TJ. Nonconventional (TL-encoded) major histocompatibility complex molecules present processed viral antigen to cytotoxic T lymphocytes. J Exp Med 1991; 174:133-8.

[4] Zaghouani H, Kuzu Y, Kuzu H, Brumeanu TD, Steinman RM, Bona CA. Contrasting efficacy of presentation by MHC class I and class II products when peptides are administrated within a common protein carrier, self-immunoglobulin. Eur J Immunol 1993; 23:2746.

[5] Gordon D. Influenza in man. In: Kilbourne E, The influenza viruses and influenza ed. Academic press, New York, 1975: 395-443.

[6] Giamarellos-Bourboulis EJ, Raftogiannis M, Antonopoulou A, Baziaka F, Koutoukas P, Savva A, et al. Effect of the Novel Influenza A (H1N1) Virus in the Human Immune System. PloS ONE 2009; 4(12):e8393.-2750.

[7] Mills KHG, McGuirk P. Antigen-specific regulatory T cells: their induction and role in infection. Seminars Immunol 2004; 16:107-117.

[8] Majlessi J, Lo-Man R, Leclerc C. Regulatory B and T cells in infections. Microbes Infect 2008; 10:1030-35.

[9] Vahlenkamp TW, Tompkins MB, Tompkins WAF. The role of CD4+CD25+ regulatory T cells in viral infections. Veterinary Immunol Immunopathol 2005; 108:219-25.

[10] Haeryfar SM, DiPaolo RJ, Tscharke DC, Bennink JR, Yewdell JW. Regulatory T cells suppress CD8+ T cell responses induced by direct priming and cross-priming and moderate immunodominance disparities. J Immunol 2005; 174:3344-51.

[11] Hurwitz JL, Hackett CJ. Influenza-specific suppression: contribution of major viral proteins to the generation and function of T suppressor cells. J Immunol 1985; 135:2134-39.

[12] Sun J, Madan R, Karp CL, Braciale TJ. Effector T cells control lung inflammation during acute influenza virus infection by producing IL-10. Nat Med 2009; 15:277-84.

[13] Smith RH, Ziola B. Cyclophosphamide and dimethyl dioctadecyl ammonium bromide immunopotentiate the delayed-type hypersensitivity response to inactivated enveloped viruses. Immunology 1986; 58(2):245-50.

[14] Sakaguchi S. Naturally arising Foxp3-expressing CD25+CD4+ regulatory T cells in immunological tolerance to self and non-self. Nat Immunol 2005; 6:345-52.

[15] Sakaguchi S, Sakaguchi N, Asano M, Itoh M, Toda M. Immunologic self-tolerance maintained by activated T cells expressing IL-2 receptor alpha-chains (CD25). Breakdown of a single mechanism of self-tolerance causes various autoimmune diseases. J Immunol 1995; 155:1151-64.

[16] Darrasse-Jeze G, Klatzmann D, Charlotte F, Salomon BL, Cohen JL. CD4+CD25+ regulatory/suppressor T cells prevent allogeneic fetus rejection in mice. Immunol Lett 2006; 102(1):106-9.

[17] Lee MK th, Moore DJ, Jarrett BP, Lian MM, Deng S, Huang X, et al. Promotion of allograft survival by CD4+CD25+ regulatory T cells: evidence for in vivo inhibition of effector cell proliferation. J Immunol 2004; 172:6539-44.

[18] Valzasina B, Piconese S, Guiducci C, Colombo MP. Tumor-induced expansion of regulatory T cells by conversion of CD4+CD25- lymphocytes is thymus and proliferation independent. Cancer Res 2006; 66:4488-95.

[19] Levings MK, Roncarolo MG. T-regulatory-1 cells: A novel subset of CD4 T cells with immunoregulatory properties. J Allergy Clin Immunol 2000; 106:109-112.

[20] McGuirk P, McCann C, Mills KH. Pathogen-specific T regulatory 1 cells induced in the respiratory tract by a bacterial molecule that stimulates interleukin 10 production by dendritic cells: a novel strategy for evasion of protective T helper type 1 responses by Bordetella pertussis. J Exp Med 2002; 195:221-31.

[21] Plebanski M, Flanagan KL, Lee EA, Reece WH, Hart K, Gelder C, et al. Interleukin 10-mediated immunosuppression by a variant CD4 T cell epitope of Plasmodium falciparum. Immunity 1999; 10:651-60.

[22] Lavelle EC, McNeela E, Armstrong ME, Leavy O, Higgins SC, Mills KH. Cholera toxin promotes the induction of regulatory T cells specific for bystander antigens by modulating dendritic cell activation. J Immunol 2003; 171:2384-92.

[23] Suvas S, Azkur AK, Kim BS, Kumaraguru U, Rouse BT. CD4+CD25+ regulatory T cells control the severity of viral immunoinflammatory lesions. J Immunol 2004; 172:4123-32.

[24] Iwashiro M, Messer RJ, Peterson KE, Stromnes IM, Sugie T, Hasenkrug KJ. Immunosuppression by CD4+ regulatory T cells induced by chronic retroviral infection. Proc Natl Acad Sci USA 2001; 98:9226-30.

[25] MacDonald AJ, Duffy M, Brady MT, McKiernan S, Hall W, Hegarty J, et al. CD4 T helper type 1 and regulatory T cells induced against the same epitopes on the core protein in hepatitis C virus-infected persons. J Infect Dis 2002; 185:720-7.

[26] Sugimoto K, Ikeda F, Stadanlick J, Nunes FA, Alter HJ, Chang KM. Suppression of HCV-specific T cells without differential hierarchy demonstrated ex vivo in persistent HCV infection. Hepatology 2003; 38:1437-48.

[27] Cabrera R, Tu Z, Xu Y, Firpi RJ, Rosen HR, Liu C, et al. An immunomodulatory role for CD4(+)CD25(+) regulatory T lymphocytes in hepatitis C virus infection. Hepatology 2004; 40:1062-71.

[28] Lund JM, Hsing L, Pham TT, Rudensky AY. Coordination of early protective immunity to viral infection by regulatory T cells. Science 2008; 320(5880):1220-24.

[29] Oswald-Richter K, Grill SM, Shariat N, Leelawong M, Sundrud MS, Haas DW, et al. HIV infection of naturally occurring and genetically reprogrammed human regulatory T-cells. PLoS Biol 2004; 2:E198.

[30] Aandahl EM, Michaelsson J, Moretto WJ, Hecht FM, Nixon DF. Human CD4+ CD25+ regulatory T cells control T-cell responses to human immunodeficiency virus and cytomegalovirus antigens. J Virol 2004; 7 8:2454-9.

[31] Kinter AL, Hennessey M, Bell A, Kern S, Lin Y, Daucher M, et al. CD25(+)CD4(+) regulatory T cells from the peripheral blood of asymptomatic HIV-infected individuals regulate CD4(+) and CD8(+) HIV-specific T cell immune responses in vitro and are associated with favorable clinical markers of disease status. J Exp Med 2004; 200:331-43.

[32] Weiss L, Donkova-Petrini V, Caccavelli L, Balbo M, Carbonneil C, Levy Y. Human immunodeficiency virus-driven expansion of CD4+CD25+ regulatory T cells, which suppress HIV-specific CD4 T-cell responses in HIV-infected patients. Blood 2004; 104:3249-56.

[33] Karube K, Ohshima K, Tsuchiya T, Yamaguchi T, Kawano R, Suzumiya J, et al. Expression of FoxP3, a key molecule in CD4CD25 regulatory T cells, in adult T-cell leukaemia/lymphoma cells. Br J Haematol 2004; 126:81-4.

[34] Yamano Y, Takenouchi N, Li HC, Tomaru U, Yao K, Grant CW, et al. Virus-induced dysfunction of CD4+CD25+ T cells in patients with HTLV-I-associated neuroimmunological disease. J Clin Invest 2005; 115:1361-8.

[35] Rouse BT, Sarangi PP, Suvas S. Regulatory T cells in virus infections. Immunol Rev 2006; 212:272-86.

[36] Casares S, Hurtado A, McEvoy RC, Sarukhan A, von Boehmer H, Brumeanu TD. Down-regulation of diabetogenic CD4+ T cells by a soluble dimeric peptide-MHC class II chimera. Nat Immunol 2002; 3:383-91.

[37] Brumeanu T-D, Casares S, Bot A, Bona C.A. Immunogenicity of a contiguous T-B synthetic epitope of the PR/8/34 influenza virus, J Virol 1997; 10:129-136.

[38] Hori S, Nomura T, Sakaguchi S. Control of regulatory T cell development by the transcription factor Foxp3. Science 2003; 299:1057-61.

[39] Stoica-Nazarov C, Surls J, Bona C, Casares S, Brumeanu TD. CD28 signaling in T regulatory precursors requires p56lck and rafts integrity to stabilize the Foxp3 message. J Immunol 2009; 182:102-10.

[40] Bot A, Casares S, Bot S, von Boehmer H, Bona C. Cellular mechanisms involved in protection against influenza virus infection in transgenic mice expressing a TCR receptor specific for class II hemagglutinin peptide in CD4+ and CD8+ T cells. J Immunol 1998; 160:4500-7.

[41] Ahmadzadeh M, Hussain SF, Farber DL. Heterogeneity of the memory CD4 T cell response: persisting effectors and resting memory T cells. J Immunol 2001; 166:926-35.

[42] Bingaman AW, Patke DS, Mane VR, Ahmadzadeh M, Ndejembi M, Bartlett ST, et al. Novel phenotypes and migratory properties distinguish memory CD4 T cell subsets in lymphoid and lung tissue. Eur J Immunol 2005; 35:3173-86.

[43] Hogan RJ, Zhong W, Usherwood EJ, Cookenham T, Roberts AD, Woodland DL. Protection from respiratory virus infections can be mediated by antigen-specific CD4(+) T cells that persist in the lungs. J Exp Med 2001; 193:981-6

[44] Kirberg J, Baron A, Jakob S, Rolink A, Karjalainen K, von Boehmer H. Thymic selection of $CD8^+$ single positive cells with a class II major histocompatibility complex-restricted receptor. J Exp Med 1994; 180:25-34.

[45] Walker MR, Carson BD, Nepom GT, Ziegler SF, Buckner JH. De novo generation of antigen-specific CD4+CD25+ regulatory T cells from human CD4+CD25- cells. Proc Natl Acad Sci U S A 2005; 102:4103-8.

[46] Thornton AM, Shevach EM. Suppressor effector function of CD4+CD25+ immunoregulatory T cells is antigen nonspecific. J Immunol 2000; 164:183-90.

[47] Andersson J, Tran DQ, Marko P, Davidson TS, Ramsey H, O'Shea JJ, et al. CD4+ Foxp3+ regulatory T cells confer infectious tolerance in TGF-β dependent manner. J Exp Med 2008; 205:1975-81.

[48] Lio CW, Hsieh CS. A two-step process for thymic regulatory T cell development. Immunity 2008; 28:100-11.

[49] Burchill MA, Yang J, Vang KB, Moon JJ, Chu HH, Lio CW, et al. Linked T cell receptor and cytokine signaling govern the development of the regulatory T cell repertoire. Immunity 2008; 28:112-21.

[50] Yu X, Tsibane T, McGraw PA, House FS, Keefer CJ, Hicar MD, et al. Neutralizing antibodies derived from the B cells of 1918 influenza pandemic survivors. Nature 2008; 445:532-36.

[51] Brown DM, Roman E, Swain SL. CD4 T cell responses to influenza infection. Seminars Immunol 2004; 16: 171-7.

[52] Catron DM, Rusch LK, Hataye J, Itano AA, Jenkins MK. CD4+ T cells that enter the draining lymph nodes after antigen injection participate in the primary response and become central-memory cells. J Exp Med 2006; 203:1045-54.

[53] Verhoeven D, Teijaro JR, Farber DL. Heterogeneous memory T cells in antiviral immunity and immunopathology. Viral Immunol 2008; 21:99-113.

[54] Welsh RM and Selin LK. No one is naive: the significance of heterologous T-cell immunity. Nat Rev Immunol 2002; 2:417-26.

[55] Mozdzanowska K, Maiese K, Gerhard W. Th cell-deficient mice control influenza virus infection more effectively than Th- and B-cell deficient mice: evidence for a Th-independent contribution by B cells to virus clearance. J Immunol 2000; 164: 2635-43.

[56] Flynn KJ, Belz GT, Altman JD, Ahmed R, Woodland DL, Doherty PC. Virus-specific CD8+ T cells in primary and secondary influenza pneumonia. Immunity 1998; 8:683-91.

[57] Strutt TM, McKinstry K, Swain SL. Functionally diverse subsets in CD4 T cell responses against influenza. J Clin Immunol. 2009; 29:145-50.

[58] McKinstry KK, Golech S, Lee WH, Huston G, Weng NP, Swain SL. Rapid default transition of CD4 T cell effectors to functional memory cells. J Exp Med 2007; 204:2199-2211.

[59] Ban Y, Tozaki T, Tobe T, Jacobson EM, Concepcion ES, Tomer Y. The regulatory T cell gene FOXP3 and genetic susceptibility to thyroid autoimmunity: an association analysis in Caucasian and Japanese cohorts. J Autoimmun 2007; 28:201-7.

[60] Moore AC, Gallimore A, Draper Sj, Watkins KR Gilbert SC, Hill AV. Anti-CD25 antibody enhancement of vaccine-induced immunogenicity: increased durable cellular immunity with reduced immunodominance. J Immunol 2005; 175:7264-73.

[61] Shimizu J, Yamazaki S, Takahashi T, Ishida Y, Sakaguchi S. Stimulation of CD25(+)CD4(+) regulatory T cells through GITR breaks immunological self-tolerance. Nat Immunol 2002; 3:135-42.

[62] Stephens GL, McHugh RS, Whitters MJ, Young DA, Luxenberg D, Carreno BM, et al. Engagement of glucocorticoid-induced TNFR family-related receptor on effector T cells by its ligand mediates resistance to suppression by CD4+CD25+ T cells. J Immunol 2004; 173:5008-20.

[63] Liu G, Burns S, Huang G, Boyd K, Proia RL, Flavell RA, et al. The receptor S1P1 overrides regulatory T cell-mediated immune suppression through Akt-mTOR. Nat Immunol 2009; 10:769-77.

[64] Pasare C, Medzhitov R. Toll pathway-dependent blockade of CD4+CD25+ T cell-mediated suppression by dendritic cells. Science 2003; 299:1033-36.

[65] Yang Y, Huang CT, Huang X, Pardoll DM. Persistent toll-like receptor signals are required for reversal of regulatory T cell-mediated CD8 tolerance. Nat Immunol 2004; 5:508-15.

Figure legends

Figure 1. Effect of T-reg enrichment on B-cell responses upon PR8 viral vaccination. (A) Groups of BALB/c mice (n=6) were infused or not 3 days prior to i.p. PR8 immunization (200 μg viral protein/mouse) with $CD4^+CD25^+$ T-reg cells ($6.5x10^6$ cells per mouse). Fourteen days (top) and forty-two days later (bottom), the anti-PR8 total serum IgG, IgG1, and IgG2a levels were measured by ELISA at 1/100 dilution using PR8 virus-coated plates (5 μg protein per mL) as described. Results are expressed as geometric mean of μg/ml ± SD between sera from individual mice calculated based on the OD values (λ = 450nm) obtained in ELISA, and a calibration curve using an anti-PR8 IgG Ab. (B) Hemagglutination Inhibition Assay (HAI) was performed for the same groups of mice like in panel A. The HAI Ab titer was assigned as the last inhibitory dilution of serum. Shown is one of two representative experiments (p^* <0.005 between two experiments).

Figure 2. Effect of T-reg enrichment on the primary T helper cell responses to PR8 viral vaccination. (A) Primary T-cell proliferative response of splenocytes (10^6 cells) from T-reg enriched ($6.5x10^6$ cells/mouse) or not from BALB/c mice (n=6) immunized with 200 μg of UV-inactivated PR8 viral protein/mouse (14 days post-immunization) upon *in vitro* stimulation with $HA_{110-120}$ synthetic peptide (40 μg/mL) or Con A (2 μg/mL). The OD units refers to the index of proliferation measured at λ=490 nm ± SD among triplicate samples from the same experiment. (B) Cytokine production in supernatants from the splenocytes of the same groups of mice upon *in vitro* stimulation with HA peptide or Con A (as in panel A) and measured by Luminex. The index of

cytokine secretion is expressed as the pg/mL value of stimulated samples (HA or Con A) divided by the pg/mL value of the non-stimulated samples (NIL, media alone). Results are expressed as the geometric mean of the index of cytokine secretion $\pm$ SD among triplicate samples from the same experiment. Shown is (panels A and B) one of two representative experiments ($p^* = 0.002$, between two experiments). (C) Relative mRNA expression of STAT4, T-bet, STAT6, GATA3, and cMAF in aliquot samples from the same groups of mice as in panels A and B and in the absence of *in vitro* re-stimulation. Shown are the mean values $\pm$ SD for 3 individual mice in each group. (D) Cytokine production in cell culture supernatants of splenocytes from BALB/c, RAG2 KO mice pre-infused with $74x10^6$ cells/mouse of either total spleen cells (n=3), or T-reg-depleted spleen cells (n=3), or saline (n=3), and then immunized 1 day later i.p. with inactivated PR8 virus (100 μg/mouse). Spleen cells of RAG2 KO recipients were collected 8 days post-immunization, stimulated for 2 days *in vitro* with purified PR8 virus (10 μg viral protein/10^6 cells) or ConA (1 μg/10^6 cells), and cytokine secretion in culture supernatants was measured by Luminex. The signal-to-noise from aliquot wells left non-stimulated was subtracted from each sample. Results from individual mice are expressed as mean pg/mL $\pm$ SD among triplicate samples from the same experiment. Shown are the results of one of two representative experiments ($p^* = 0.004$ between experiments).

Figure 3. Effect of T-reg enrichment on the memory T helper cell response to PR8 viral vaccination. (A) Cytokine production in supernatants from the splenocytes (10^6 cells) of T-reg enriched ($6.5x10^6$ cells/mouse) or not from BALB/c mice (n=6) immunized with 200 μg of UV-inactivated PR8 virus/mouse (42 days post-

immunization) upon *in vitro* re-stimulation with $HA_{110-120}$ synthetic peptide (40 μg/mL) or Con A (2 μg/mL) and measured by Luminex. The index of cytokine secretion is expressed as the pg/mL value of stimulated samples ($HA_{110-120}$ peptide or Con A) divided by the pg/mL value of the non-stimulated samples (NIL, media alone). Results are expressed as the geometric mean of the index of cytokine secretion $\pm$ SD among triplicate samples from the same experiment. Shown is one of two representative experiments (p*=0.0042 between two experiments). (B) Kinetics in the frequency of $CD4^+CD44^{high}$ memory T-cells from the splenic cells of T-reg enriched ($6.5x10^6$ cells/mouse) or not from BALB/c mice (n=6) immunized or not with 200 μg of UV-inactivated PR8 viral protein/mouse, before, and after 14 and 42 days post-immunization. Cells were stained with CD3-FITC, CD4-PerCP, and CD44-PE Ab conjugates (BD PharMingen) and the number of $CD3^+CD4^+CD44^{high}$-gated cells was measured by FACS among 10^5 cell events. Shown are individual mice (n=6) from each group of mice ($p< 0.005$ between individual mice).

Figure 4. The suppressogenic function of T-reg cells upon PR8 viral vaccination. Groups of RAG2 KO, RIP-PR8/HA Tg mice (n=5 mice/group) were infused i.p. with splenic TCR-PR8/HA CD4 diabetogenic T-cells ($2x10^5$ cells/mouse, diabetes control group) (*panel* A), or with splenic $CD4^+$ memory T-cells from PR8 immunized BALB/c mice ($2x10^5$ cells/mouse) harvested 42 days post-immunization) (*panel* B). Inserts show the H&E staining of a representative pancreatic section from one recipient mouse in each group, 30 and respectively, 60 days after cell transfer. Glycemia values are indicated for individual mice in each group. Upper limit of normoglycemia (200 mg/dL, dotted line)

was previously determined on a large cohort of naïve RAG2 KO, RIP-PR8/HA Tg mice after overnight fastening. (C) RAG2 KO, RIP-PR8/HA Tg mice (n=5) were infused i.p. with splenic $CD4^+$ memory T-cells from T-reg enriched/PR8-immunized BALB/c mice harvested 42 days post-immunization. Thirty-five days after cell infusion (dark arrow) mice were co-infused i.p. with TCR-PR8/HA diabetogenic T-cells ($2x10^5$ cells/mouse) and glycemia monitored on a bi-weekly basis. Shown are the H&E staining of pancreatic sections from one representative naïve (non-infused) RAG2 KO, RIP-PR8/HA Tg mouse that lacks pancreatic infiltration (left insert), and one representative RAG2 KO, RIP-PR8/HA Tg mouse 35 days after co-infusion of TCR-PR8/HA diabetogenic cells showing a limited, peri-islet infiltration with lymphocytes (right insert).

Figure 5. Glucose tolerance test in RAG2 KO, RIP-PR8/HA Tg recipient mice of BALB/c PR8-specific T-regs induced by vaccination. (A) Naïve RAG2 KO, RIP-PR8/HA Tg mice (n=7, normoglycemia control group), or infused i.p. with splenic TCR-PR8/HA diabetogenic T-cells (n=4, diabetes control group) (panel B), or RAG2 KO, RIP-PR8/HA Tg mice (n=3) infused i.p. with splenic $CD4^+$ memory T-cells ($2x10^5$ cells/mouse) from BALB/c mice immunized with PR8 virus and harvested 42 days post-immunization (panel C), or RAG2 KO, RIP-PR8/HA Tg mice (n=3) infused i.p. with splenic $CD4^+$ memory T-cells ($2x10^5$ cells/mouse) from T-reg enriched, BALB/c mice immunized with PR8 virus and harvested 42 days post-immunization (panel D) were fasted overnight and then injected i.p. with glucose in saline (60 mg/mouse). Blood glucose levels were determined at various intervals of time during a 180-min period after

glucose load. Upper limit of normoglycemia (200 mg/dL) in naïve RAG2 KO, RIP-PR8/HA Tg mice after overnight fastening is indicated (dotted line).

Figure 6. Frequency of $CD4^+Foxp3^+$ T-regs upon T-reg enrichment in naïve BALB/c mice before and after PR8 viral vaccination. Splenic T-cells from BALB/c T-reg enriched (*panel B*) or not (*panel A*) that were immunized or not with 200 μg of UV-inactivated PR8 viral protein/mouse were surface stained with CD3-FITC, CD4-PerCP and intra-nuclear stained with Foxp3 Ab-PE conjugates 14 and 42 days post-immunization. Shown are the mean values for individual mice (framed histograms) in each group of mice indicating the percent of $Foxp3^+$ T-reg cells at various time-points $\pm$ SD (n=6 mice/group) in one of two representative experiments ($p^* < 0.005$ between experiments). (C) Foxp3 mRNA expression in splenocytes collected from BALB/c, RAG2 KO mice pre-infused with $74x10^6$ cells/mouse of either total spleen cells (n=3), or T-reg-depleted spleen cells (n=3), or saline (n=3), and then immunized with PR8 virus in saline 1 day later (100 μg/mouse). Spleen cells of RAG2 KO recipients were collected 8 days post-immunization, and Foxp3 mRNA expression was determined 8 days post-immunization in individual mice by real-time RT-PCR. Results are expressed as mean of relative mRNA expression from individual mice $\pm$ SD ($p^* = 0.005$ between experiments).

Figure 7. Antigen-specificity of $CD4^+Foxp3^+$ T-regs induced by PR8 viral vaccination. *Panel A*, RAG2 KO, RIP-PR8/HA Tg mice (n=3) co-infused i.p. with TCR-PR8/HA diabetogenic cells ($2x10^5$ cells/mouse) and $CD4^+$ splenic T-cells ($2x10^5$ cells/mouse) from BHK-immunized BALB/c mice. *Panel B*, RAG2 KO, RIP-PR8/HA Tg

mice (n=5) co-infused i.p. with TCR-PR8/HA diabetogenic cells ($2x10^5$ cells/mouse) and $CD4^+$ splenic T-cells ($2x10^5$ cells/mouse) from BHK-immunized BALB/c mice and enriched in T-reg cells ($6.5x10^6$ cells added/mouse) prior to immunization. The CD4 splenic T-cells from BHK-immunized BALB/c mice were collected 42 days after immunization. Plots indicate the level of blood glucose in individual mice till reaching the hyperglycemic status. Inserts in panels A and B show the H&E staining of pancreatic sections from one representative recipient mouse in each group. As illustrated, both groups of mice showed heavy pancreatic infiltration of β-islets with lymphocytes 35 days after cell co-infusion. Dotted line indicates the upper limit of normoglycemia (200 mg/dL).

A

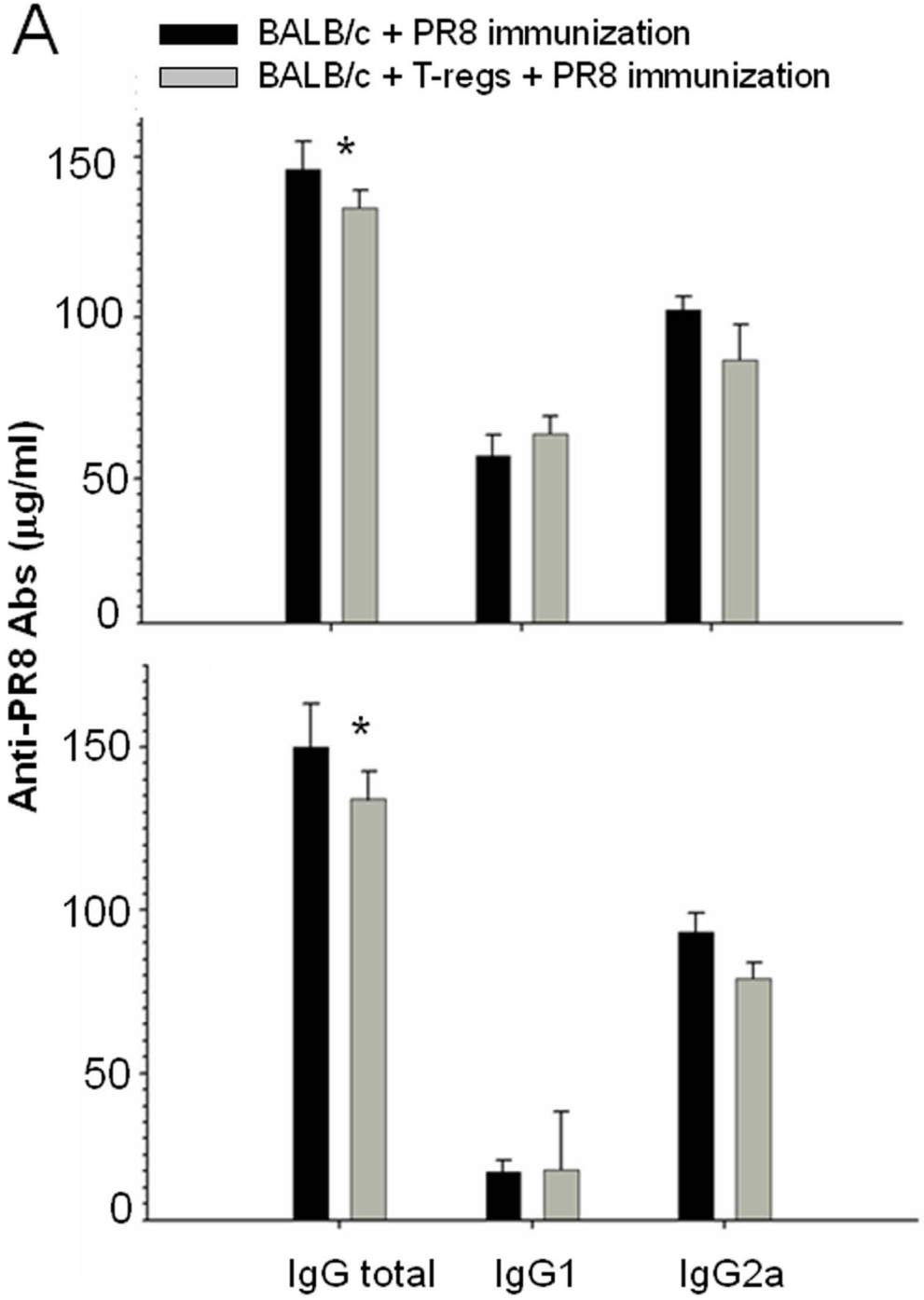

B

Group of mice:	PR8 virus HI titers:
PR8-immunized and analyzed 14 days post-immunization	1/320 - 1/640
T-regs infused prior to PR8-immunization and analyzed14 days post-immunization	1/240 - 1/640
PR8-immunized and analyzed 42 days post-immunization	1/160-1/320
T-regs infused prior to PR8-immunization and analyzed 42 days post-immunization	1/160-240

Vaccine, Surls et al., Fig. 1.

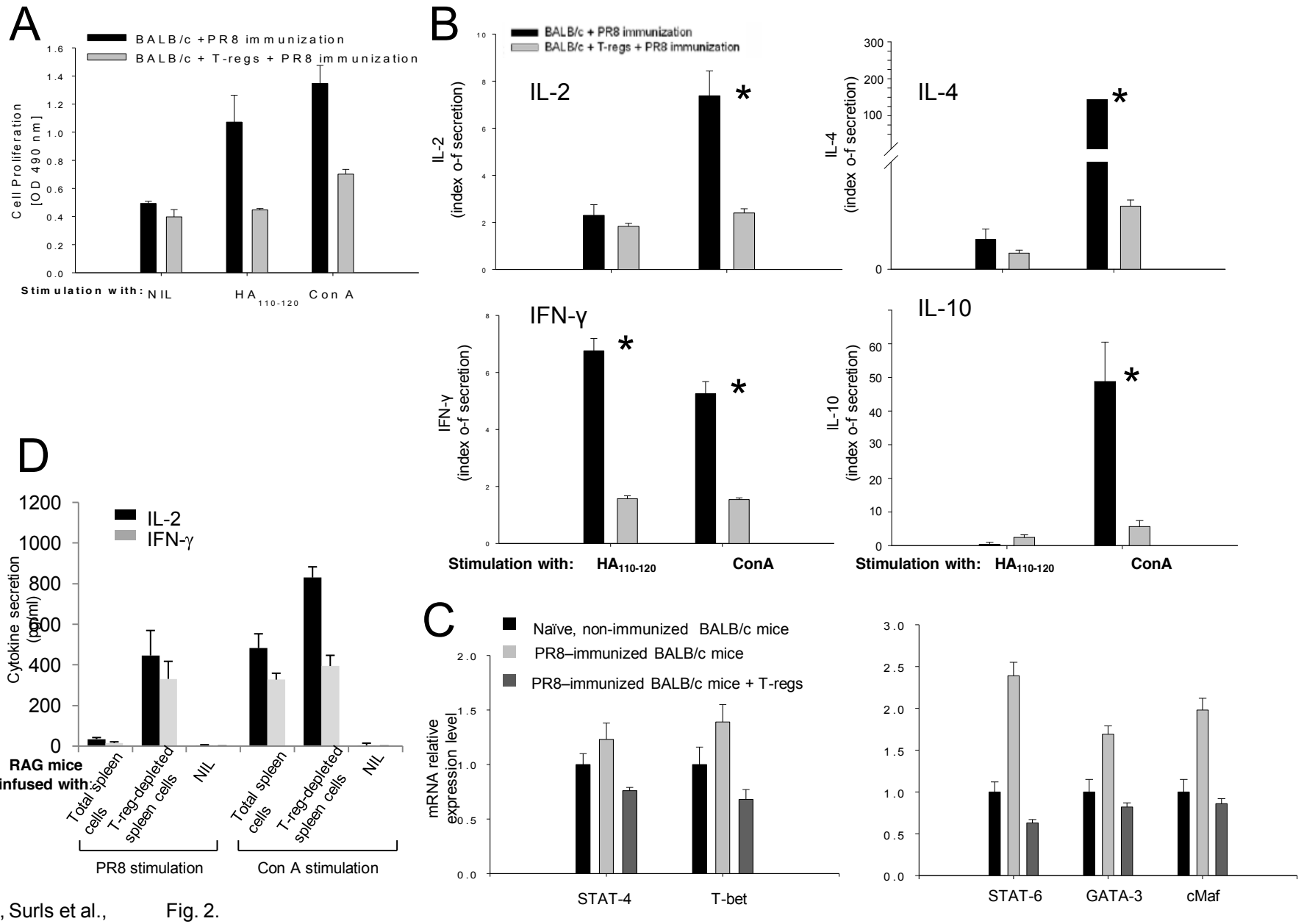

Vaccine, Surls et al., Fig. 2.

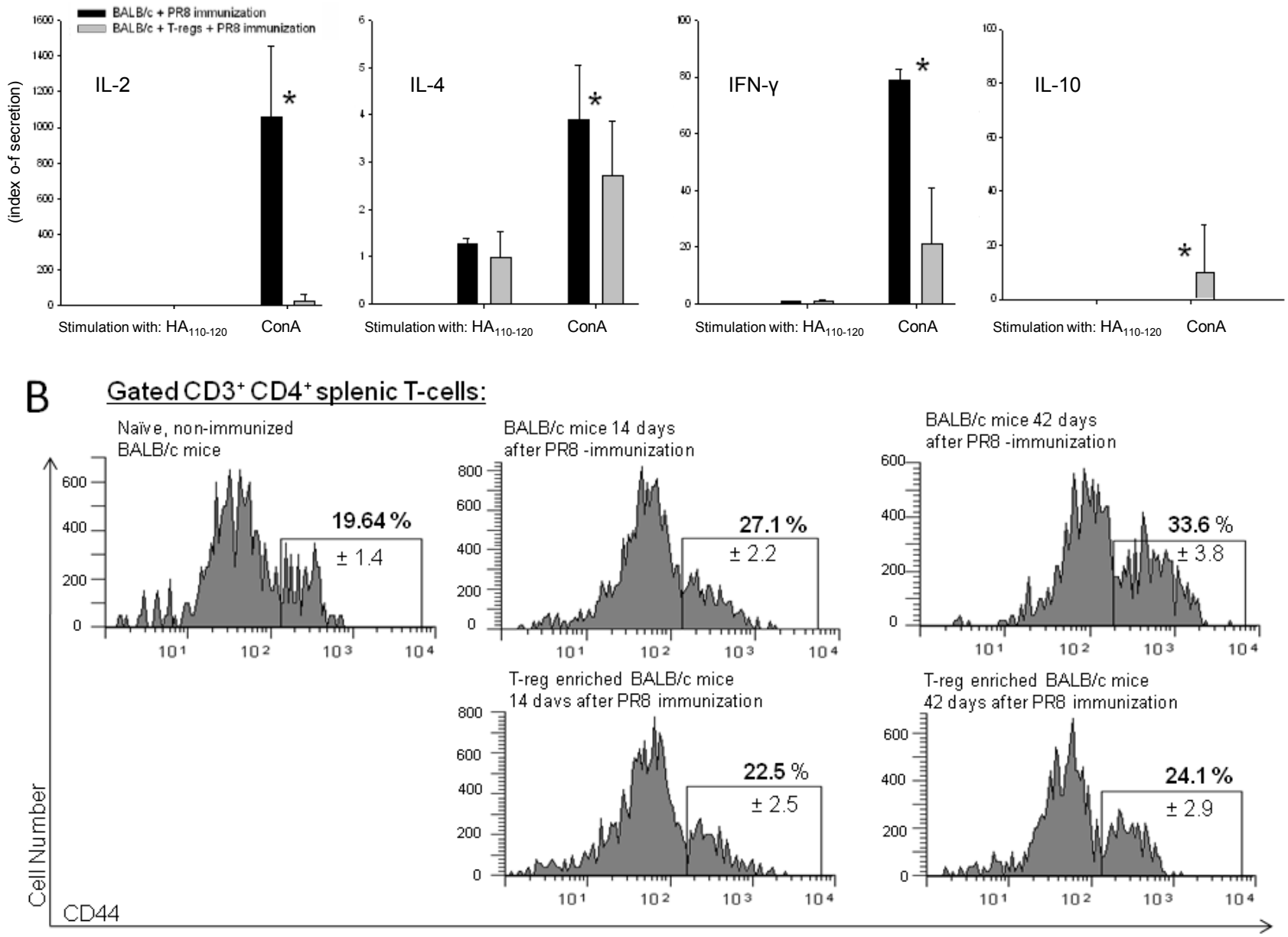
A
BALB/c + PR8 immunization
BALB/c + T-regs + PR8 immunization
(index o-f secretion)
IL-2
IL-4
IFN-γ
IL-10
Stimulation with: HA110-120
ConA
B
Gated CD3+ CD4+ splenic T-cells:
Naïve, non-immunized BALB/c mice
19.64 %
± 1.4
BALB/c mice 14 days after PR8 -immunization
27.1 %
± 2.2
BALB/c mice 42 days after PR8 -immunization
33.6 %
± 3.8
T-reg enriched BALB/c mice 14 davs after PR8 immunization
22.5 %
± 2.5
T-reg enriched BALB/c mice 42 days after PR8 immunization
24.1 %
± 2.9
Cell Number
CD44

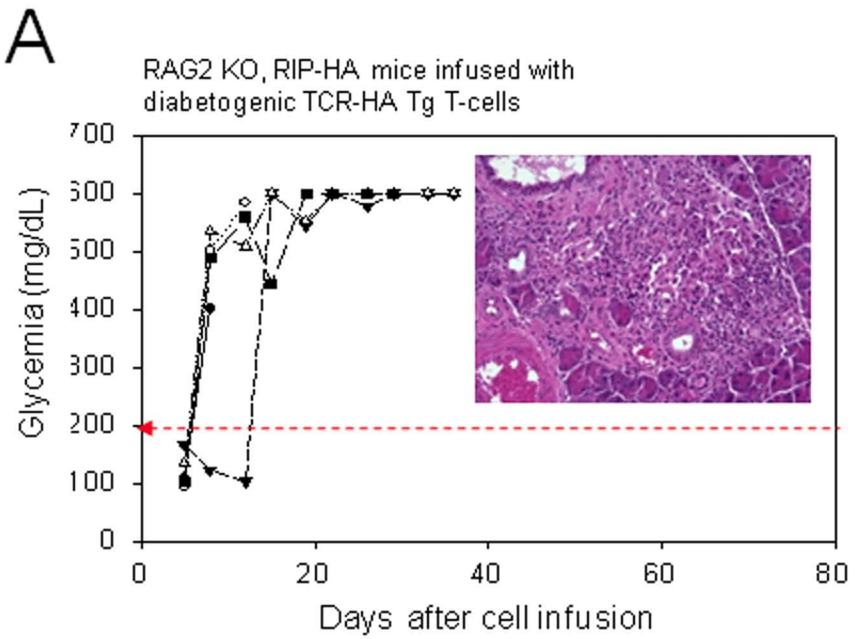
A
RAG2 KO, RIP-HA mice infused with
diabetogenic TCR-HA Tg T-cells
Glycemia (mg/dL)
0
100
200
300
400
500
600
700
0
20
40
60
80
Days after cell infusion

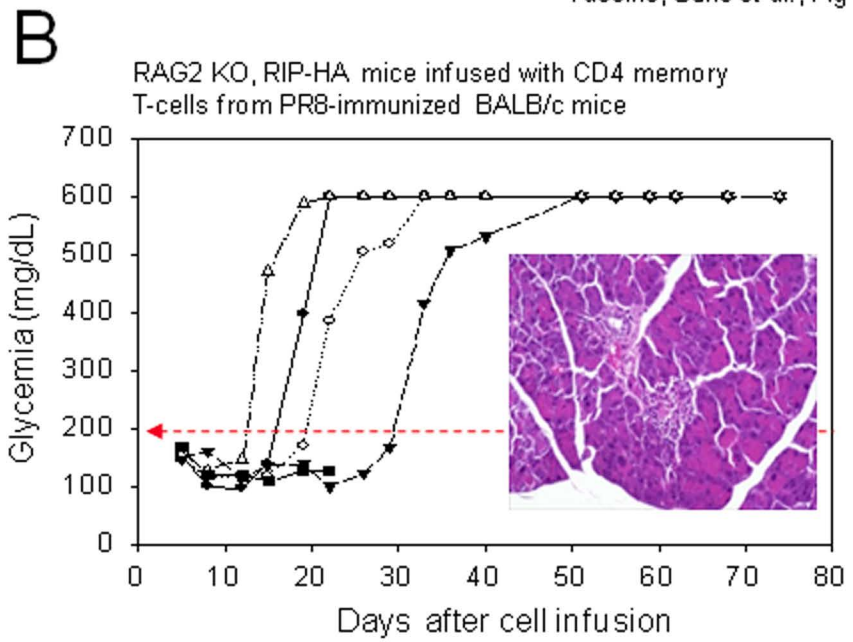
B
RAG2 KO, RIP-HA mice infused with CD4 memory
T-cells from PR8-immunized BALB/c mice
Glycemia (mg/dL)
0
100
200
300
400
500
600
700
0
10
20
30
40
50
60
70
80
Days after cell infusion

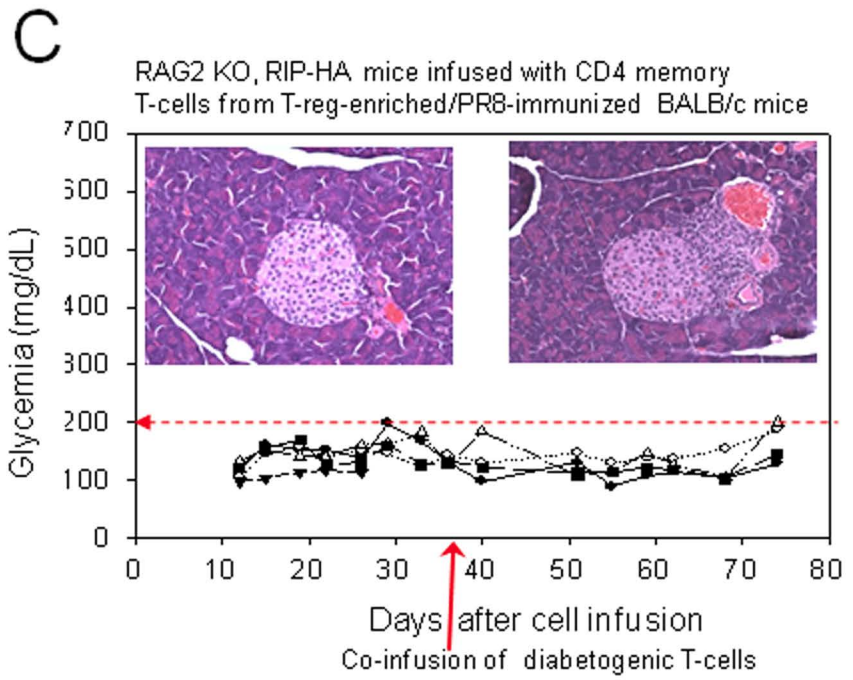
C
RAG2 KO, RIP-HA mice infused with CD4 memory
T-cells from T-reg-enriched/PR8-immunized BALB/c mice
Glycemia (mg/dL)
0
100
200
300
400
500
600
700
0
10
20
30
40
50
60
70
80
Days after cell infusion
Co-infusion of diabetogenic T-cells

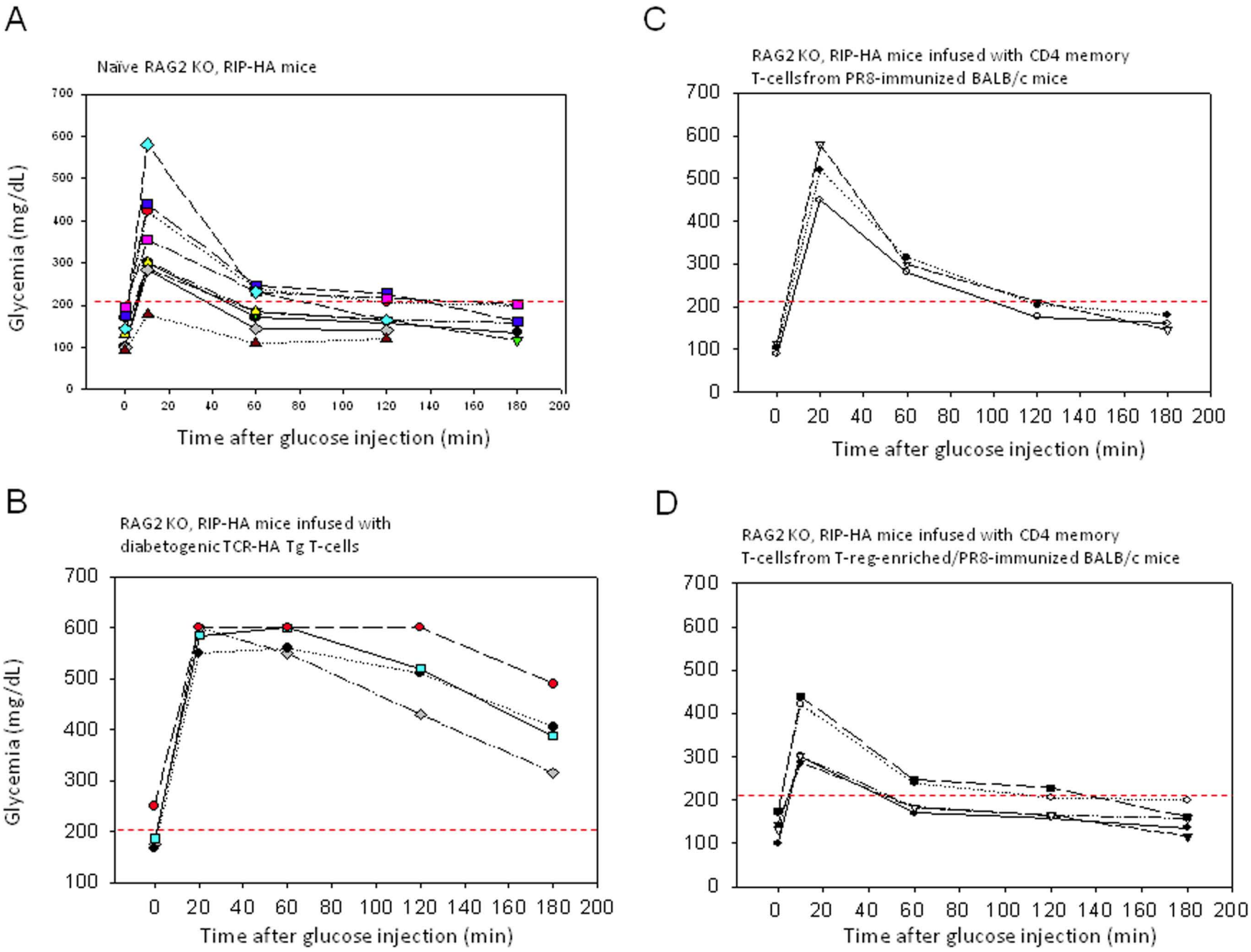
A
Naïve RAG2 KO, RIP-HA mice
Glycemia (mg/dL)
Time after glucose injection (min)
B
RAG2 KO, RIP-HA mice infused with
diabetogenic TCR-HA Tg T-cells
Glycemia (mg/dL)
Time after glucose injection (min)
C
RAG2 KO, RIP-HA mice infused with CD4 memory
T-cells from PR8-immunized BALB/c mice
Time after glucose injection (min)
D
RAG2 KO, RIP-HA mice infused with CD4 memory
T-cells from T-reg-enriched/PR8-immunized BALB/c mice
Time after glucose injection (min)

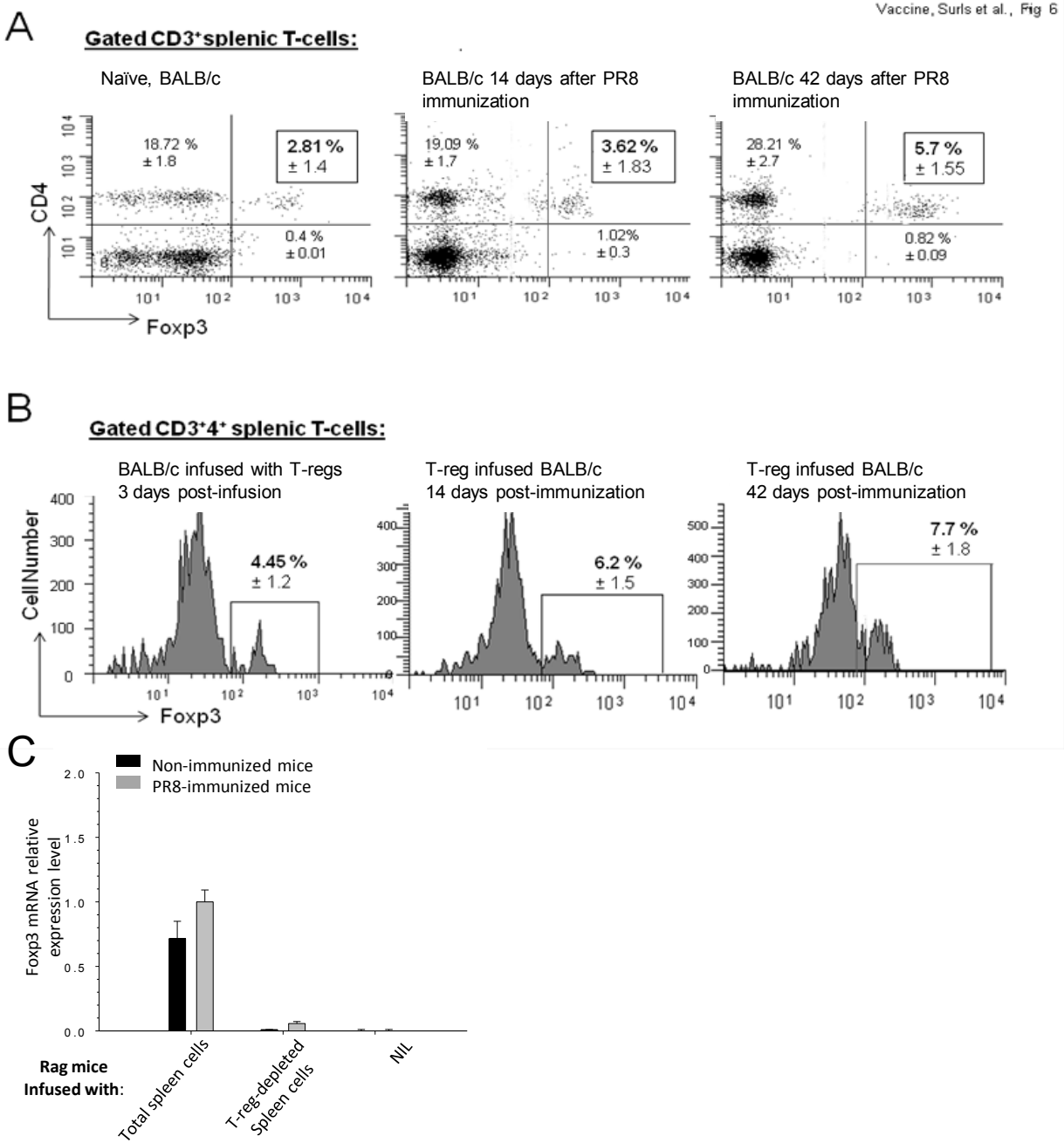
A
Gated CD3+splenic T-cells:
Naïve, BALB/c
BALB/c 14 days after PR8 immunization
BALB/c 42 days after PR8 immunization
18.72 % ± 1.8
2.81 % ± 1.4
0.4 % ± 0.01
19.09 % ± 1.7
3.62 % ± 1.83
1.02% ± 0.3
28.21 % ± 2.7
5.7 % ± 1.55
0.82 % ± 0.09
CD4
Foxp3
B
Gated CD3+4+ splenic T-cells:
BALB/c infused with T-regs 3 days post-infusion
T-reg infused BALB/c 14 days post-immunization
T-reg infused BALB/c 42 days post-immunization
4.45 % ± 1.2
6.2 % ± 1.5
7.7 % ± 1.8
Cell Number
Foxp3
C
Non-immunized mice
PR8-immunized mice
Foxp3 mRNA relative expression level
Rag mice Infused with:
Total spleen cells
T-reg-depleted Spleen cells
NIL

A.

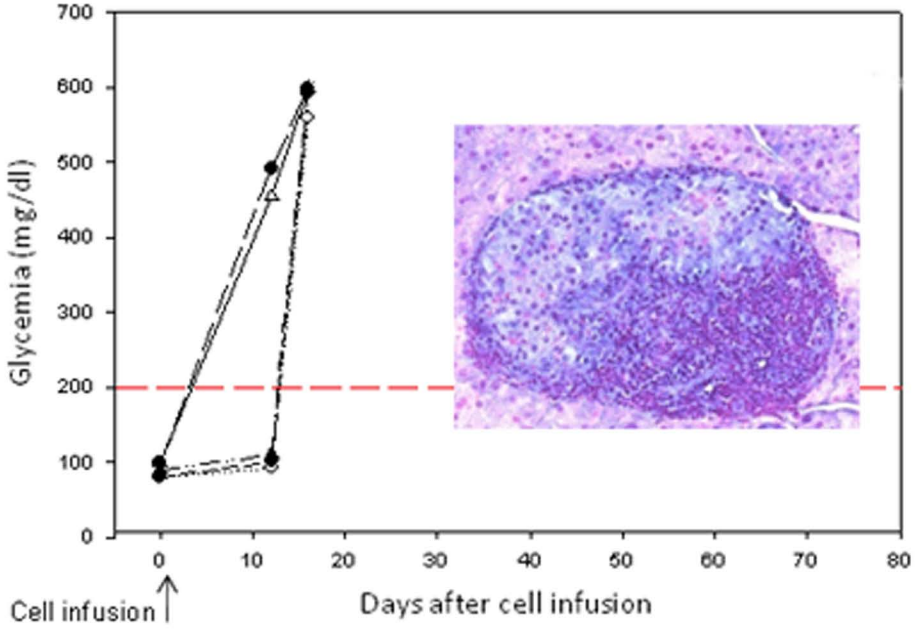
Glycemia (mg/dl)
700
600
500
400
300
200
100
0
0
10
20
30
40
50
60
70
80
Cell infusion
Days after cell infusion

B.

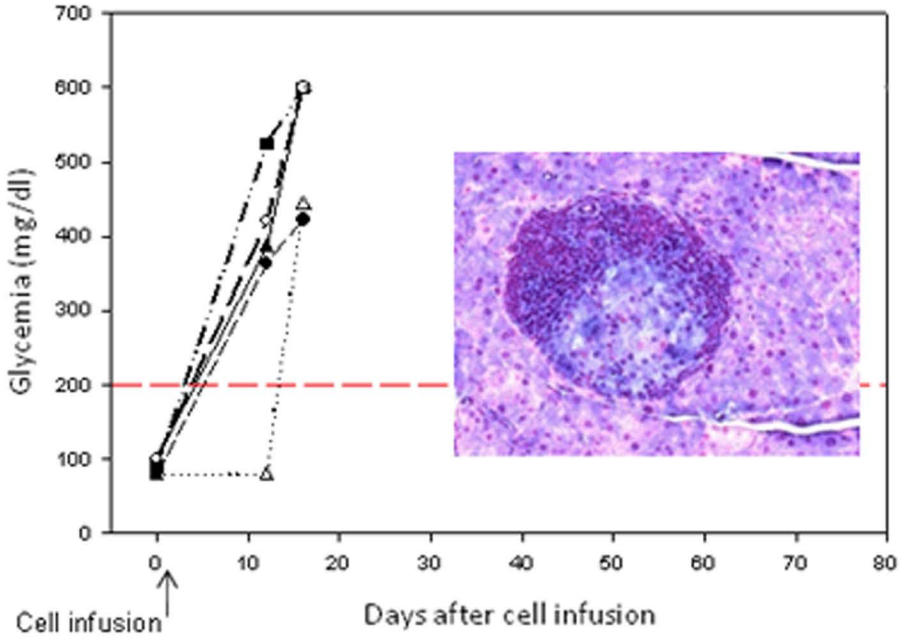
Glycemia (mg/dl)
700
600
500
400
300
200
100
0
0
10
20
30
40
50
60
70
80
Cell infusion
Days after cell infusion

Manuscript 2

Increased Membrane Cholesterol in Lymphocytes Diverts T-cells Toward an Inflammatory Response

Jacqueline Surls[1], Cristina Nazarov-Stoica[1], Margaret Kehl[1], Sofia Casares[1, 2], and Teodor-D. Brumeanu[1,*,£]

[1] Department of Medicine, Division of Immunology, Uniformed Services University of the Health Sciences, Bethesda, Maryland, 20814, U.S.A.

[2] Naval Medical Research Center, Infectious Diseases Directorate-Malaria Program, Silver Spring, Maryland 20910, U.S.A.

* Address correspondence to T-D. Brumeanu, Uniformed Services University of the Health Sciences, Department of Medicine, Division of Immunology, #A3074, Bethesda, MD 20814. Tel. +1 301 295 3608; FAX: +1 301 295 3557.

Email address: tbrumeanu@usuhs.edu

£ This work was supported by a grant from Uniformed Services University of Health Sciences (RO83ZK) to T-D.B.

ABSTRACT

Cell signaling for T-cell growth, differentiation, and apoptosis is initiated in the cholesterol-rich microdomains of the plasma membrane known as lipid rafts. Herein, we investigated whether enrichment of membrane cholesterol in lipid rafts effects antigen-specific CD4 T-helper cell functions. Enrichment of membrane cholesterol by 40-50% following squalene administration in mice was paralleled by an increased number of resting CD4 T helper cells in periphery. We also observed sensitization of the Th1 cell differentiation machinery that occurred through the redistribution of IL-2Rα, IL-4Rα, and IL-12Rβ2 subunits to lipid rafts, and increased STAT-4 and STAT-5 phosphorylation following membrane cholesterol enrichment. Antigen stimulation or CD3/CD28 polyclonal stimulation of membrane cholesterol-enriched, resting CD4 T-cells followed a path of Th1 differentiation, which was more vigorous in the presence of increased IL-12 secretion by APCs enriched in membrane cholesterol. Enrichment of membrane cholesterol in antigen-specific, autoimmune Th1 cells fostered their organ-specific reactivity, as confirmed in an autoimmune mouse model for diabetes. However, membrane cholesterol enrichment in $CD4^+$ $Foxp3^+$ T-reg cells did not alter their suppressogenic function. These findings revealed a differential regulatory effect of membrane cholesterol on the function of CD4 T-cell subsets. This first suggests that membrane cholesterol could be a new therapeutic target to modulate immune cell functions, and second that increased membrane cholesterol in various physiopathological conditions may bias the immune system toward an inflammatory Th1 type of response.

Introduction

Plasma membrane cholesterol plays a critical role in cell signaling by stabilizing protein receptors within close proximity to liquid-ordered phase microdomains called lipid rafts [1]. With few exceptions, most functional receptors are sequestrated within lipid rafts prior to ligand ligation and downstream signaling [2]. Lipid rafts can constitute up to 30-40% of the mammalian cell membrane [3-6]. Ligand-mediated clustering of neighboring receptor subunits into rafts leads to the assembly of fully functional receptors able to signal the T cell development, maturation, activation and differentiation [7-10]. These processes occur upon formation of T cell-APC immunological synapse and TCR-peptide-MHC complex interactions [11,12]. Clustering of rafts leading to T cell-APC immunological synapse formation may also occur in a non antigen-specific manner upon cross-linking of GM1 gangliosides by bacterial proteins such as cholera toxin B-subunit [13-15], or cross-linking of carbohydrate moieties of various protein receptors by galectins [16,17].

Un-esterified cholesterol is the major component of lipid rafts, and its content is homeostatically regulated by extracellular uptake from blood circulating LDL [18,19] and *de novo* intracellular synthesis [20]. Fine alterations in the amount of membrane cholesterol leads to re-organization of the lipid raft architecture, which in turn affects many T-cell functions such as a proliferation [21,22], blunting IL-2 production, or TCR signaling [23,24] by incomplete or defective coupling of CD3/TCR receptor with its signaling modules [25-27]. Alterations in the cholesterol-rich lipid rafts of T-cell membranes can be induced *in vitro* either by depletion of cholesterol using cyclodextrins, filipin, nystatin [28], or by cholesterol addition using hydroxypropyl-β-cyclodextrin [29].

Current therapeutic strategies aimed at immune regulation may also alter membrane cholesterol content, and thus inadvertently modify the architecture of protein receptors. Thus, glucocorticoids suppress the immune system and reduce inflammation in several disease settings, in part, by preventing compartmentalization of raft-associated proteins like LAT, LCK, FYN [30]. We and others show that certain therapeutic HMG-CoA reductase inhibitors like Lovastatin, a cholesterol lowering drug, can also lower the amount of T-cell membrane cholesterol and result in altered TCR signaling [31,32]. Though some pharmaceutical immune regulatory agents lower membrane cholesterol while aiming to down-regulate of T-cell function, little is known about the affect of membrane cholesterol enrichment on T-cell function.

Early studies using *in vivo* administration of radio-labeled squalene demonstrated its ability to integrate into the cholesterol biosynthetic pathway and generate cholesterol [33]. Squalene is a late precursor of intracellular cholesterol synthesis that is being used as an adjuvant to enhance the human immune responses upon vaccination [34], but its immunomodulatory mechanism(s) remain largely unknown. Reports indicate that squalene treatment, or as little as 1% of dietary squalene, can limit the development of preneoplastic lesions involved in colon carcinogenesis [35-37]. In humans, squalene is ubiquitously found in the blood at very low concentrations due to its rapid turnover [38], while in the skin and adipose tissue at higher concentrations [39].

Herein, we questioned whether enrichment of membrane cholesterol in rafts by squalene administration affects cell differentiation of antigen-specific CD4 T-helper cells and suppressogenicity of CD4 *Foxp3* T-regulatory (T-reg) cells in mice expressing antigen-specific CD4 T-cells and CD4 *Foxp3* T-reg cells. A single dose of squalene, well

below the liver toxicity level, was followed by a significant increase in membrane cholesterol by most lymphocyte subsets, particularly by the CD4 T helper and CD4 *Foxp3* T-regulatory (T-reg) cells. This increase in membrane cholesterol was paralleled by an increase in the number of resting CD4 T-cells in the spleen, and it favored Th1 differentiation of CD4 T-cells while having no effect on the suppressogenic function of CD4 *Foxp3* T-regulatory cells.

Material and Methods

Mice

To generate mice bearing antigen-specific CD4 T-cells and (GFP)-labeled $CD4^{+}$*Foxp3*$^{+}$ T-regulatory cells, the HA-specific TCR transgenic (TCR-HA Tg) mice expressing the 14.3d T-cell receptor that recognizes the $HA_{110\text{-}120}$-CD4 T-cell immunodominant epitope of the hemagglutinin protein (HA) from the A/PR/8/34 influenza virus [40] were crossed with BALB/c mice expressing GFP under the *Foxp3* promoter (Bar harbor, Maine, USA). The F1 hybrids (*Foxp3*-$GFP^{+/-}$, TCR-$HA^{+/-}$) were used as the source of antigen-(HA) specific CD4 T helper and *Foxp3*$^{+}$CD4 T-reg cells. Since the *Foxp3* gene is expressed on X chromosome, *Foxp3*-$GFP^{+/+}$ homozygous females were crossed with TCR-$HA^{+/+}$ homozygous Tg males to obtain 100% heterozygous F1 offspring for both the TCR-HA and *Foxp3*-GFP transgenes. The F1 hybrids were genotyped by PCR and analyzed by FACS for *Foxp3*, GFP, and TCR-HA expression in CD4 T-cells. Some 30-35% of $CD4^{+}$ T-cells and $CD4^{+}$*Foxp3*-GFP^{+} T-cells expressed TCR-HA in the spleen of F1 hybrids as measured by FACS using a TCR-$HA_{110\text{-}120}$ clonotypic mAb (#6.5 mAb). The RAG2 KO, RIP-HA Tg mice expressing the PR8 influenza HA viral protein in the pancreatic β-cell

islets under the rat insulin promoter [40] were used in adoptive cell transfer experiments as a read-out system for the HA-specific (diabetogenic) function of TCR-HA CD4 T-cells and for the regulatory function of CD4 *Foxp3* T-reg cells. Adoptively transferred TCR-HA Tg T-cells in RAG2 KO, RIP-HA Tg mice induces fulminate diabetes within two weeks post transfer [41], while the HA-specific CD4 *Foxp3* T-reg cells have a down-regulatory effect on diabetes onset [42,43]. All mice were housed in pathogen-free conditions at Uniformed Services University of Health Sciences/Laboratory Animal Medicine facility. Experiments and care/welfare were in agreement with the Federal and Local regulations under an approved Institutional Animal Care and Use Committee protocol at Uniformed Services University of Health Sciences.

Cell isolation

Single-cell suspensions of $CD4^+$ or $CD25^+$ Treg-depleted cells were prepared by negative sorting from the spleen of untreated or squalene treated mice. The $CD25^{hi}$ expression was found on more than 90% of TCR-$HA^{+/-}$, *Foxp3*-$GFP^{+/-}$ T-reg cells by FACS using triple staining with CD4, *Foxp3*, and CD25-dye conjugates (BD Biosciences, San Jose, CA, USA). Negative sorting of cells was preferred for lipid rafts studies, since positive sorting using specific ligands or antibodies cross-link plasma membrane receptors leading to clustering and re-organization of rafts, and thereby introducing errors in data interpretation. The $CD4^+$ splenocytes were negatively-sorted on mouse CD4 columns (R&D Systems, Minneapolis, MN, USA) according to the manufacturer's instructions. To obtain CD4 T-cells devoid of $CD4^+$ $CD25^+$ (TCR-$HA^{+/-}$, *Foxp3*-$GFP^{+/-}$ T-reg) cells, negatively-sorted CD4 splenocytes were incubated at room temperature for 30 min. with

CD25 Ab (5 μg/10^6 cells, mAb clone# 7D4, ATTC) followed by incubation with a PE-labeled anti-CD25 Ab and enrichment on anti-PE antibody-magnetic beads according to the manufacturer's instructions (Miltenyi Biotech, Auburn, CA, USA). The effluent (untouched) cell fraction was collected as the $CD4^+$T-reg-depleted cell population. The *Foxp3*-GFP T-reg cells from the spleen of *Foxp3*-$GFP^{+/-}$ TCR-$HA^{+/-}$ (F1) hybrids were also negatively-sorted by FACS based on GFP fluorescence. In some experiments, the HA-specific T-cells from both the TCR-HA Tg mice and *Foxp3*-$GFP^{+/-}$ TCR-$HA^{+/-}$ (F1) mice were FACS-sorted in cell preparations stained with the 6.5 mAb clonotypic mAb conjugated to an APC fluorochrome. The clonotypic 6.5 mAb is a rat IgG1 that recognizes the TCR-$HA_{110-120}$ on T-cells. It does not cross-link the TCR-HA or the rafts, nor trigger TCR signaling [44]. To isolate splenic APCs, single-cell suspensions of splenocytes were incubated on a plastic surface in RPMI for 2 h at 37° C, 5% CO_2. The adherent cells were detached by trypsinization, washed in PBS, and then rested in RPMI for 2 h before assayed.

In Vivo protocols

Squalene treatment: *Foxp3*-$GFP^{+/-}$, TCR-$HA^{+/-}$ double transgenic (dTg) mice (F1 hybrids) were injected intraperitoneally (i.p.) with one or four doses of 180 μg squalene (Sigma, Atlanta, GA, USA) emulsified 3:1 in saline. At various time-points after the last injection, the blood, liver and spleen were collected for histology, *in vitro* bioassays, serum lipid electrophoresis, FACS analysis, and adoptive cell transfer experiments. Several splenic lymphocyte subsets were analyzed for the amount of membrane cholesterol by FACS at various time-points after the last injection.

Adoptive cell transfer: $2x10^5$ or 10^4 negatively-sorted CD25-depleted $CD4^+$ splenic cells (diabetogenic T-cells), or representing or CD4 *Foxp3*-$GFP^{+/-}$ T-cells (T-reg cells) from *Foxp3*-$GFP^{+/-}$ TCR-$HA^{+/-}$ (F1) mice were transferred or co-transferred i.p. into RAG2 KO RIP-HA Tg mice. The onset of autoimmune diabetes in RAG2 KO RIP-HA Tg recipients was monitored based on blood glucose values using Accu-Check glucose meter and glucose test strips (Roche, Indianapolis, IN, USA). Mice were considered diabetic after two consecutive readings of glycemia above 200 mg/dL.

Western blot analyses

Single-cell suspension of splenocytes or negatively-sorted $CD4^+$ splenocytes ($8.5x10^7$) from untreated or squalene treated (180 μg/mouse) F1 mice were prepared 3 days post-squalene injection. Cells were washed with PBS and lysed for 30 min on ice in a buffer containing 0.1% SDS, 0.5% NP-40, 10mM Tris, 150 mM NaCl, 1 mM Na_3VO_4, 16 mM EDTA, and a cocktail of protease inhibitors (pH 7, Roche, Indianapolis, IN, USA). Protein cell extracts were analyzed by SDS-PAGE and Western blot under denaturing/reducing conditions (1% SDS/0.5% 2-ME) using 8-25 gradient Phastgels (GE Life Sciences, Piscataway, NJ, USA) or 10-20% Tris-HCl Ready gels (BioRad, Hercules, CA, USA). Gels were either silver-stained or electrotransferred onto PVDF membranes (Millipore, Billerica, MA, USA). Transferred membranes were blocked with 5% BSA in PBS and probed with anti-mouse phosphotyrosine-HRP conjugate (mouse IgG1 Ab clone# Clone 179003, R&D). Aliquots of protein cell extracts were precipitated either with anti-mouse CD3, CD28, IL-4Rα, IL-2Rα, or IL-12Rβ2 Abs for 2 h at room temperature, the immunoprecipitates were isolated by incubation with agarose-protein

A/G beads (Pierce, Rockford, IL, USA) for 2 h at room temperature, and the beads were washed twice in PBS, and then boiled for 5 min in SDS-2ME sample buffer followed by a 5 min centrifugation at 5,000 rpm to remove the agarose beads. Supernatants were then electrophoresed, and electrotransferred onto PVDF membranes (Millipore, Auburn, CA, USA) blocked with 5% BSA in PBS and probed with Abs specific for phosphorylated ZAP-70, PI3K, STAT-6, STAT-4, or STAT-5 (Abcam, Cambridge, MA, USA). PVDF membranes were washed, and bound anti-phospho Abs were detected by isotype specific secondary anti-IgG-HRP Ab-conjugates (Cell Signaling). The HRP signal was visualized in a Kodak Imaging Analyzer by chemiluminescence using a Pierce ECL western blotting substrate (Pierce, Rockford, IL, USA) according to the manufacturer's instructions.

T cell bioassays

Single-cell suspensions of splenocytes (10^6 cells) from individual mice were incubated in round bottom 96-well plates with RPMI complete media containing $HA_{110-120}$ synthetic peptide (40 μg/mL) at 5% CO_2 and 37°C. Cytokine secretion in the cell culture supernatants was measured by Luminex, i.e., 24 h of stimulation for IL-2 secretion and 36 h of stimulation to measure IL-4 and IFN-γ secretion. For the APC-CD4 T-cell co-culturing experiments, the CD4 T cells (10^6) and APCs ($5x10^5$) from untreated or squalene treated mice were pulsed or not with $HA_{110-120}$ synthetic peptide (40 μg/mL). For the T-cell suppression experiments, T-regs were co-cultured in 96-well plates with HA-specific CD4 T-cells at 1:1 ratio ($2x10^6$ total cell number/well) in the presence of $HA_{110-120}$ peptide (40 μg/mL) for 48 h at 5% CO_2 and 37°C, and the IL-4 and IFN-γ secretion in cell culture supernatants was measured by Luminex. Cytokines concentration

was measured in Multiplex mouse cytokines kits using a Luminex instrument (Luminex Corporation, Austin, TX, USA) and a 5 parameter logistics model equation (MasterplexQT software, Miraibio, San Francisco, CA, USA) according to the manufacturer's instructions.

Histology

The liver or spleen from untreated or squalene treated mice was frozen in Tissue-Tek O.C.T. compound (VWR, Batavia, IL, USA). Frozen liver sections were mounted on glass slides, permeabilized with digitonin, and stained for cholesterol with hematoxylin-eosin and Sudan IV (Histoserv, Germantown, MD, USA). Images were captured using the Eclipse Nikon microscope and NIS-Elements AR Nikon software (Nikon, Melville, NY). To identify cytosolic cholesterol accumulation and lipoidic microdroplets, frozen spleen sections were mounted on glass slides and stained with Oil-red O staining (ORO) and hematoxylin-eosin. Briefly, mounted spleen sections were stained in 36% Oil red O/Triethyl phosphate working solution for 10 min (Sigma-Aldrich, Atlanta, GA, USA), washed in tap water, and then counterstained with Harris' hematoxylin (Sigma-Aldrich, Atlanta, GA, USA). Slides were mounted with VectaShield Hard Set Mounting medium containing DAPI (Vector Laboratories, Burlingame, CA, USA) and analyzed by phase contrast microscopy using a Zeiss instrument (Thornwood, NY, USA).

Phase Contrast and Confocal laser scanning microscopy (CLSM)

Negatively-sorted CD4 T-cells (10^6 cells) from the spleen of individual mice previously treated or not with squalene were co-stained with 1.5 µl CTB-FITC conjugate (Sigma)

and anti-CD4 Ab-PE conjugate (BD Biosciences) for 30 min at 4°C, on ice. CTB is a specific ligand for the GM1 glycosphingolipid resident moieties of the lipid rafts [45]. To visualize the IL-2Rα, IL-4Rα, or IL-12Rα subunits in the lipid rafts of negatively-sorted CD4 T-cells (10^6 cells), single cell suspensions (10^6 cells) were co-stained with specific anti-receptor Ab-PE conjugates (BD Biosciences) and CTB-FITC conjugate. Stained cells were washed twice in PBS/BSA 1% and mounted onto glass slides using Vectashield containing DAPI stain (Vector Laboratories Inc., Birmingham, CA) to identify cell nuclei. Distribution of GM1 resident moiety in the cholesterol-rich rafts of plasma membrane was captured as 2D images, and the GM1 content was measured based on CTB-FITC cell intensity using a ZEISS 710 Confocal Laser Scanning Microscope equipped with ZEISS ZEN 2009 analysis software (Thornwood, NY, USA). To analyze receptor distribution in the lipid rafts, resting CD4 T-cells from the squalene treated or untreated mice were triple stained with DAPI, GM1-CTB, and either anti IL-2Rα-APC, anti-IL-4Rα–PE, or anti-IL-12Rβ2–PE conjugates (BD Biosciences).

Flow Cytometry

Single-cell suspension of splenocytes (10^6 cells) from untreated or squalene treated mice were stained for 30 min at 4°C for surface markers or intracellular cytokine synthesis using specific antibody-dye conjugates (BD Biosciences) or their isotype controls. In some experiments, cells were co-stained with Filipin III (Sigma) to measure the amount of cholesterol in the plasma membrane. Mean fluorescence intensity (MFI) of Filipin III or Ab-dye conjugates was measured by FACS at the single-cell level in 10^4-10^5 cell events acquired with a LSR II Becton-Dickinson instrument equipped with the WINLIST

analysis software (Verity, Topsham, ME, USA). FACS measurements of membrane cholesterol was estimated by the MFI values of Filipin III as described [46]. Filipin III binds specifically to un-esterified cholesterol present in the plasma membrane of lipid rafts [47]. Spectrophotometric measurements between $\lambda_{excitation} = 340$ and 380 nm and $\lambda_{emission}$=385-470 nm ruled out the possibility that Filipin III may stain squalene possibly attached or incorporated into the plasma membrane.

Real-Time RT-PCR

Total RNA and cDNA from splenocytes was extracted using Pure-Link Micro and Midi RNA Purification Systems (Invitrogen, Carlsbad, CA, USA) and High Capacity cDNA Archive kit (Applied Biosystems, Foster City, CA, USA), respectively. The primers for murine HMG-CoA reductase were forward-5'GAATGCCTTGTGATTGGAGTTG3', and reverse- 5'GCCGAA GCAGCACATGATCT3'; specific primers for Squalene epoxidase, T-bet, GATA-3, IL-2Rα, IL-12Rβ_2, and IL–4Rα were purchased from Applied Biosystems. Measurement of gene products expression was carried in an ABI Prism 7700 equipped with SDS 1.9.1 analysis software (Applied Biosystems), as previously described [48]. The relative mRNA levels were estimated in reference to the 18S rRNA (Applied Biosystems).

Serum lipid electrophoresis

Fresh mouse serum from untreated or squalene treated mice was assessed for the fractions of high density lipoproteins (HDL), low density lipoproteins (LDL), and very low density lipoproteins (VLDL) using the QuickGel Cholesterol kit and an

electrophoretic system from Helena Laboratories (Beaumont, TX, USA) according to the manufacturer's protocol. The lipoprotein fractions were quantified based on the number and intensity of pixels per each electrophoretic band using the SCION Image analysis software (Scion Corp. Frederick, MD, USA).

Statistics

Significance of results between untreated and squalene treated groups for the MFI values measured by FACS, cytokines concentration in Luminex, RNA expression level in RT-PCR, and blood glucose values, was determined by the unpaired Student's *t*-test for which *P* values <0.05 were considered significant. For each cytokine measured by Luminex, means were compared across groups using one-way analysis of variance (ANOVA) followed by Tukey's post-hoc pairwise comparisons. *P* values <0.05 were considered statistically significant.

Results

Squalene treatment up-regulates membrane cholesterol in various lymphocyte subsets

Squalene is a late cholesterol precursor that can be efficiently taken up by hepatocytes and converted into cholesterol when administered intravenously [33]. Herein, we measured the content and distribution of membrane cholesterol in various splenic lymphocyte subsets following i.p. injection of squalene (emulsified 3:1 in saline) in F1 hybrid mice (TCR-HA$^{+/-}$, *Foxp3*-GFP$^{+/-}$ mice).

F1 mice were treated i.p. with 0, 1, or 4 doses of squalene (180 μg/dose). Seven days after the last injection, negatively-sorted, resting CD4 splenic T-cells from each group

were stained with Filipin III and analyzed for the amount of membrane cholesterol by FACS. The kinetics of membrane cholesterol accumulation in resting CD4 T-cells from F1 mice given a single dose of squalene (180μg/mouse) indicated that the peak cholesterol load occurs after 7 days, with a gradual decrease within the following two weeks till reaching physiological levels (data not shown). Four injections of squalene (180μg/dose/mouse) administered within a week interval significantly increased the amount of membrane cholesterol in CD4 T-cells (45% MFI increase) as compared with those from untreated (control) mice. However, no significant difference was observed between mice given one or four doses of squalene (40% *vs*. 45% MFI increase) (**Figure 1A**). This may be explained by the saturation limit of either the cellular uptake of squalene or the intracellular trafficking of cholesterol from the cytosol to the plasma membrane in CD4 T-cells. A slight homogenous accumulation of cholesterol in the spleen was visualized by phase contrast microscopy in oil-red-o stained cross-sections from F1 mice treated with 4 doses but not a single dose of squalene (**Figure 1B**). Membrane cholesterol accumulation in resting CD4 T-cells upon squalene administration appeared to be an active process regulated by genes involved in cholesterol synthesis, since an increase in the mRNA expression levels of *HMG-CoA reductase* and *Squalene epoxidase* by 30% and 15% respectively, was detected 3 days after a single dose of squalene (**Figure 1C**).

We have previously showed that accumulation of membrane cholesterol in resting CD4 T-cells is a developmental feature and that the content of membrane cholesterol is stable between 2 and 4 months of age in mice [49]. To avoid physiological alterations in

T-cell membrane cholesterol content, all experiments were carried out in 3 month-old F1 mice when the amount of membrane cholesterol is most stable.

Seven days after a single dose of squalene (180 μg/mouse), single-cell level flow cytometry analysis revealed that the amount of membrane cholesterol in CD4 *Foxp3* splenic T regulatory cells was also increased by 40 to 50% (**Figure 1D**). Resting B-cells, and dendritic cells from the spleen of F1 mice given a single dose of squalene (180 μg/mouse) also showed an increase (5-10%) in membrane cholesterol, albeit less dramatic when compared to CD4 and CD8 T-cells (**Figure S1**).

A single-dose of squalene administration (180 μg/mouse) was consistently associated with altered CD4 T-cell frequencies within the pool of resting splenocytes, as analyzed by flow cytometry 7 days post-injection. Thus, the number of resting CD4 T-cells was increased by 20-22%, whereas the number of CD4 *Foxp3* T-cells, CD8 T-cells, $CD19^+$ B-cells, and $CD11c^+$ dendritic cells remained relatively unchanged (**Figures 1 and S1**). Furthermore, CLSM analysis of the resident lipid raft marker GM1 in negatively-sorted, resting CD4 splenic cells from F1 mice injected with a single dose of squalene (180 μg/mouse) showed that membrane cholesterol enrichment was associated not only with a higher GM1 expression, but also with a more homogeneous distribution as compared with lower GM1 expression and more heterogeneous distribution in resting CD4 splenic cells from untreated mice (**Figure 2**).

To determine the extent to which *in vivo* squalene administration may affect cholesterol metabolism in the liver, the electrophoretic profile of serum cholesterol fractions and rate of cholesterol accumulation in liver were analyzed. F1 mice given a single dose of squalene (180 μg/mouse) showed no significant alterations in the ratio of

serum cholesterol fractions or cholesterol accumulation in the liver 7 days post-injection (data not shown). However, four doses of squalene (180 μg/dose/mouse) administered once a week led to an increase in the high density lipid fraction (HDL) in serum 7 days after the last injection (**Figure S2-A**), and a modest accumulation of cholesterol in liver tissue (**Figure S2-B**). Of note, all biofunctional assays in this study were carried out in 3 month-old F1 mice injected with a single i.p. dose of squalene (180 μg/mouse), for which no alterations in serum cholesterol fractions or liver cholesterol accumulation were detected. Early studies showed that LDL serum cholesterol increases upon inhibition of hepatic squalene synthesis by zaragozic acid [50].

In summary, these results indicate that exogenous squalene can be efficiently taken up by various subsets of resting peripheral lymphocytes and is constantly associated with an increase in membrane cholesterol, particularly in resting CD4 T-cells. Squalene administration was also followed by an increased frequency of resting CD4 T-cells (~20% increase), but had no significant effect on the frequency of CD4 *Foxp3* T-reg cells, CD8 T-cells, B-cells, and dendritic cells in the spleen.

Cholesterol enrichment in CD4 T-cell membrane sensitizes the Th1 signaling modules in the absence of T-cell stimulation

Cholesterol-rich plasma membrane microdomains (lipid rafts) play a critical role in early intracellular signaling towards many cell functions. These signaling events can be detected by phosphorylation of various protein receptors and their adaptor molecules, as well as by the recruitment of various kinases to their intracellular domains. Herein, we questioned whether enrichment of membrane cholesterol in resting CD4 splenic T-cells

may alter the baseline of tyrosine phosphorylation in several signal transduction molecules critical for cell differentiation. First, the protein patterns from total lysates of negatively-sorted, resting CD4 splenic T-cells from untreated or squalene treated (180 μg/mouse) F1 mice showed no detectable quantitative alterations 3 days post-injection, as the number and intensity of SDS-PAGE protein bands were similar in both groups of mice (**Figure 3A**). However, a modest increase in the 55 to 100 kDa tyrosine phosphorylated proteins was detected in the T-cell lysates from squalene treated mice (**Figure 3B**).

Analysis of several protein kinases and transducer molecules required for downstream signaling of T-cell differentiation, i.e., IL-12R, IL-4R and their signaling molecules, revealed a differential modulatory effect of membrane cholesterol in resting CD4 T-cells in the absence of antigen stimulation (**Figure 3C**). During T-cell differentiation, binding of IL-12 to IL-12Rβ2 leads to STAT-4 phosphorylation in Th1 cells [51], whereas binding of IL-4 to IL-4R leads to STAT-6 phosphorylation in Th2 cells [52]. Data depicted in **figure 3C** showed that resting CD4 splenic T-cells enriched in membrane cholesterol had an increased baseline of STAT-4 phosphorylation and a decreased baseline of STAT-6 phosphorylation. A number of additional signaling events supporting the T-cell growth and survival also occur during Th1 cell differentiation. Thus, binding of IL-2 to IL-2R promotes recruitment and phosphorylation of JAK kinases on the IL-2Rβ chain, which in turn mediates the assembly of a fully functional IL-2Rαβγ followed by STAT-5 phosphorylation, heterodimerization, and translocation to the nucleus where it binds to restriction elements in the gene promoter of several genes. [53,54]. The basal level of phosphorylated STAT-5 was increased in resting CD4 T-cells upon enrichment

of membrane cholesterol (**Figure 3C**). Furthermore, during Th1 differentiation the CD3 chains are assembled together with the T cell receptor (TCR) α and β chains in the cell membrane to form a fully functional CD3/TCR complex. The ζ–chain of CD3/TCR complex expresses phosphorylated ITAM motifs that are crucial for recruitment and docking of phosphorylated ZAP-70 [55]. Membrane cholesterol enrichment in resting CD4 splenic T-cells led to an increased base level of phosphorylated ZAP-70 kinase (**Figure 3C**). In addition to CD3/TCR and cytokine receptor signaling, CD28 co-stimulation through ligation by B7 molecules expressed by APCs provides sustained CD3/TCR signaling and promotes Th1 cell survival [55,56]. An early event of CD28 ligation is the recruitment and phosphorylation of PI3K on its intra-cytoplasmic tail. Our data consistently showed that enrichment of membrane cholesterol in resting CD4 splenic T-cells had little if any effect on the phosphorylation and recruitment of PI3K to the CD28 intra-cytoplasmic tail (**Figure 3C**).

Further analysis of resting CD4 splenic T-cells from untreated and squalene treated F1 mice was carried out by CLSM to visualize the membrane distribution of IL-12Rβ2 and IL-4Rα subunits that recruit STAT-4 in Th1 differentiating cells and respectively STAT-6 in Th2 differentiating cells. CLSM analysis of IL-2Rα revealed a differential re-organization of this receptor subunit within lipid rafts, as well as IL-4Rα and IL-12Rβ2, 7 days after squalene treatment. In differentiating CD4 T-cells, the autocrine IL-2 secretion and IL-2R up-regulation on cell surface play a critical role for the cell growth and proliferation. The first observation was that these receptor subunits were easily detected in the rafts upon squalene treatment (**Figure 4**). Secondly, the IL-2Rα and IL-4Rα subunits were visualized as capping rafts microdomains, whereas the IL-12Rβ2 subunit

was more dispersed in the rafts (**Figure 4,** *enlargements*). Third, squalene treatment was paralleled by increased mRNA expression level, particularly for IL-4Rα and IL-12Rβ2 subunits in resting CD4 T-cells (**Figure 5A**). Fourth, the level of cell surface expression of either receptor was not significantly increased by squalene treatment as determined by the MFI values in single-cell level FACS analysis (**Figure 5B**). Conceivably, a differential receptor re-distribution in the rafts detectable by CLSM implies that the unique structure of each receptor and the amount of cholesterol in the microdomains could both play important roles. The mechanism by which spatiotemporal re-organization of IL-2R, IL-4R, and IL-12R in the rafts microdomains of resting CD4 T-cells upon membrane cholesterol enrichment remains to be further investigated.

Together, these data indicate that enrichment of membrane cholesterol in resting CD4 T-cells by 40 to 50% can sensitize the Th1 signaling machinery by means of rafts re-distribution of cytokine receptors and increased phosphorylation of signaling modules critical for Th1 cell differentiation.

Cholesterol enrichment in the CD4 T-cell membrane fosters type 1 cell differentiation in the presence of T-cell stimulation

Since enrichment of membrane cholesterol in resting CD4 T-cells increased the phosphorylation of signaling modules involved in Th1 differentiation in the absence of T-cell stimulation, we next investigated whether enrichment of membrane cholesterol in CD4 T-cells and/or antigen presenting cells (APCs) under stimulation may affect the outcome of T-cell differentiation. For this, the cytokine secretion profiles from various combinations of negatively-sorted CD4 T-cells and APCs isolated from untreated or

squalene treated (180 μg) F1 mice ($HA_{110-120}$-specific TCR) were analyzed in the presence of antigen-specific ($HA_{110-120}$) stimulation or non antigen-specific CD3/CD28 polyclonal stimulation.

Co-cultures of membrane cholesterol-enriched, resting CD4 T-cells and $HA_{110-120}$ pulsed APCs enriched in membrane cholesterol showed the highest secretion of IL-2 and IFN-γ and the lowest IL-4 secretion (**Figure 6A**). The amount of IL-2 and IFN-γ secreted by resting CD4 T-cells stimulated with $HA_{110-120}$-pulsed APCs was 30-35% lower when T-cells were not enriched in membrane cholesterol, indicating that membrane cholesterol enrichment in both CD4 T-cells and APCs provides the strongest Th1 polarization. Thus, while the HA-specific CD4 T-cells stimulated with $HA_{110-120}$ peptide usually developed a Th1/Th2 mixed response, those from squalene treated mice developed a predominant Th1 response. Because membrane cholesterol enrichment in APCs augmented IFN-γ secretion by antigen-specific CD4 T-cells, and IL-12 secretion by APCs is known to up-regulate IFN-γ secretion by CD4 T-cells, we next compared the steady-state of IL-12 secretion by unstimulated APCs from untreated and squalene treated F1 mice. The baseline of IL-12 secretion was near the limit of detection in APCs cultured from untreated (control) mice, while being significantly higher in APCs cultured from squalene treated mice (**Figure S3**). This may well explain why IFN-γ secretion by CD4 T-cells was significantly augmented in the presence of HA-pulsed APCs enriched in membrane cholesterol. The base level of IL-6 secretion, but not IL-1α secretion by APCs was also slightly increased upon membrane cholesterol enrichment (**Figure S3**), which indicated a differential effect of membrane cholesterol not only on CD4 T-cell function, but also on APC function.

Furthermore, total spleen cells harvested 7 days after squalene injection were stimulated in culture with CD3/CD28 Abs. These cultures showed a larger number of proliferating CD4 splenic T-cells positive for intracellular IFN-γ than for IL-4 detected by FACS (**Figure 6B**). This corresponded with a significant 8 fold-increase in T-bet mRNA expression and only a 2 fold-increase in GATA-3 mRNA expression measured by real-time RT-PCR (**Figure S4**).

Together, the results demonstrate that stimulation of CD4 T-cells leads preferentially to a Th1 response when plasma membrane cholesterol is enriched by 40-50%. The Th1 response was more vigorous when APCs were also enriched in membrane cholesterol, as they secreted higher amounts of IL-12, a major cytokine driving Th1 cell differentiation.

Enrichment of membrane cholesterol fosters the reactivity of autoimmune Th1 cells

To determine whether membrane cholesterol enrichment by *in vivo* squalene administration alters the reactivity of antigen-specific ($HA_{110-120}$) Th1 cells *in vivo*, we took advantage of a RAG2 KO, RIP-HA Tg mouse model in which autoimmune diabetes (type 1 diabetes, T1D) is induced by i.p. infusion of splenic CD4 T-cells ($2.5x10^5$ cells) from TCR-HA Tg mice. In this model of inducible T1D, hyperglycemia is detected within 7 to 10 days after transfer of diabetogenic, $HA_{110-120}$-specific Th1 cells [57].

Using this T1D mouse model, we first tested our F1 hybrid mouse for the expression level and diabetogenicity of TCR-$HA^{+/-}$ $CD4^+$ (*Foxp3*$^{-/-}$) T-cells in the spleen. Similar to the parental TCR-$HA^{+/+}$ homozygous Tg mice, the spleen of F1 hybrid mice expressed ~40% of TCR-$HA^{+/-}$ $CD4^+$ (*Foxp3*$^{-/-}$) T-cells according to FACS measurements using a TCR-HA clonotypic antibody (# 6.5 mAb). The spleen of F1 hybrid mice also contained

a similar number of $CD4^+$ *Foxp3*-$GFP^{+/-}$ T-reg cells as the parental *Foxp3*-$GFP^{+/+}$ homozygous Tg mice (1-3%). The diabetogenic potential of TCR-$HA^{+/-}$ Tg CD4 splenic T-cells from F1 hybrid mice (TCR-$HA^{+/-}$, *Foxp3*-$GFP^{+/-}$ dTg mouse) was tested by transferring i.p. $2.5x10^5$ negatively-sorted $CD4^+$ (*Foxp3*-$GFP)^{-/-}$ splenic T-cells into RAG2 KO, RIP-HA Tg mice. The RAG2 KO, RIP-HA Tg recipients developed hyperglycemia by 8-10 days after cell transfer, whereas those receiving either $CD4^+$ (*Foxp3*-$GFP)^{+/-}$ T-reg cells from the same F1 donors or CD4 splenic T-reg cells from *Foxp3*-$GFP^{+/+}$ Tg parental mice did not (**Figure 7A**). This clearly demonstrated that only the $CD4^+$TCR-$HA^{+/-}$ (*Foxp3*-$GFP^{-/-}$) splenic T-cells, but not the $CD4^+$ TCR-$HA^{+/-}$ *Foxp3*-$GFP^{+/-}$ or $CD4^+$*Foxp3*-$GFP^{+/+}$ splenic T-reg cells have diabetogenic potential.

To determine whether enrichment of membrane cholesterol in $CD4^+$TCR-$HA^{+/-}$ (*Foxp3*-$GFP^{-/-}$) may affect their diabetogenic potential, splenocytes from untreated and squalene treated F1mice (180 μg squalene/mouse) were isolated 7 days post-injection and depleted of $CD4^+$*Foxp3*-$GFP^{+/-}$ T-regs, followed by negative-sorting of diabetogenic $CD4^+$TCR-$HA^{+/-}$ T-cells. Purified diabetogenic $CD4^+$(*Foxp3*-depleted) TCR-$HA^{+/-}$ T-cells ($1x10^4$ cells/mouse) from squalene treated or untreated F1 mice were then transferred into RAG2 KO, RIP-HA Tg mice, and glycemia (read out for T1D onset) was monitored bi-weekly. Data depicted in **figure 7B** show that the cumulative incidence of hyperglycemia in RAG2 KO, RIP-HA Tg recipients of diabetogenic $CD4^+$(*Foxp3*-depleted), TCR-$HA^{+/-}$ T-cells from untreated F1 mice was 50%, whereas in those receiving the same type of cells from squalene treated F1 mice was increased to almost 80%. These results indicated that the enrichment of membrane cholesterol in *self*-reactive (diabetogenic) Th1 cells fostered their diabetogenic potential.

Cholesterol enrichment in CD4 Foxp3 T-reg cell membrane does not affect their suppressogenic function

Naturally-born CD4 T-cells expressing the master regulatory gene *Foxp3* are the archetype of T-regulatory (T-reg cells). T-reg cells maintain T-cell and B-cell homeostasis and can also restrict immune responses to various *self* and foreign antigens [58]. We have shown above that a single dose of squalene (180 μg/mouse) resulted in a 40 to 50% increase of membrane cholesterol in CD4 *Foxp3* T-reg cells (**Figure 1D**). We next investigated whether their function was altered by membrane cholesterol enrichment. For this, resting CD4 T-cells expressing the $HA_{110-120}$-specific TCR (T effector cells, T-eff) were negatively-sorted from the spleen of untreated or squalene treated (180 μg/mouse) F1 mice 7 days post-injection. FACS-sorted GFP^+ T-reg cells were also negatively-sorted by FACS from the spleen of untreated or squalene treated (180 μg/mouse) F1 mice 7 days post-injection. The supernatants from 2-day co-cultures of several combinations of T-reg cells and CD4 T-eff cells in the presence of $HA_{110-120}$-pulsed APCs from untreated or squalene treated F1 mice were further assessed for the secretion of IL-2 and major Th1 and Th2 cytokines (IFN-γ and IL-4, respectively) in parallel with mRNA expression level of T-bet, a critical transcription factor that up-regulates IFN-γ synthesis in Th1 cells. We previously reported that the level of T-bet mRNA expression strongly correlates with the suppressogenic capacity of CD4 *Foxp3* T-regs on the proliferation and cytokine secretion of conventional $CD4^+$(*Foxp3*$^-$) T-cells (T-eff cells) [48].

Interestingly, if considering the effect of membrane cholesterol on CD4 Th1 differentiation in the previous experiments, the CD4 *Foxp3* T-regs were able to induce similar levels of suppression on IL-2, IFN-γ, and IL-4 secretion by conventional CD4 T-cells (T-eff cells) regardless of membrane cholesterol enrichment (**Figure 8A**). This was consistent with a lack of alteration in the T-bet mRNA expression in T-effector cells, as determined by real-time RT-PCR (**Figure 8B**).

Discussion

Cholesterol-rich microdomains known as lipid rafts are postulated to be a driving force in immunological synapse formation and critical for T-cell signaling [1,59-61]. Squalene is a late precursor of cholesterol that is readily incorporated by hepatocytes and proficiently integrated into the cholesterol biosynthesis pathway after intravenous administration in humans [33]. Herein, we found that a single intraperitoneal injection of squalene leads to a significant enrichment of membrane cholesterol in resting lymphocytes, particularly T lymphocytes. The plasma membrane of CD4 T-cells and CD4 *Foxp3* T-reg cells showed a 40-50% increase in membrane cholesterol above baseline after a single dose of squalene, most likely due to a differential threshold for membrane cholesterol compared with other lymphocyte subsets. Squalene enrichment of membrane cholesterol was paralleled by an increased number of resting CD4 splenic T-cells in the absence of T-cell stimulation. This was consistent with early studies showing that provision of cholesterol through high and low density lipoproteins sustains a continuous homeostatic proliferation of T lymphocytes [62-64]. Recently, a cholesterol-rich diet or hypercholesterolemia in mice was associated with an increased number of

splenic CD4 T-cells [65]. In contrast, Atorvastatin-induced inhibition of HMG CoA reductase, a critical enzyme required for cholesterol synthesis, led to a reduction in the number of T-cells in humans [66]. The molecular mechanism(s) by which membrane cholesterol promotes lymphocyte proliferation remains largely unknown. We found that squalene enrichment of membrane cholesterol in resting CD4 T-cells was paralleled by increased IL-2 secretion, a powerful autocrine growth factor for T-cells. This may well explain why the rate of homeostatic proliferation was increased in resting CD4 T-cells enriched in membrane cholesterol.

Spatiotemporal partitioning of protein receptors in lipid rafts influences their signaling status in T-cells, not only in a ligand-specific manner but also by re-partitioning of neighboring receptors and co-receptors [67]. We questioned whether squalene enrichment of membrane cholesterol in the absence of TCR ligation may affect the spatiotemporal partitioning of protein receptors and consequently the tyrosine phosphorylation events critical for recruitment of signaling kinases in CD4 T-cells. The protein synthesis in resting CD4 splenic T-cells was quantitatively unaltered after enrichment of membrane cholesterol. However, fine alterations in tyrosine phosphorylation of several signaling modules associated with receptors involved in Th1/Th2 cell differentiation were detected. Higher amounts of phospho-STAT-4 recruited on IL-12Rβ2, phospho-STAT-5 on IL-2Rα, and phospho-ZAP-70 recruited on TCR/CD3 ζ-chain were detected in resting CD4 T-cells enriched in membrane cholesterol, in contrast to phospho-STAT-6 recruited on IL-4Rα that dropped below baseline. Increased ability of IL-12Rβ2 to recruit phospho-STAT-4 and of IL-2Rα to recruit phospho-STAT-5 was consistent with increased IFN-γ, and respectively IL-2

secretion upon CD3/CD28 ligation [68]. These protein receptors have a particular partitioning in the lipid rafts of resting T-cells. Thus, most of TCR α and β chains in resting T-cells reside in the non raft domains, whereas the ζ–chain resides in the raft microdomains [69,70]. The IL-12Rβ2 is mostly located in the non-raft microdomains, whereas IL-12Rβ1 is located in the raft microdomains, and the ligation through IL-12 leads to a functional IL-12R [71]. The IL-2Rα-chain (CD25) is mostly located in the rafts of resting CD4 T-cells independent of ligation by IL-2 [68,72], whereas the IL-2Rβ-chain is mostly located in the non-raft microdomains [73]. While the IL-2Rα-chain binds IL-2 with high affinity and lacks signaling ability, the intracellular tail of IL-2Rβ-chain expresses several tyrosine phosphorylated sites as docking sites for JAK kinases, which in turn mediates STAT-5 phosphorylation and dimerization. It has been suggested that a functional IL-2Rαβγ able to promote phosphorylation/dimerization of STAT-5 is assembled mostly in the non-raft microdomains of the plasma membrane [74]. The IL-4Rα chain resides mostly in the rafts and assembles with the common γ chain to form a functional receptor [75].

Interestingly, the ability of the CD28 receptor to recruit PI3K was not affected by membrane cholesterol enrichment in resting CD4 T-cells. The CD28 receptor resides mostly in the raft microdomains during T-cell signaling [76]. These opposing signaling events that occurred solely by cholesterol enrichment in the plasma membrane, strongly suggest that not only receptor ligation but also an increase in rafts cholesterol can lead to spatiotemporal re-partitioning of protein receptors in CD4 T-cells. To this, a large body of evidence indicates that pharmacological alterations in rafts composition like changes in cholesterol content are sufficient to induce re-distribution of protein receptors and their

signaling modules in the plasma membrane [reviewed in [77]. A question that remains to be addressed is to what extent squalene enrichment of membrane cholesterol versus squalene itself leads to re-distribution of protein receptors in T-cells? That is because squalene administration in mice up-regulated expression of HMG Co reductase, a critical up-stream enzyme required not only for cholesterol synthesis, but also for generation of small geranylgeranyl and farnesyl radicals actively involved in protein trafficking from cytosol to the plasma membrane [reviewed in [78]. This seems worthy of further investigation, as early studies showed that squalene itself protects rats against cyclophosphamide-induced toxicity by scavenging free radicals and reactive oxidative species [79].

Besides increasing the number of resting CD4 T-cells, squalene enrichment of membrane cholesterol sensitized the Th1 signaling modules in the absence of T-cell stimulation, i.e., STAT-4, STAT-5, and TCR/ZAP-70. Th1 sensitization was significantly augmented in the presence of increased IL-12 secretion by APCs. IL-12 secreted by macrophages and dendritic cells is a well known inflammatory Th1 inducing cytokine whose synthesis is contributed by TLR3 and TLR4 using MyD88 as a common adaptor molecule for down-stream signaling [80]. Although the effect of cholesterol loading in APCs was not the focus of this study, the intimate mechanism by which cholesterol-rich rafts interferes with TLRs signaling and genetic regulation of IL-12 synthesis in APCs is worth being explored. In this study, squalene enrichment of membrane cholesterol in resting CD4 T-cells led to a spatiotemporal re-distribution of IL-2Rβ2 subunit in the rafts according to CLSM analysis, a driving event towards Th1 differentiation. Furthermore, squalene enrichment of membrane cholesterol in the presence of antigen or CD3/CD28

stimulation led to a vigorous Th1 differentiation. This was consistent with an increased reactivity of antigen-specific, diabetogenic Th1 cells in a mouse model for inducible T1D, and with previous findings showing that cholesterol lowering statin therapy can lead to the beneficial reversal of Th1 to Th2 polarization in psoriasis patients associated with hyperlipidemia [81].

Foxp3^{+} T-reg cells represent a particular subset of the CD4 T-cell population. A recent study showed that the number of splenic T-regs mice peaked at 4 weeks and decreased gradually between 8 and 20 weeks during a cholesterol-rich diet in mice, and this coincided with an increased number of inflammatory Th1 cells over the same period of time [65]. The same study concluded that hypercholesterolemia impairs the T-reg pool but not the migration of inflammatory cells to atherosclerotic lesions. However, our data showed that squalene enrichment of membrane cholesterol did not alter the splenic T-reg frequency. We also found that unlike conventional CD4 T-cells that were polarized toward a Th1 phenotype, the T-reg suppressogenic function remained unaltered after squalene enrichment of membrane cholesterol in CD4 *Foxp3* T-reg cells or CD4 T effector cells.

Together, these data revealed differential regulatory effects of membrane cholesterol on the function of CD4 T-cell subsets, suggesting that membrane cholesterol could be a new therapeutic target to modulate immune cell functions in various physiopathological conditions.

Acknowledgments: We thank Mrs. Karen Wolcott for help with Luminex assays and FACS-sorting of lymphocyte subsets.

References

1. Lingwood D, Simons K (2010) Lipid rafts as a membrane-organizing principle. Science 327: 46-50.
2. Thomas S, Kumar RS, Brumeanu TD (2004) Role of lipid rafts in T cells. Arch Immunol Ther Exp (Warsz) 52: 215-224.
3. Gidwani A, Holowka D, Baird B (2001) Fluorescence Anisotropy Measurements of Lipid Order in Plasma Membranes and Lipid Rafts from RBL-2H3 Mast Cells†. Biochemistry 40: 12422-12429.
4. Prior IA, Muncke C, Parton RG, Hancock JF (2003) Direct visualization of Ras proteins in spatially distinct cell surface microdomains. J Cell Biol 160: 165-170.
5. Simons K, Toomre D (2000) Lipid rafts and signal transduction. Nat Rev Mol Cell Biol 1: 31-39.
6. Stevens TJ, Arkin IT (2000) Do more complex organisms have a greater proportion of membrane proteins in their genomes? Proteins 39: 417-420.
7. Saint-Ruf C, Panigada M, Azogui O, Debey P, von Boehmer H, et al. (2000) Different initiation of pre-TCR and gammadeltaTCR signalling. Nature 406: 524-527.
8. Ebert PJ, Baker JF, Punt JA (2000) Immature CD4+CD8+ thymocytes do not polarize lipid rafts in response to TCR-mediated signals. J Immunol 165: 5435-5442.
9. Leitenberg D, Balamuth F, Bottomly K (2001) Changes in the T cell receptor macromolecular signaling complex and membrane microdomains during T cell development and activation. Semin Immunol 13: 129-138.
10. de Mello Coelho V, Nguyen D, Giri B, Bunbury A, Schaffer E, et al. (2004) Quantitative differences in lipid raft components between murine CD4+ and CD8+ T cells. BMC Immunol 5: 2.
11. Poloso NJ, Roche PA (2004) Association of MHC class II-peptide complexes with plasma membrane lipid microdomains. Curr Opin Immunol 16: 103-107.
12. Gombos I, Detre C, Vamosi G, Matko J (2004) Rafting MHC-II domains in the APC (presynaptic) plasma membrane and the thresholds for T-cell activation and immunological synapse formation. Immunol Lett 92: 117-124.
13. Anderson HA, Hiltbold EM, Roche PA (2000) Concentration of MHC class II molecules in lipid rafts facilitates antigen presentation. Nat Immunol 1: 156-162.
14. Horejsi V (2005) Lipid rafts and their roles in T-cell activation. Microbes Infect 7: 310-316.
15. Mitchell JS, Kanca O, McIntyre BW (2002) Lipid microdomain clustering induces a redistribution of antigen recognition and adhesion molecules on human T lymphocytes. J Immunol 168: 2737-2744.
16. Liu SD, Whiting CC, Tomassian T, Pang M, Bissel SJ, et al. (2008) Endogenous galectin-1 enforces class I-restricted TCR functional fate decisions in thymocytes. Blood 112: 120-130.
17. Demetriou M, Granovsky M, Quaggin S, Dennis JW (2001) Negative regulation of T-cell activation and autoimmunity by Mgat5 N-glycosylation. Nature 409: 733-739.
18. Ho YK, Brown S, Bilheimer DW, Goldstein JL (1976) Regulation of low density lipoprotein receptor activity in freshly isolated human lymphocytes. J Clin Invest 58: 1465-1474.

19. Verhoeye FR, Descamps O, Husson B, Hondekijn JC, Ronveaux-Dupal MF, et al. (1996) An improved method for detection of low density lipoprotein receptor defects in human T lymphocytes. J Lipid Res 37: 1377-1384.
20. Lehoux JG, Kandalaft N, Belisle S, Bellabarba D (1985) Characterization of 3-hydroxy-3-methylglutaryl coenzyme A reductase in human adrenal cortex. Endocrinology 117: 1462-1468.
21. Fulop T, Jr., Douziech N, Goulet AC, Desgeorges S, Linteau A, et al. (2001) Cyclodextrin modulation of T lymphocyte signal transduction with aging. Mech Ageing Dev 122: 1413-1430.
22. Nix M, Stoffel W (2000) Perturbation of membrane microdomains reduces mitogenic signaling and increases susceptibility to apoptosis after T cell receptor stimulation. Cell Death Differ 7: 413-424.
23. Fulop T, Larbi A, Wikby A, Mocchegiani E, Hirokawa K, et al. (2005) Dysregulation of T-cell function in the elderly : scientific basis and clinical implications. Drugs Aging 22: 589-603.
24. Harikumar KG, Puri V, Singh RD, Hanada K, Pagano RE, et al. (2005) Differential effects of modification of membrane cholesterol and sphingolipids on the conformation, function, and trafficking of the G protein-coupled cholecystokinin receptor. J Biol Chem 280: 2176-2185.
25. Hillyard DZ, Cameron AJ, McDonald KJ, Thomson J, MacIntyre A, et al. (2004) Simvastatin inhibits lymphocyte function in normal subjects and patients with cardiovascular disease. Atherosclerosis 175: 305-313.
26. Jury EC, Isenberg DA, Mauri C, Ehrenstein MR (2006) Atorvastatin restores Lck expression and lipid raft-associated signaling in T cells from patients with systemic lupus erythematosus. J Immunol 177: 7416-7422.
27. Kabouridis PS, Janzen J, Magee AL, Ley SC (2000) Cholesterol depletion disrupts lipid rafts and modulates the activity of multiple signaling pathways in T lymphocytes. Eur J Immunol 30: 954-963.
28. Tani-ichi S, Maruyama K, Kondo N, Nagafuku M, Kabayama K, et al. (2005) Structure and function of lipid rafts in human activated T cells. Int Immunol 17: 749-758.
29. Nguyen DH, Espinoza JC, Taub DD (2004) Cellular cholesterol enrichment impairs T cell activation and chemotaxis. Mech Ageing Dev 125: 641-650.
30. Van Laethem F BE, Smyth LA, Andris F, Bex F, et al. (2001) Glucocorticoids attenuate T cell receptor signaling. J Exp Med 803-814.
31. Goldman F, Hohl RJ, Crabtree J, Lewis-Tibesar K, Koretzky G (1996) Lovastatin inhibits T-cell antigen receptor signaling independent of its effects on ras. Blood 88: 4611-4619.
32. Brumeanu TD, Goldstein R, Casares S (2006) Down-regulation of autoreactive T-cells by HMG CoA reductase inhibitors. Clin Immunol 119: 1-12.
33. Eidinoff ML, Knoll JE, Marano BJ, Kvamme E, Rosenfeld RS, et al. (1958) Cholesterol biosynthesis: studies related to the metabolic role of squalene. J Clin Invest 37: 655-659.
34. Mbow ML, De Gregorio E, Valiante NM, Rappuoli R (2010) New adjuvants for human vaccines. Curr Opin Immunol 22: 411-416.

35. Murakoshi M, Nishino H, Tokuda H, Iwashima A, Okuzumi J, et al. (1992) Inhibition by squalene of the tumor-promoting activity of 12-O-tetradecanoylphorbol-13-acetate in mouse-skin carcinogenesis. Int J Cancer 52: 950-952.
36. Rao CV, Newmark HL, Reddy BS (1998) Chemopreventive effect of squalene on colon cancer. Carcinogenesis 19: 287-290.
37. Van Duuren BL, Goldschmidt BM (1976) Cocarcinogenic and tumor-promoting agents in tobacco carcinogenesis. J Natl Cancer Inst 56: 1237-1242.
38. Loud AV, Bucher NL (1958) The turnover of squalene in relation to the biosynthesis of cholesterol. J Biol Chem 233: 37-41.
39. Tilvis RS, Miettinen TA (1983) Dietary squalene increases tissue sterols and fecal bile acids in the rat. Lipids 18: 32-36.
40. Casares S, Hurtado A, McEvoy RC, Sarukhan A, von Boehmer H, et al. (2002) Down-regulation of diabetogenic CD4+ T cells by a soluble dimeric peptide-MHC class II chimera. Nat Immunol 3: 383-391.
41. Kirberg J, Baron A, Jakob S, Rolink A, Karjalainen K, et al. (1994) Thymic selection of CD8+ single positive cells with a class II major histocompatibility complex-restricted receptor. J Exp Med 180: 25-34.
42. Fisson S, Djelti F, Trenado A, Billiard F, Liblau R, et al. (2006) Therapeutic potential of self-antigen-specific CD4+ CD25+ regulatory T cells selected in vitro from a polyclonal repertoire. Eur J Immunol 36: 817-827.
43. Surls J, Nazarov-Stoica C, Kehl M, Casares S, Brumeanu TD (2010) Differential effect of CD4+Foxp3+ T-regulatory cells on the B and T helper cell responses to influenza virus vaccination. Vaccine 28: 7319-7330.
44. Casares S, Bona CA, Brumeanu TD (1997) Engineering and characterization of a murine MHC class II-immunoglobulin chimera expressing an immunodominant CD4 T viral epitope. Protein Eng 10: 1295-1301.
45. Thomas S, Kumar RS, Casares S, Brumeanu TD (2003) Sensitive detection of GM1 lipid rafts and TCR partitioning in the T cell membrane. J Immunol Methods 275: 161-168.
46. Castanho MA, Coutinho A, Prieto MJ (1992) Absorption and fluorescence spectra of polyene antibiotics in the presence of cholesterol. J Biol Chem 267: 204-209.
47. Muller CP, Stephany DA, Winkler DF, Hoeg JM, Demosky SJ, Jr., et al. (1984) Filipin as a flow microfluorometry probe for cellular cholesterol. Cytometry 5: 42-54.
48. Nazarov-Stoica C, Surls J, Bona C, Casares S, Brumeanu TD (2009) CD28 signaling in T regulatory precursors requires p56lck and rafts integrity to stabilize the Foxp3 message. J Immunol 182: 102-110.
49. Brumeanu TD, Preda-Pais A, Stoica C, Bona C, Casares S (2007) Differential partitioning and trafficking of GM gangliosides and cholesterol-rich lipid rafts in thymic and splenic CD4 T cells. Mol Immunol 44: 530-540.
50. Ness GC, Zhao Z, Keller RK (1994) Effect of squalene synthase inhibition on the expression of hepatic cholesterol biosynthetic enzymes, LDL receptor, and cholesterol 7 alpha hydroxylase. Arch Biochem Biophys 311: 277-285.
51. Kaplan MH, Sun YL, Hoey T, Grusby MJ (1996) Impaired IL-12 responses and enhanced development of Th2 cells in Stat4-deficient mice. Nature 382: 174-177.

52. Kaplan MH, Schindler U, Smiley ST, Grusby MJ (1996) Stat6 is required for mediating responses to IL-4 and for development of Th2 cells. Immunity 4: 313-319.
53. Cantrell DA, Collins MK, Crumpton MJ (1988) Autocrine regulation of T-lymphocyte proliferation: differential induction of IL-2 and IL-2 receptor. Immunology 65: 343-349.
54. Cantrell D, Smith K (1984) The interleukin-2 T-cell system: a new cell growth model. Science 224: 1312.
55. Chan AC, Irving BA, Fraser JD, Weiss A (1991) The zeta chain is associated with a tyrosine kinase and upon T-cell antigen receptor stimulation associates with ZAP-70, a 70-kDa tyrosine phosphoprotein. Proc Natl Acad Sci U S A 88: 9166-9170.
56. Lenschow DJ, Walunas TL, Bluestone JA (1996) CD28/B7 system of T cell costimulation. Annu Rev Immunol 14: 233-258.
57. Bot A, Casares S, Bot S, von Boehmer H, Bona C (1998) Cellular mechanisms involved in protection against influenza virus infection in transgenic mice expressing a TCR receptor specific for class II hemagglutinin peptide in CD4+ and CD8+ T cells. J Immunol 160: 4500-4507.
58. Sakaguchi S (2005) Naturally arising Foxp3-expressing CD25+CD4+ regulatory T cells in immunological tolerance to self and non-self. Nat Immunol 6: 345-352.
59. Zeyda M, Stulnig TM (2006) Lipid Rafts & Co.: an integrated model of membrane organization in T cell activation. Prog Lipid Res 45: 187-202.
60. Owen DM, Oddos S, Kumar S, Davis DM, Neil MA, et al. (2010) High plasma membrane lipid order imaged at the immunological synapse periphery in live T cells. Mol Membr Biol 27: 178-189.
61. Simons K, Gerl MJ (2010) Revitalizing membrane rafts: new tools and insights. Nat Rev Mol Cell Biol 11: 688-699.
62. Cuthbert JA, Lipsky PE (1987) Provision of cholesterol to lymphocytes by high density and low density lipoproteins. Requirement for low density lipoprotein receptors. J Biol Chem 262: 7808-7818.
63. Cuthbert JA, Lipsky PE (1987) Regulation of lymphocyte proliferation by cholesterol: the role of endogenous sterol metabolism and low density lipoprotein receptors. Int J Tissue React 9: 447-457.
64. Cuthbert JA, Lipsky PE (1986) Promotion of human T lymphocyte activation and proliferation by fatty acids in low density and high density lipoproteins. J Biol Chem 261: 3620-3627.
65. Maganto-Garcia E, Tarrio ML, Grabie N, Bu DX, Lichtman AH (2011) Dynamic changes in regulatory T cells are linked to levels of diet-induced hypercholesterolemia. Circulation 124: 185-195.
66. Ganesan A, Crum-Cianflone N, Higgins J, Qin J, Rehm C, et al. (2011) High dose atorvastatin decreases cellular markers of immune activation without affecting HIV-1 RNA levels: results of a double-blind randomized placebo controlled clinical trial. J Infect Dis 203: 756-764.
67. Matko J, Szollosi J (2002) Landing of immune receptors and signal proteins on lipid rafts: a safe way to be spatio-temporally coordinated? Immunol Lett 82: 3-15.

68. Matko J, Bodnar A, Vereb G, Bene L, Vamosi G, et al. (2002) GPI-microdomains (membrane rafts) and signaling of the multi-chain interleukin-2 receptor in human lymphoma/leukemia T cell lines. Eur J Biochem 269: 1199-1208.
69. Montixi C, Langlet C, Bernard AM, Thimonier J, Dubois C, et al. (1998) Engagement of T cell receptor triggers its recruitment to low-density detergent-insoluble membrane domains. EMBO J 17: 5334-5348.
70. Xavier R, Brennan T, Li Q, McCormack C, Seed B (1998) Membrane compartmentation is required for efficient T cell activation. Immunity 8: 723-732.
71. Canda-Sanchez A, Salgado FJ, Perez-Diaz A, Varela-Gonzalez C, Arias P, et al. (2009) Differential distribution of both IL-12Rbeta chains in the plasma membrane of human T cells. J Membr Biol 227: 1-12.
72. Li QR, Ma J, Wang H, Li JS (2005) Interleukin-2alpha receptor in membrane lipid rafts. Transplant Proc 37: 2395-2397.
73. Goebel J, Forrest K, Morford L, Roszman TL (2002) Differential localization of IL-2- and -15 receptor chains in membrane rafts of human T cells. J Leukoc Biol 72: 199-206.
74. Marmor MD, Julius M (2001) Role for lipid rafts in regulating interleukin-2 receptor signaling. Blood 98: 1489-1497.
75. Rao R, Logan B, Forrest K, Roszman TL, Goebel J (2004) Lipid rafts in cytokine signaling. Cytokine Growth Factor Rev 15: 103-110.
76. Viola A, Schroeder S, Sakakibara Y, Lanzavecchia A (1999) T lymphocyte costimulation mediated by reorganization of membrane microdomains. Science 283: 680-682.
77. Fessler MB, Parks JS (2011) Intracellular lipid flux and membrane microdomains as organizing principles in inflammatory cell signaling. J Immunol 187: 1529-1535.
78. Zhang FL, Casey PJ (1996) Protein prenylation: molecular mechanisms and functional consequences. Annu Rev Biochem 65: 241-269.
79. Senthilkumar S, Devaki T, Manohar BM, Babu MS (2006) Effect of squalene on cyclophosphamide-induced toxicity. Clin Chim Acta 364: 335-342.
80. Krummen M, Balkow S, Shen L, Heinz S, Loquai C, et al. (2010) Release of IL-12 by dendritic cells activated by TLR ligation is dependent on MyD88 signaling, whereas TRIF signaling is indispensable for TLR synergy. J Leukoc Biol 88: 189-199.
81. Ghazizadeh R, Tosa M, Ghazizadeh M (2011) Clinical improvement in psoriasis with treatment of associated hyperlipidemia. Am J Med Sci 341: 394-398.

Figure legends

Figure 1. **Squalene administration leads to accumulation of membrane cholesterol in resting CD4 T-cells**. **(A)** Seven days after the last squalene injection, negatively-sorted splenic CD4 cells from individual untreated (purple line), squalene treated mice with a single dose (black line), or squalene treated mice with 4 doses (red line) within a week interval were co-stained with CD3-PE, CD4-FITC, and Filipin III (180 μg/dose/mouse, n=5/group). Shown is the amount of membrane cholesterol of gated $CD3^+CD4^+$ splenic cells as measured by MFI of Filipin III in FACS at single-cell level in one representative mouse from each group (*left panel*). *Right panel*, F1 hybrid mice (n=7/group) were injected i.p. (black line) or not (red line) with a single dose of squalene (180 μg/mouse) and 7 days later negatively-sorted splenic CD4 cells from individual mice were co-stained with CD3-PE, CD4-FITC, and Filipin III. Shown is the percentage of gated $CD4^+$ T-cells ± standard deviation (SD) and MFI values of Filipin III ± SD before and after squalene injection as collected among 700 cell events in gated population of $CD3^+4^+$ T-cells for one of three representative experiments. **(B)** Cholesterol accumulation in the spleen was identified by Oil Red O (ORO) staining of frozen spleen sections, counter-stained with hematoxylin from untreated or squalene treated mice given 1 or 4 doses (180 μg/mouse), and analyzed 7 days after the last injection (n=3/group). *First panel*, spleen section from untreated mouse. *Second panel*, spleen section from squalene treated mouse given 1 dose. *Third panel*, spleen section from squalene treated mouse given 4 doses. *Last panel*, positive control for ORO lipid droplet staining in adipocytes. Shown is one representative ORO stained section in each group. Dark arrows indicate ORO stain. **(C)** Quantitative real-time RT-PCR of HMG-CoA reductase mRNA and Squalene epoxidase

mRNA extracted from negatively-sorted CD4 splenocytes isolated from individual untreated (light bars) or squalene treated (dark bars) with a single dose of squalene (180 μg/mouse) F1 hybrid mice (n=5/group) and analyzed 7 days post-injection. Y axis indicates the mean fold increase in mRNA expression level relative to the endogenous 18S rRNA expression level (control ± standard deviation, SD). *P value <0.05. Shown is one of two representative experiments. **(D)** FACS measurements of $CD3^+4^+$*Foxp3*$^+$ T-reg cells from negatively-sorted $CD4^+$ splenic cells of the same F1 mouse groups analyzed in panel A that were co-stained with CD3-PE and Filipin III. Shown is the percentage of gated $CD4^+Foxp3^+$ T-reg cells ± SD and MFI values of Filipin III ± SD collected among 500 cell events in the gated population of GFP^+-*Foxp3*/GFP^+ cells from one mouse in each group from two representative experiments.

Figure 2. **Squalene induced accumulation of membrane cholesterol in resting CD4 T-cells alters the partitioning of lipid rafts**. Negatively-sorted $CD4^+$ splenocytes were isolated from the spleen of untreated or squalene treated (single 180 μg dose/mouse) F1 mice 7 days post-injection. Cells were co-stained with CD4-PE, CTB-FITC and DAPI and analyzed by CLSM. *Upper panels,* quadrants indicating single-color stained cells at X40 magnification from untreated (*left column*) and squalene treated F1 mouse (*right column*): *upper left* quadrant, CTB-FITC staining (green); *upper right* quadrant, CD4-PE stain (red); *lower left* quadrant, DAPI staining of nuclei (blue), and *lower right* quadrant, merged channels for CTB-FITC, CD4-PE and DAPI staining. *Middle panels*, merged CTB-FITC, CD4-PE and DAPI staining of clusters of splenocytes from untreated and squalene treated F1 mouse at X220 magnification. *Bottom panels,* color intensity

quantification for cell clusters shown in the middle panels using the using the ZEISS ZEN 2009 analysis software. Of note, the amount of GM1 moiety revealed by CTB-FITC (green) in merged channel 2 is significantly higher for the CD4 T-cells from squalene treated mouse than that of the untreated mouse. Shown is one of three mice analyzed in each group.

Figure 3. Tyrosine phosphorylation patterns of major signaling modules of T helper differentiation upon enrichment of membrane cholesterol. (A) SDS-PAGE silver stain of pooled, negatively-sorted $CD4^+$ splenic T-cell lysates from F1 mice (n=4/group) untreated (*left lane*) or squalene treated (single dose of 180 μg, *right lane*) 3 days post-injection shows no detectable quantitative alterations in the protein bands between the two groups of mice. **(B)** Tyrosine phosphorylation patterns of the same samples in panel *A* were blotted with anti-phosphorylated tyrosine Ab-HRP conjugate. Of note, the amount of 55-100 kDa phosphorylated protein bands is increased in mice treated with squalene. **(C)** Immunoprecipitation of pooled splenic $CD4^+$ T-cell lysates from F1 mice treated or not with squalene (180 μg/mouse, n=4/group) 3 days post-injection was carried out for IL-12Rβ2, IL-2Rα, IL-4Rα, CD28, or CD3 receptors using specific Abs, and probed with specific anti-phospho Abs for STAT4, STAT5, STAT6, PI3K, and ZAP-70 kinases. Only the phosphorylated STAT-4, STAT-5, and ZAP-70 in squalene treated mice were significantly enhanced. Shown is one of two representative experiments.

Figure 4. Distribution of cytokine receptors in the lipid rafts of resting CD4 T-cells before and after squalene treatment. Resting CD4 T-cells from individual F1 mice

(n=5/group) before and 7 days after squalene treatment (180 μg/mouse) were analyzed for interleukin receptor expression and distribution at the single-cell level by CLSM. Cells were stained with IL-4Rα-, IL-12Rβ2-, or IL-2Rα–PE conjugates, and co-stained for GM1 ganglioside by CTB- FITC conjugate and for nuclei with DAPI. First column indicates single-channel color for DAPI staining (blue), second column indicates GM1 staining (green), third column indicates interleukin receptor (IL-Rs) staining (red), and last column indicates merged channels at X63 magnification. *Top-two rows*, indicate cells from untreated (*upper row*) and squalene treated mice (*lower row*) stained for IL-4Rα. *Middle-two rows*, indicate cells from untreated (*upper row*) and squalene treated mice (*lower row*) stained for IL-12Rβ2. *Bottom-two rows*, indicate cells from untreated (*upper row*) and squalene treated mice (*lower row*) stained for IL-2Rα. Arrows indicate presence of IL-Receptor co-expression with the GM1 resident of lipid rafts. Enlargements of the merged channels are depicted to the *right* along with two different angles of the membrane for each IL-Receptor at X220 magnification. Shown are representative images in one of three experiments.

Figure 5. Alteration in cytokine receptors mRNA expression after squalene enrichment of membrane cholesterol in resting lymphocytes. (A) Quantitative real-time RT-PCR of IL-4Rα, IL-12Rβ2, and IL-2Rα mRNA extracted from peripheral blood lymphocytes of individual F1 mice (n=5/group) analyzed before squalene treatment (dark bars) and 7 days after squalene injection (180 μg/mouse) (light bars). Y axis indicates the mean fold increase in mRNA expression level relative to the endogenous 18S rRNA expression level (control ± SD). **P* values <0.05. **(B)** Aliquots samples in panel A were

stained with CD4-FITC conjugate, co-stained either with IL-4Rα-PE or IL-12Rβ2-PE or IL-2Rα-PE conjugates, and analyzed by FACS at the single-cell level for the surface IL-Rs expression level based on MFI measurements. Shown are the IL-Rs MFI values ± SD measured in individual mice before and after squalene treatment. Of note, no significant changes occurred in the IL-Rs expression on cell surface after squalene treatment (*p values >0.05).

Figure 6. Squalene induced accumulation of membrane cholesterol in resting CD4 T cells favors Th1 polarization under antigen-specific or non antigen specific stimulation (A) Isolated adherent splenocytes (APCs, $5x10^5$) from individual untreated or squalene treated (180 μg) F1 hybrid mice, were pulsed (+) or not pulsed (-) with $HA_{110-120}$ synthetic peptide (40 μg/mL/10^6 cells) *in vitro* 7 days after squalene injection, and co-cultured with negatively-sorted CD4 splenic T-cells (10^6 cells) from the same groups of mice, treated or not with squalene (Sq) (n=4/group). Various cell co-culture combinations are shown on the X-axis, where (+) indicates presence and (–) indicates absence from the culture. Cell-culture supernatants were collected 24-48 h later, and secretion of IL-2, IL-4, and IFN-γ (Y-axis) was measured in pg/ml by Luminex. Bars represent average ± SD. Differences among groups were highly significant (brackets, p <0.001) for cytokines with the following exceptions denoted by §: For IL-4, co-culture in column 6 differed significantly from column 5 (p =0.047) but not from column 3 (p =0.097). No significant difference was observed between co-cultures in column 3 and 5 for any of the three cytokines. **(B)** Intracellular cytokine staining for IFN-γ (*left panels*) and IL-4 (*right panels*) in splenic cells and CD4-gated splenic cells from individual

untreated (*top panels*) and squalene treated F1 mice (*bottom panels*) (n =3/group) were stimulated for 48 h with anti-CD3/CD28 Abs (2.5μg each/10^6 cells). Shown are the overlapped FACS histograms of gated $CD4^+$ T cells synthesizing IL-4 or IFN-γ (red cell events), and total splenic cells (dark cell events) from squalene treated or untreated F1 mice, 7 days after squalene treatment. R1 gate indicates the percent of low-proliferating cell population whereas the R2 gate indicates the percent high proliferating cell population in each experiment. Dead cells are shown in the un-gated cell population below the R1 gate. Shown is one of two representative experiments.

Figure 7. Squalene enrichment of membrane cholesterol fosters the autoreactivity of antigen-specific Th1 diabetogenic cells. (A) Diabetogenicity of antigen ($HA_{110-120}$)-specific CD4 splenic Th1 cells was determined in RAG2 KO, RIP-HA mouse model for inducible type 1 diabetes (T1D). The $HA_{110-120}$-specific CD4 splenic T-cells ($2x10^5$ cells) from either F1 mice (*Foxp3*-$GFP^{+/-}$ TCR-$HA^{+/-}$ mice) (filled circle), or from parental *Foxp3*-$GFP^{+}/^{+}$ mice (open circle) were infused alone, or in combination with *Foxp3*-GFP sorted splenic cells ($2x10^5$ cells) from Fl mice (filled triangle) or *Foxp3*-GFP sorted cells ($2x10^5$ cells) from parental *Foxp3*-$GFP^{+}/^{+}$ mice (open triangle) into RAG2 KO, RIP-HA Tg recipient mice (n =5 mice /group). Shown is the mean glycemia values for individual mice in each group ± SD. Horizontal dark line indicates the upper limit of euglycemia (200 mg/dL) previously determined in a large cohort of non manipulated RAG2 KO RIP-HA Tg recipients (n=20). Of note, only the antigen ($HA_{110-120}$)-specific CD4 splenic T-cells, but not T-regs or other non-antigen ($HA_{110-120}$)-specific T-cells were able to induce hyperglycemia in RAG2 KO, RIP-HA Tg recipients. **(B)** Diabetogenicity of antigen

($HA_{110-120}$)-specific CD4 splenic Th1 cells from squalene treated F1 mice was tested in the same RAG2 KO, RIP-HA mouse model for inducible T1D described in panel A. The $HA_{110-120}$-specific CD4 splenic T-cells ($2x10^4$ cells) from squalene treated (180 μg/mouse) 7 days post-treatment or untreated F1 mice were first depleted of *Foxp3*$^+$ splenic cells, and then infused i.p. in RAG2 KO, RIP-HA Tg recipients (n=10 mice/group). Shown is the cumulative incidence of hyperglycemia (X-axis) from two separate experiments where each experiment had n=5 mice/group. Cumulative incidence of hyperglycemia was calculated by dividing the number of mice per group that developed two consecutive readings of hyperglycemia (>200 mg/dL) by the total number of mice and then multiplied by 100.

Figure 8. Squalene enrichment of membrane cholesterol in CD4$^+$*Foxp3*$^+$ T-reg cells does not alter their suppressogenic function. (A) T-reg suppression of $HA_{110-120}$ -specific CD4 T-effector (T-eff) cells from untreated or squalene treated (single dose of 180 μg/mouse) F1 mice (n=4/group) has been tested in an *in vitro* suppression assay. Isolated $HA_{110-120}$-pulsed APCs ($5x10^5$) were co-cultured for 48 h with FACS-sorted HA-specific CD4$^+$ T-eff cells (10^6 cells) and FACS-sorted *Foxp3*-GFP$^+$ T-regs (10^6 cells) from either untreated or squalene treated (Sq) F1 mice. Various cell co-culture combinations from individual mice are shown in the X-axis, where (+) indicates the presence and (–) indicates the absence of cells in the culture system. Cell-culture supernatants from each Treg/T-eff combination were then measured for secreted IFN-γ (Th1 cytokine) and IL-4 (Th2 cytokine) by Luminex (Y-axis). **(B)** Quantitative real-time RT-PCR measured the T-bet mRNA extracted from triplicate wells of each T-reg/T-eff

cells combination described in panel A. The Y axis indicates the mean fold increase in mRNA expression level relative to endogenous 18S rRNA control ± SD. The mRNA relative values were normalized to the untreated T-eff co-cultures with HA-pulsed APCs (reference control sample). Shown is one of two representative experiments. No significant changes were observed in the specified profiles (brackets, *p values > 0.05).

Supplemental Figures

Figure S1. Squalene administration leads to accumulation of membrane cholesterol in several lymphocyte subsets. F1 hybrid mice (n=5/group) were injected i.p. (filled plots) or not (unfilled plots) with a single dose of squalene (180 μg/mouse) and 7 days later splenocytes were individually stained for CD8, CD22.2, CD19, or CD11c, and co-stained with CD3 and Filipin III. Shown are the percent values ± SD and MFI values of Filipin III ± SD collected among 100-800 cell events in gated populations from one of two representative experiments. Values to the left of each histogram correspond to untreated treated mice and values to the right of each histogram correspond to squalene treated mice.

Figure S2. **Effect of recurrent administration of squalene on the cholesterol metabolism (A)** Serum lipid electrophoresis of F1 mice treated i.p. with 4 doses of squalene (red line) given once a week (180 μg/dose/mouse) (lanes 1-2), or untreated mice (lanes 3-4) and analyzed 7 days after the last squalene injection. Shown are the LDL, VLDL, and HDL serum fractions of cholesterol from 4 of 10 mice analyzed. The electrophoretic bands were scanned by densitometry and quantified using the SCION

analysis software (right panel). Of note, a recurrent squalene treatment resulted in increased HDL serum fraction. **(B)** Liver accumulation of cholesterol in individual F1 mice treated i.p. with 1 or 4 doses of squalene (180μg/mouse) (n =5 mice/group) were analyzed 7 days after the last squalene injection by staining frozen liver sections with Sudan IV and hematoxylin. *Upper* panel shows the presence of cholesterol (reddish spots) in a sample of fat tissue (control cholesterol staining). *Lower left* panel, F1 mouse treated with 1 dose of squalene at X40 magnification. *Lower right* panel, F1 mouse treated with 4 doses of squalene at X40 magnification. Of note, slight increase in cholesterol accumulation (reddish areas) was detected in mice treated with 4, but not 1 dose of squalene. Shown is one representative liver section from each group of mice.

Figure S3. Squalene enrichment of membrane cholesterol in unstimulated APCs alters their cytokine secretion. Unstimulated APCs from F1 mice untreated (dark bars) or squalene treated mice (180μg/mouse) (light bars) were measured for IL-12, IL-6, and IL-1α secretion *in vitro*, 7 days after squalene treatment (n=5 mice/group). Cell culture supernatants from 2-day cultures of adherent lymphocytes harvested from individual spleens of each group of mice were measured by Luminex. Of note, only IL-12 secretion by unstimulated APCs from squalene treated mice was significantly increased (*p <0.01).

Figure S4. Alteration in T-bet and GATA-3 mRNA expression levels in splenic cells enriched for membrane cholesterol and stimulated with CD3/CD28 Abs. Quantitative real-time RT-PCR of T-bet and GATA-3 mRNA extracted from *in vitro* CD3/CD28-stimulated splenocytes from individual F1 mice treated i.p. or not with 1 dose of squalene

(180 μg) (n=5 mice/group) was carried out 7 days after squalene injection. Y axis indicates the mean fold increase in mRNA expression level relative to the endogenous 18S rRNA expression level (control ± SD). *P value is < 0.01.

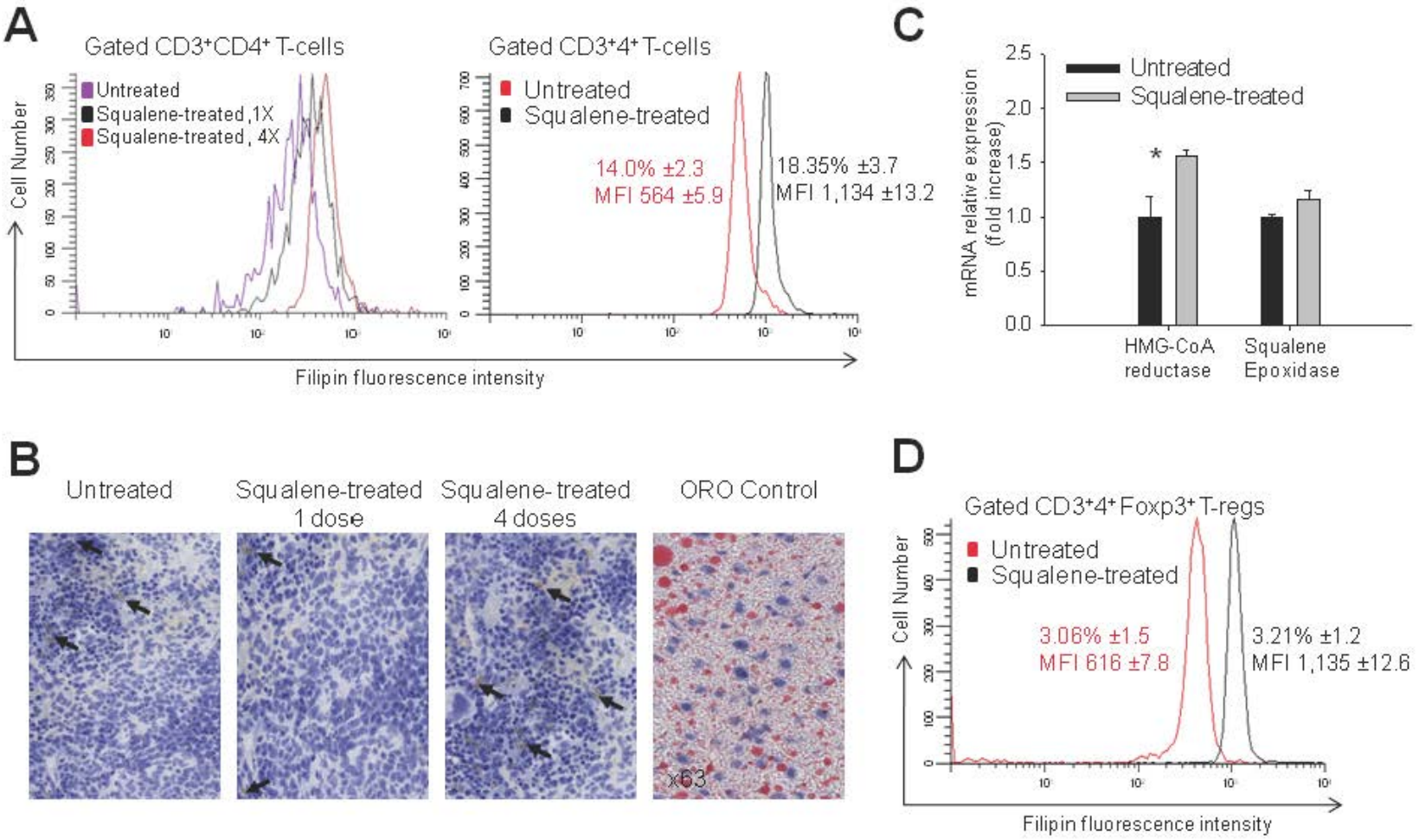
A
Gated CD3+CD4+ T-cells
Untreated
Squalene-treated,1X
Squalene-treated, 4X
Cell Number
Filipin fluorescence intensity
Gated CD3+4+ T-cells
Untreated
Squalene-treated
14.0% ±2.3
MFI 564 ±5.9
18.35% ±3.7
MFI 1,134 ±13.2
C
mRNA relative expression (fold increase)
Untreated
Squalene-treated
*
HMG-CoA reductase
Squalene Epoxidase
B
Untreated
Squalene-treated 1 dose
Squalene- treated 4 doses
ORO Control
x63
D
Gated CD3+4+ Foxp3+ T-regs
Untreated
Squalene-treated
3.06% ±1.5
MFI 616 ±7.8
3.21% ±1.2
MFI 1,135 ±12.6
Cell Number
Filipin fluorescence intensity

Figure 1

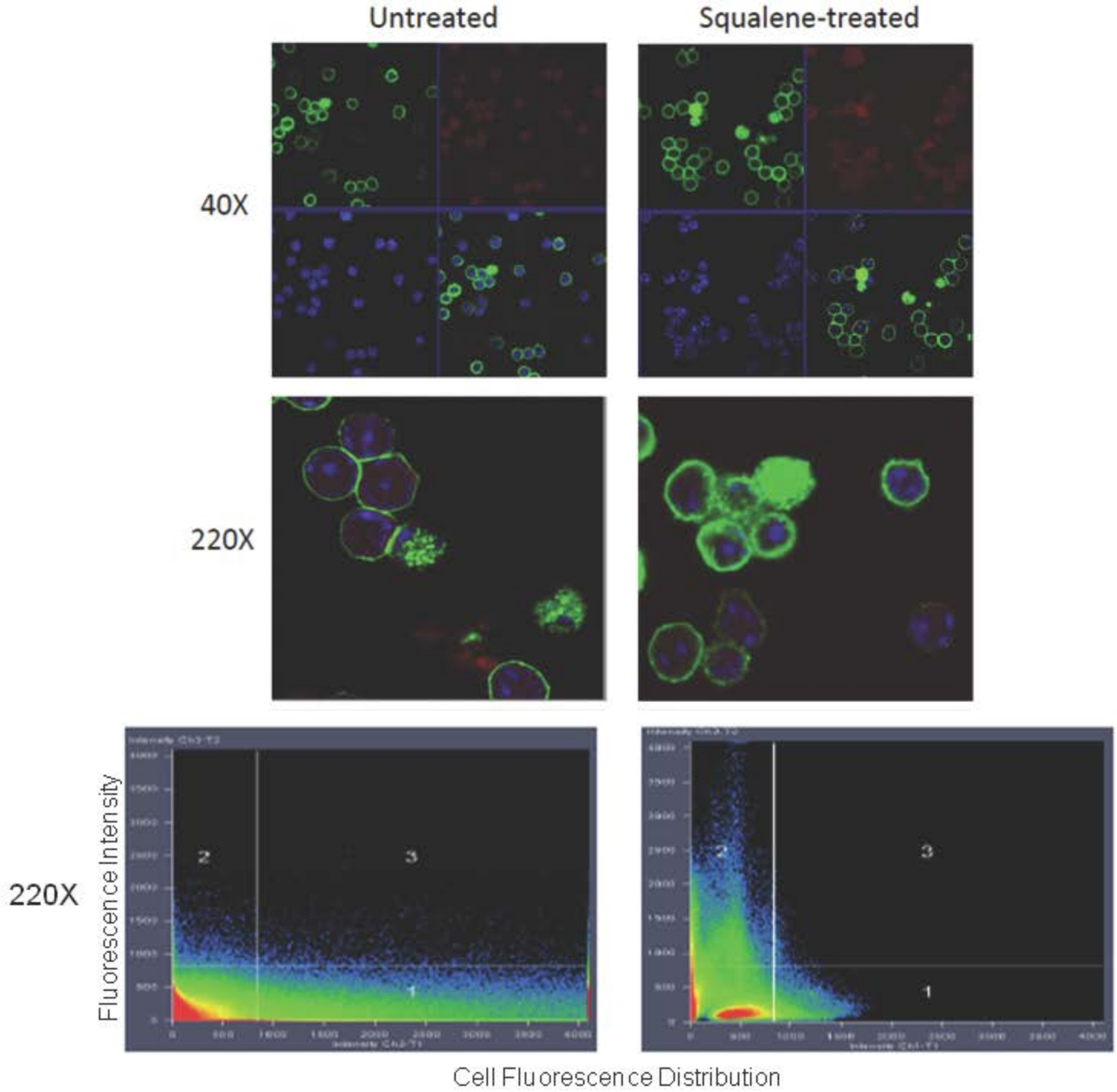
Untreated
Squalene-treated
40X
220X
220X
Fluorescence Intensity
2
3
1
2
3
1
Cell Fluorescence Distribution

Figure 2.

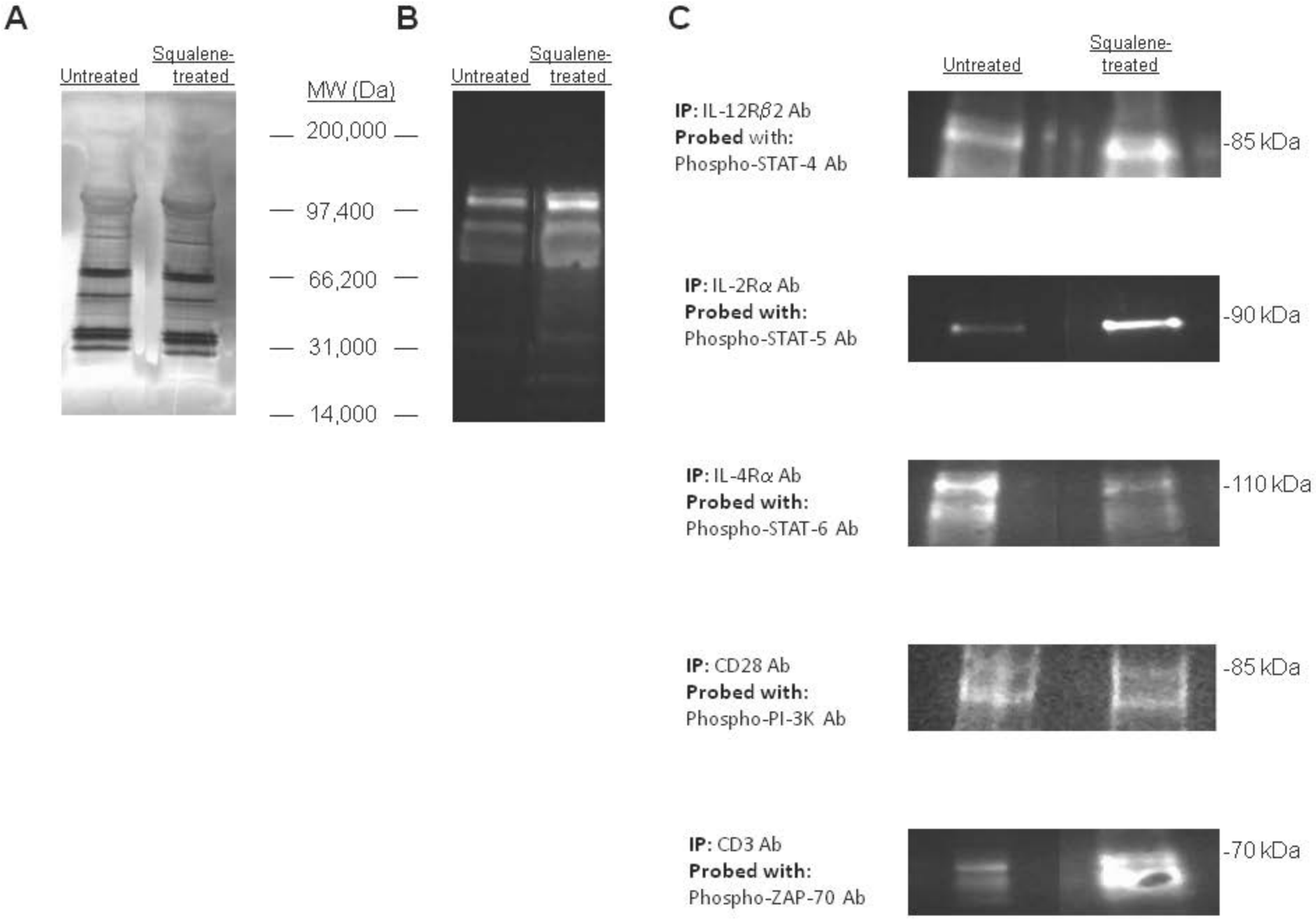
A
Untreated
Squalene-treated
MW (Da)
200,000
97,400
66,200
31,000
14,000
B
Untreated
Squalene-treated
C
Untreated
Squalene-treated
IP: IL-12Rβ2 Ab
Probed with:
Phospho-STAT-4 Ab
-85 kDa
IP: IL-2Rα Ab
Probed with:
Phospho-STAT-5 Ab
-90 kDa
IP: IL-4Rα Ab
Probed with:
Phospho-STAT-6 Ab
-110 kDa
IP: CD28 Ab
Probed with:
Phospho-PI-3K Ab
-85 kDa
IP: CD3 Ab
Probed with:
Phospho-ZAP-70 Ab
-70 kDa

Fig 3.

Figure. 4

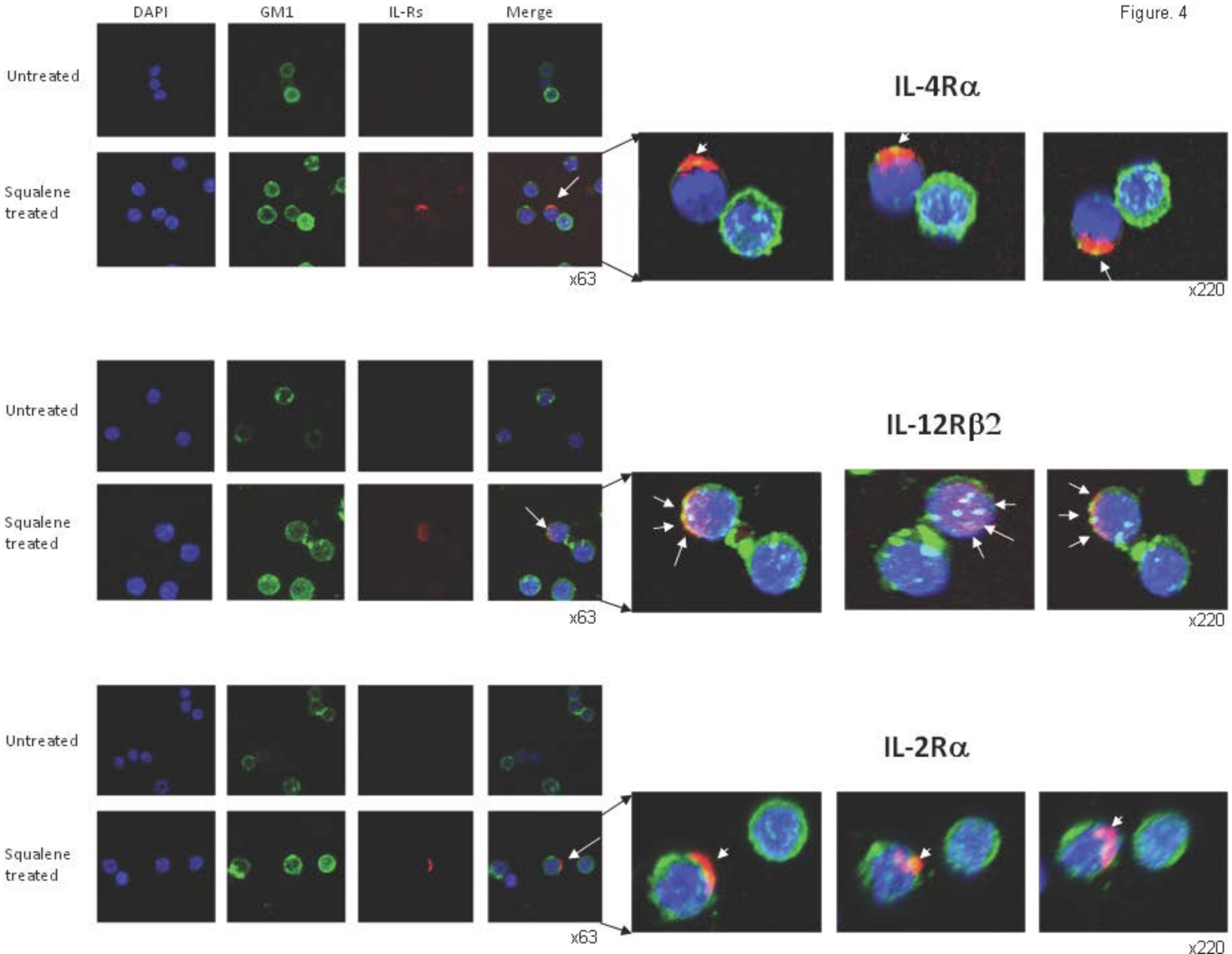
DAPI
GM1
IL-Rs
Merge
Untreated
Squalene treated
IL-4Rα
x63
x220
Untreated
Squalene treated
IL-12Rβ2
x63
x220
Untreated
Squalene treated
IL-2Rα
x63
x220

A

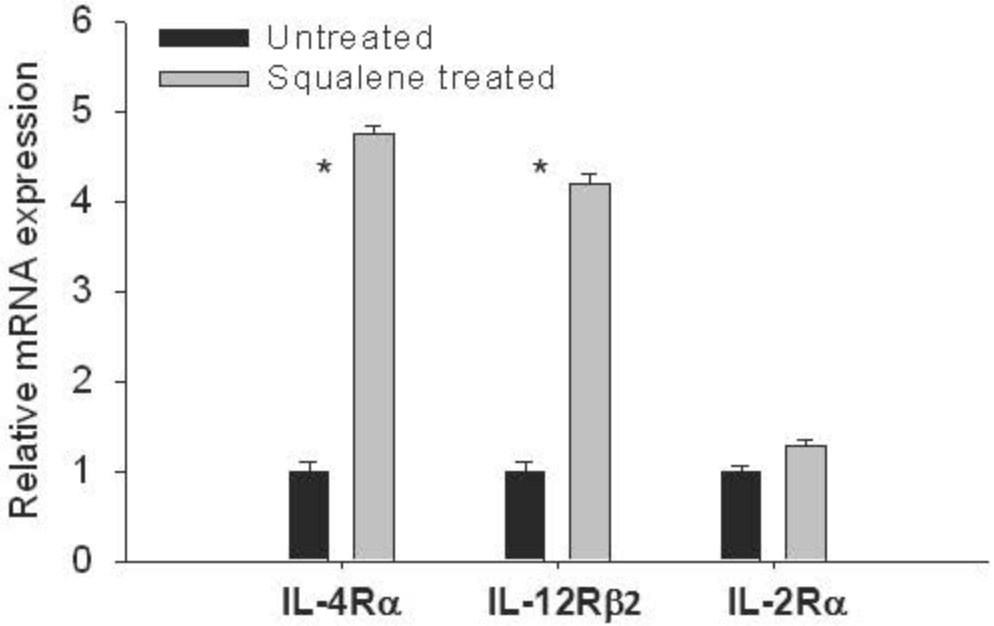

B

CD4 T-cell gated population-Receptor Expression		Before Squalene treatment	After Squalene treatment	*p values
IL-4Rα	*MFI*	*17.2* ± 1.2	*17.0* ± 0.1	*0.40*
IL-12Rβ2	*MFI*	*17.5* ± 2.4	*15.9* ± 0.5	*0.40*
IL-2Rα	*MFI*	*52.6* ± 2.3	*42.6* ± 6.6	*0.19*

Figure 5

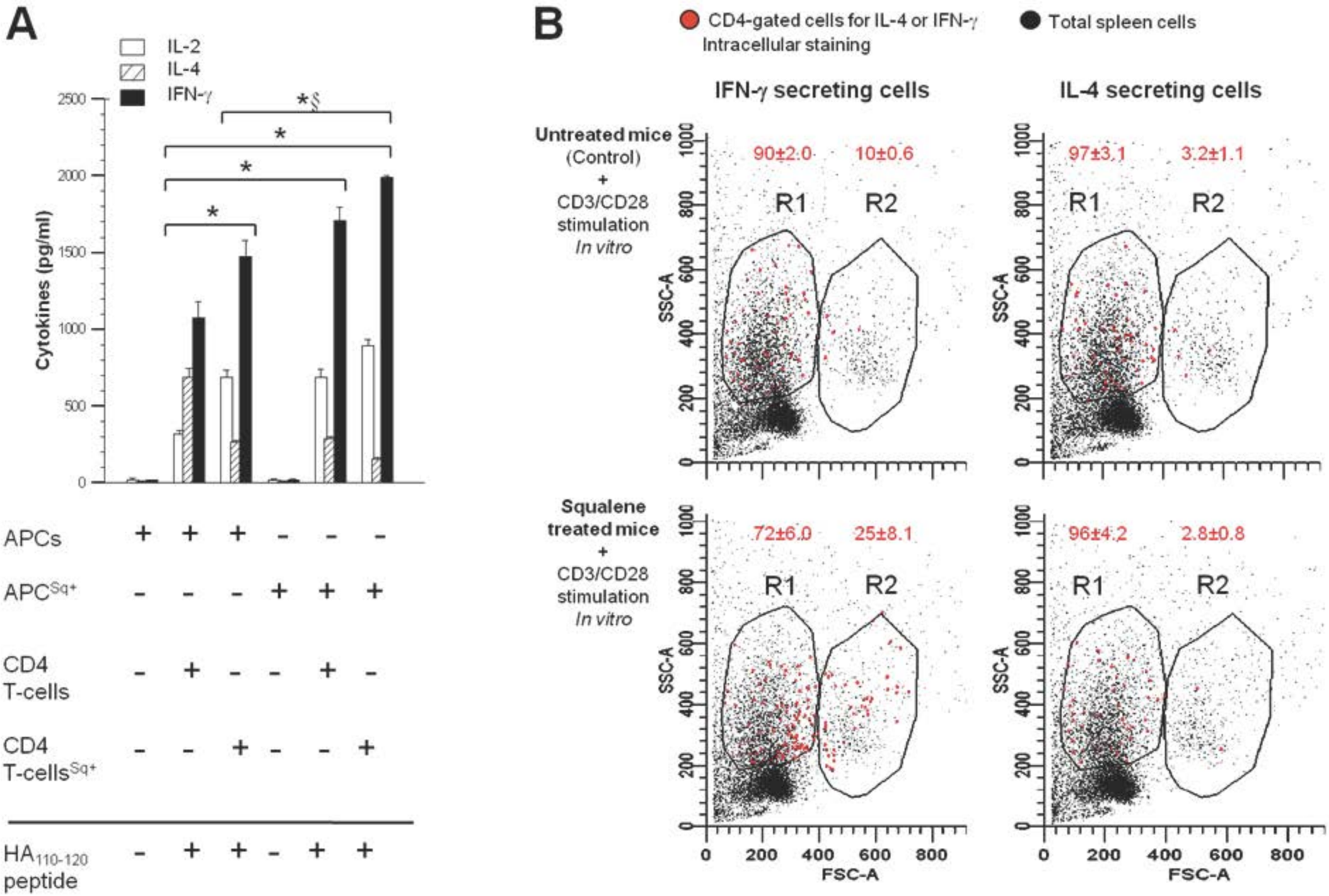
A
IL-2
IL-4
IFN-γ
Cytokines (pg/ml)
2500
2000
1500
1000
500
0
*§
*
*
*
APCs + + + - - -
APC^Sq+ - - - + + +
CD4 T-cells - + - - + -
CD4 T-cells^Sq+ - - + - - +
HA110-120 peptide - + + - + +
B
CD4-gated cells for IL-4 or IFN-γ Intracellular staining
Total spleen cells
IFN-γ secreting cells
IL-4 secreting cells
Untreated mice (Control) + CD3/CD28 stimulation In vitro
Squalene treated mice + CD3/CD28 stimulation In vitro
90±2.0
10±0.6
97±3.1
3.2±1.1
72±6.0
25±8.1
96±4.2
2.8±0.8
R1
R2
SSC-A
FSC-A
0
200
400
600
800
1000

Figure 6

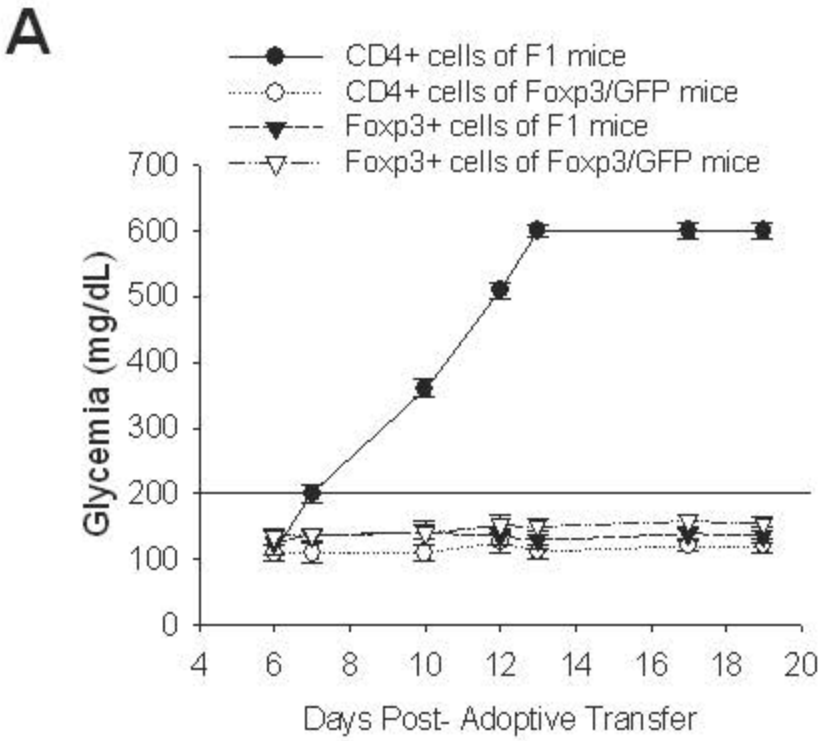
A
CD4+ cells of F1 mice
CD4+ cells of Foxp3/GFP mice
Foxp3+ cells of F1 mice
Foxp3+ cells of Foxp3/GFP mice
Glycemia (mg/dL)
0
100
200
300
400
500
600
700
4
6
8
10
12
14
16
18
20
Days Post- Adoptive Transfer

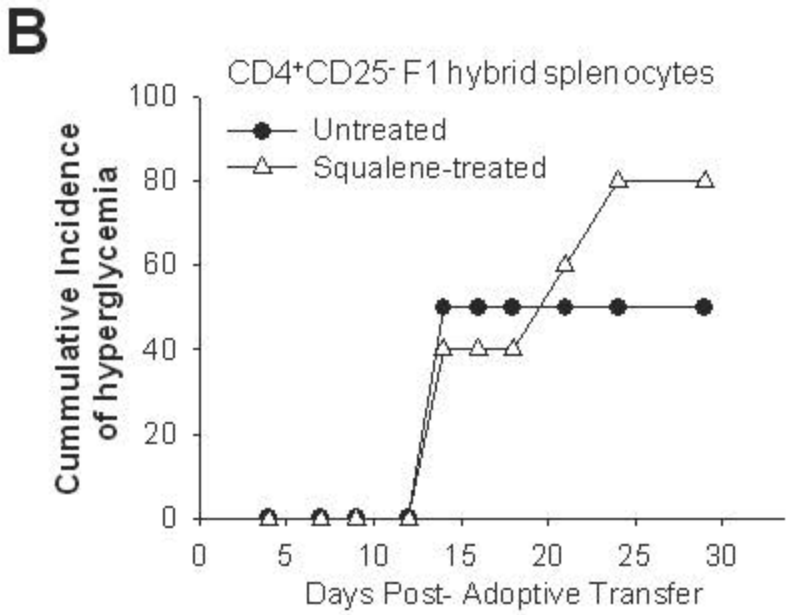
B
CD4+CD25- F1 hybrid splenocytes
Untreated
Squalene-treated
Cummulative Incidence of hyperglycemia
0
20
40
60
80
100
0
5
10
15
20
25
30
Days Post- Adoptive Transfer

Figure 7

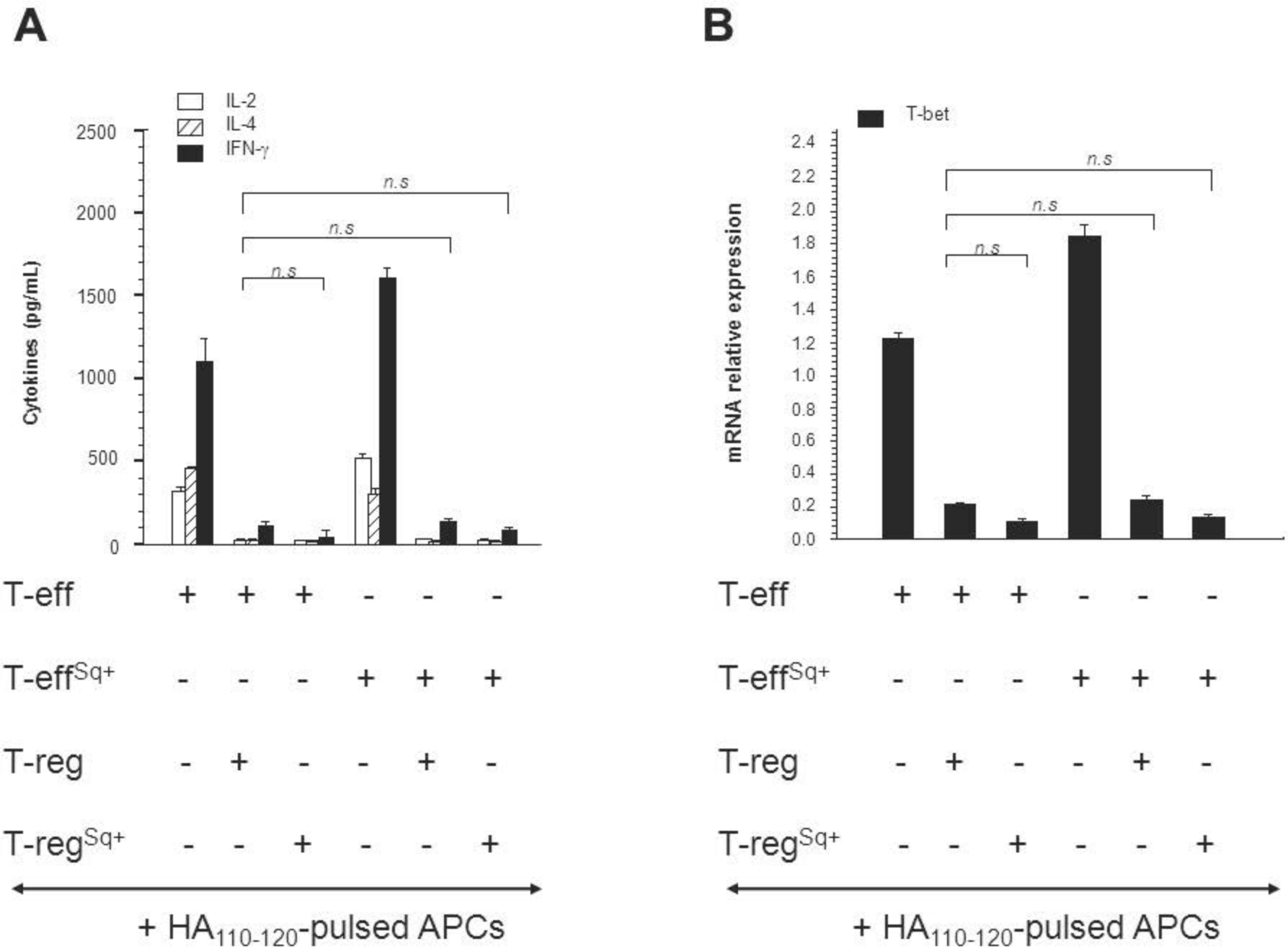
A
IL-2
IL-4
IFN-γ
Cytokines (pg/mL)
2500
2000
1500
1000
500
0
n.s
n.s
n.s
T-eff + + + - - -
T-eff^Sq+ - - - + + +
T-reg - + - - + -
T-reg^Sq+ - - + - - +
+ HA110-120-pulsed APCs
B
T-bet
mRNA relative expression
2.4
2.2
2.0
1.8
1.6
1.4
1.2
1.0
0.8
0.6
0.4
0.2
0.0
n.s
n.s
n.s
T-eff + + + - - -
T-eff^Sq+ - - - + + +
T-reg - + - - + -
T-reg^Sq+ - - + - - +
+ HA110-120-pulsed APCs

Figure 8

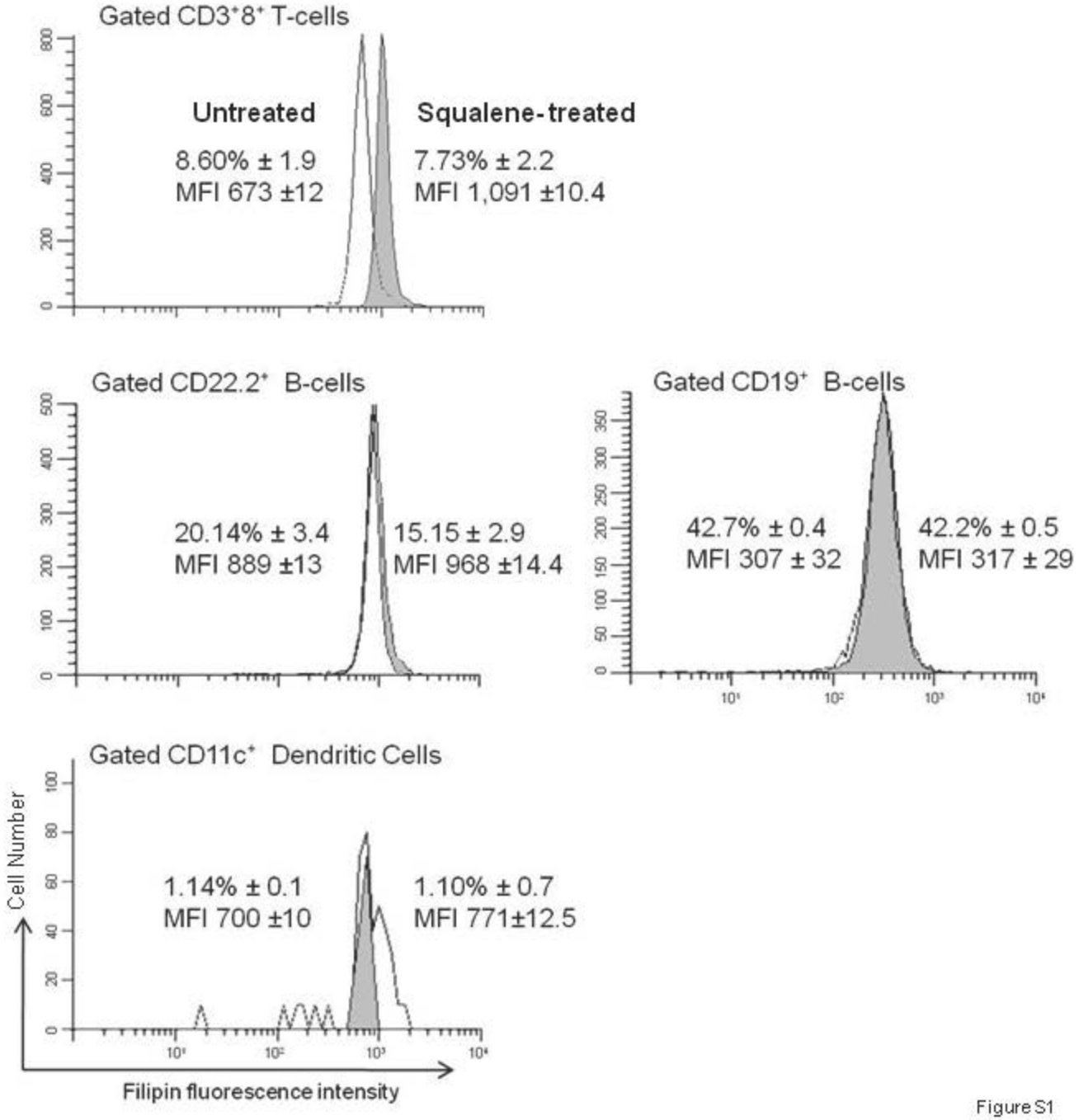
Gated CD3+8+ T-cells
Untreated
Squalene-treated
8.60% ± 1.9
MFI 673 ±12
7.73% ± 2.2
MFI 1,091 ±10.4
Gated CD22.2+ B-cells
20.14% ± 3.4
MFI 889 ±13
15.15 ± 2.9
MFI 968 ±14.4
Gated CD19+ B-cells
42.7% ± 0.4
MFI 307 ± 32
42.2% ± 0.5
MFI 317 ± 29
Gated CD11c+ Dendritic Cells
1.14% ± 0.1
MFI 700 ±10
1.10% ± 0.7
MFI 771±12.5
Cell Number
Filipin fluorescence intensity

Figure S1

A

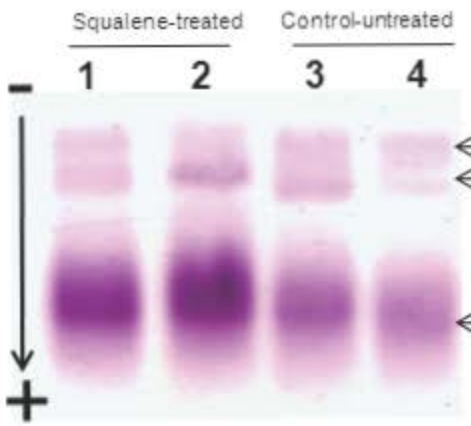

LDL
VLDL
HDL

Band densitometry analysis

1	2	3	4
13897	14232	12950	12477
10234	16736	13457	6439
15104	16290	10639	7909

B

Fat tissue (cholesterol positive staining)

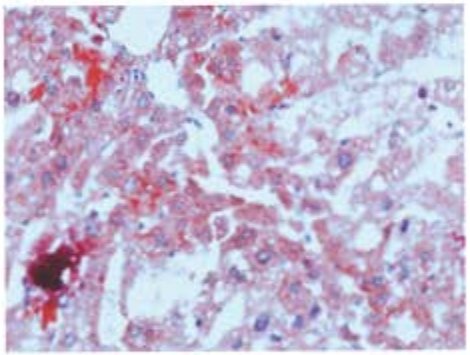

X40

Liver: untreated F1 mouse

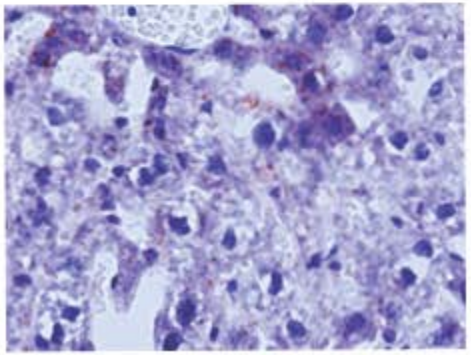

X40

Liver: Squalene-treated F1 mouse

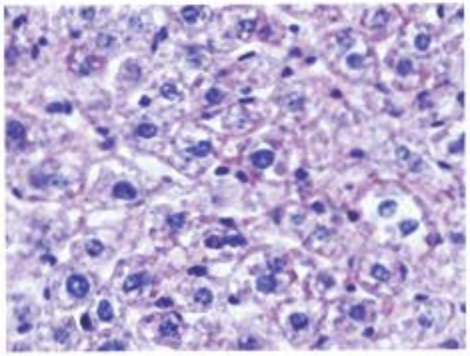

X40

Figure S2

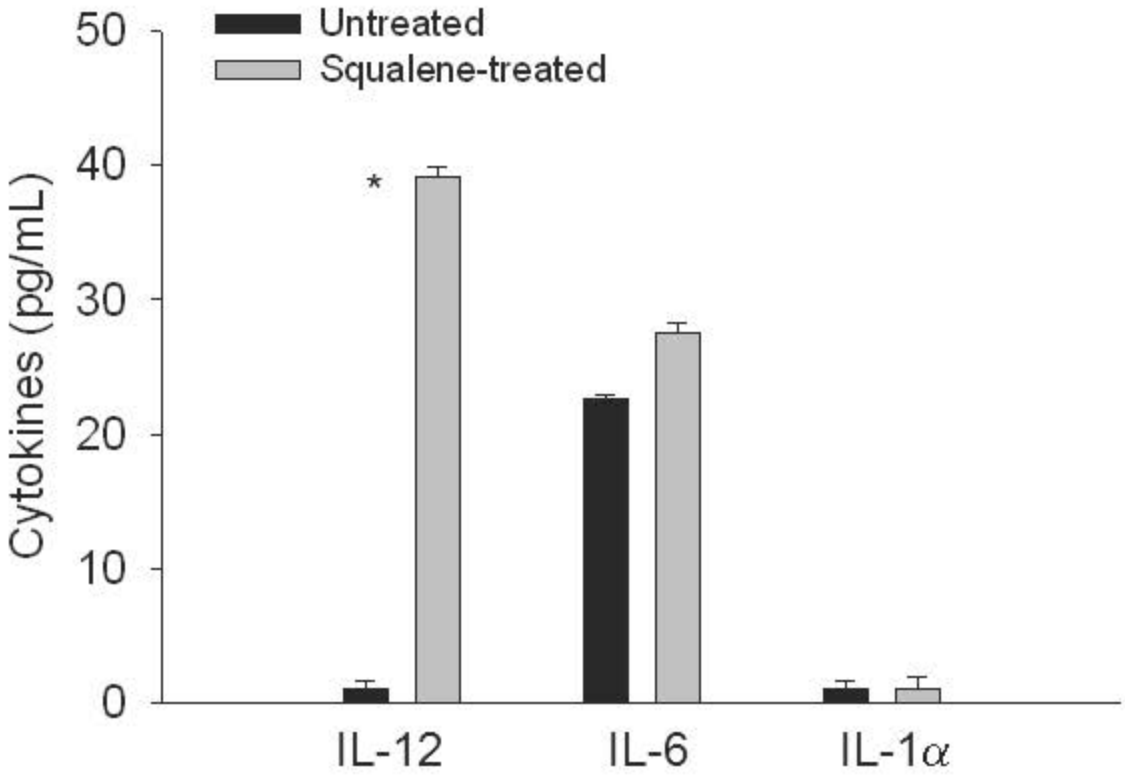
Untreated
Squalene-treated
Cytokines (pg/mL)
50
40
30
20
10
0
*
IL-12
IL-6
IL-1α

Figure S3

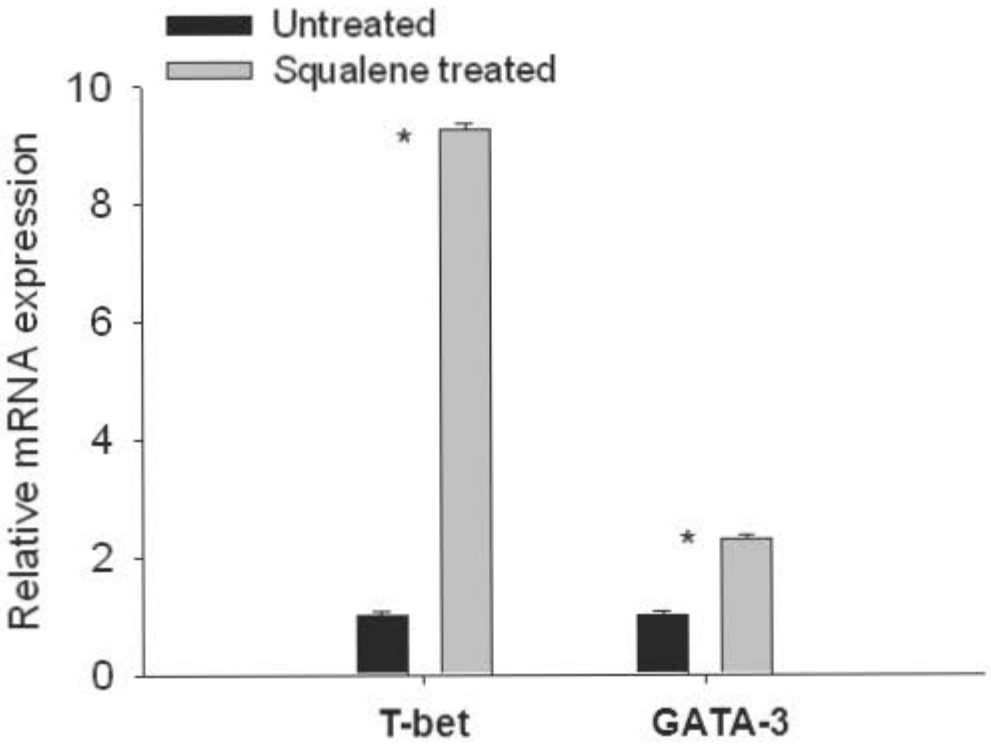
Untreated
Squalene treated
Relative mRNA expression
10
8
6
4
2
0
*
*
T-bet
GATA-3

Figure S4

Dissertation Discussion

Given the large body of evidence that argues for the suppressogenic effect of T-regs on the anti-viral immune responses, it is crucial that we extend our investigation to their effect on vaccination. In the first part of this dissertation, I found that influenza vaccination expanded the $Foxp3^+$ T-reg pool by almost 30% and 100%, 14 and respectively 42 days post-vaccination of BALB/c mice with a single dose of influenza A/PR/8/34 virus vaccine. This finding was consistent with previous reports describing an increased number of antigen-specific T-regulatory cells in the periphery of mice and humans infected with influenza [Giamarellos-Bourboulis et al 2009].

T-regs may indirectly suppress the humoral immune response by inhibition of helper T-cell function to secrete stimulatory cytokines (i.e., IL-4, IL-5, and IL-6) that are necessary for proliferation and differentiation. Recent reports suggest that T-regs can directly suppress B-cells by inducing apoptosis *in vivo* and *in vitro* in a contact-dependent manner [Iikuni et al 2009 (*in vivo study*), Zhao et al 2006, Lim et al 2005 *(in vitro studies)*]. Thus, I analyzed their effect on the influenza specific B-cell responses since they are crucial in generating neutralizing antibodies necessary for viral clearance.

However, I found no significant differences in the generation of neutralizing virus antibody titers in mice having a two-fold increase in the size of $Foxp3^+$ T-reg pool over the pre-existent pool (before vaccination) compared to control mice, as measured by hemagglutination inhibition assay. This assay is the hallmark for testing vaccine efficacy and my findings clearly indicated that T-reg enrichment in PR8 vaccinated BALB/c mice did not effect the production of PR8 neutralizing antibodies. On the contrary, I found the primary and memory virus-specific T helper responses significantly suppressed in mice

enriched with T-regs, as indicated by reductions in lymphocyte proliferation, Th1/Th2 cytokine secretion, and Th1/Th2 transcription factor mRNA expression. IL-10 secretion, being the exception, was significantly increased in stimulated splenocytes from vaccinated, T-reg enriched mice compared to mice vaccinated with PR8 alone, 42 days post-vaccination. The CD4 Th2, $Foxp3^+$ T-reg, and TR1 cell subsets are capable of secreting IL-10, along with various other immune cells under certain conditions [reviewed by Moore et al 2001, Saraiva and O'Garra 2010]. IL-10 is an anti-inflammatory cytokine that has been shown to inhibit activation and effector functions such as cytokine secretion in T-cells, monocytes, macrophages, dendritic cells, and growth and differentiation of B-cells [Moore et al 2001]. A relative increase in $CD4^+Foxp3^+$ T-regs remained by day 42 post-vaccination, therefore it is possible that T-regs contributed to the noticeable increase in IL-10 secretion upon Con A stimulation *in vitro,* since this was not seen in control mice. However, I can not be certain that $CD4^+Foxp3^+$ T-regs, indeed, are causative for the observed levels of IL-10 since total splenocytes (including T effectors) were present in the culture system.

The CD4 T-cells play an essential role in humoral immunity by providing B-cell activation and immunoglobulin isotype switching through direct interaction. They can also help indirectly through the provision of critical cytokines that support B-cell differentiation (ie., IL-4, IFN-γ, or TGF-β). Thus, IL-4 induces IgG1 and IgE, IFN-γ induces IgG2a and IgG3, and TGF-β induces IgG2b and IgA production [Coffman and Carty 1986, Snapper and Paul 1987, McIntyre et al 1993]. Despite a significant reduction in CD4 T helper responses in PR8-immunized mice enriched with T-regs compared to mice immunized with PR8 alone, I did not observe a difference in the PR8-specific Ig

response. This may suggest that other immune cells are able to provide sufficient B-cell help. B-cells themselves express TLRs like TLR7 which has been reported to engage influenza virus RNA during infection [Lund et al 2004]. Moreover, it was demonstrated that inactivated influenza virus induces activation of human B-cells [Marshall-Clarke et al 2005]. In this study we did not analyze the effect of T-reg enrichment on CD8 T-cells or NK cells which are also capable of secreting IFN-γ. However, a strong CD8 T-cell response is not generally induced by inactivated influenza virus vaccination. As for NK cells, it was reported that inactivated influenza virus vaccination augments NK activity [Schapiro et al 1990]. Others have demonstrated that both CD4 KO and CD40 KO mice generate virus-specific IgG responses following influenza immunization or infection, respectively. Moreover, these knockout strains developed protective PR8-specific neutralizing antibodies in a CD4 or CD40 independent mechanism [Sha and Compans 2000, Lee et al 2005]. Sha and Compans hypothesized that double negative $CD4^-CD8^-$ (DN) T-cells may compensate for CD4 T-cell functions to support B-cell responses in CD4 KO mice based on the observation that these mice expressed a significant increase in DN T-cell numbers compared to wildtype. According to these findings, immune cells other than CD4 T-cells may provide adequate support for the B-cell responses despite suppressed CD4 T-cell function, particularly following immunization with a high dose of virus in mice. It remains to be addressed the mechanisms by which PR8 vaccination elicits a T-independent antibody response.

In an alternative approach, I show that RAG2 KO mice adoptively transferred with syngeneic splenocytes depleted of $CD25^+$ population have significantly enhanced PR8-specific T helper cytokine secretion 8 days post-vaccination upon *in vitro* re-stimulation,

as compared to RAG2 KO reconstituted with total splenocytes. Interestingly, RAG2 KO mice reconstituted with CD25 depleted splenocytes showed an increase in relative Foxp3 mRNA expression following PR8 vaccination. This finding is consistent with a number of reports indicating that T-regs may differentiate from peripheral naïve $CD4^+$ T-cells upon encountering antigen and in the presence of TGF–β, or IL-2 and IL-15 [Walker et al 2005, Thornton et al 2000, Andersson et al 2008, Lio et al 2008].

I also addressed the suppressive function of $CD4^+25^+$ $Foxp3^+$ T-regs induced by PR8 vaccination *in vivo*. Using a BALB/c, RAG2 KO, RIP-PR8/HA transgenic mouse model in which adoptive transfer of influenza PR8/HA-specific T-effector cells (from a TCR-PR8/HA Tg mouse) induces fulminate diabetes, I found that $CD4^+CD25^+(Foxp3^+)$ T-regs induced in BALB/c mice upon vaccination with PR8 virus, abolished the diabetogenic function of PR8/HA-specific T-effector cells, even in the presence of co-infused diabetogenic T-cells, for as long as 70 days. Additionally, the PR8/HA-specific T-regs protected the pancreatic β-cell insulin secretory function upon glucose challenge testing. The antigen-specificity of PR8 induced T-regs was confirmed by an additional group of mice vaccinated with a Hong Kong virus (BHK) expressing a structurally different HA protein. In this group, the BHK/HA specific T-regs were unable to prevent the induction of diabetes upon co-infusion of diabetogenic T-cells. This clearly demonstrated that the bystander mediated suppression of BHK/HA-specific $Foxp3^+$ T-regs was ineffective in regulating the HA specific diabetogenic T-cells, as opposed to the PR8/HA specific T-regs which completely abolished their effector functions.

It is reported that individual variations in the size of T-reg compartment in various ethnic groups are correlated with susceptibility to autoimmunity [Ban et al 2007].

Additionally, patients with certain types of cancer were shown to have an expanded $CD4^+$ $CD127^{lo}$ $Foxp3^+$ T-reg pool in peripheral blood [Beyer et al 2011]. Thus, gaining a better understanding of how the T-reg pool size affects the anti-viral immune responses induced by vaccination is crucial in determining whether new vaccine strategies are needed in such individuals possessing a larger T-reg compartment.

In summary, I show that the size of $CD4^+Foxp3^+$ T-reg pool is an important modulatory component of the primary and memory T-cell responses to influenza vaccination. However, it remains to be addressed how alterations in the size of the T-reg compartment affect other vaccination types since distinct pathogens and various adjuvants elicit different types of immune responses. These findings may be particularly important for those investigating cell-mediated vaccines where a robust primary CD4 T-cell response is desired.

Several groups are investigating mechanisms to regulate T-reg function in various disease settings as well as for increasing vaccine efficacy. Potential targets for T-reg manipulation include GITR or CTLA-4 blocking antibodies [Shimizu et al 2002, Stephens et al 2004], manipulation of sphingosine 1-phospatate receptor type 1 ($S1P_1$) expression [Liu et al 2009], and engagement of specific TLRs expressed by T-regs to suppress their function [Pasare et al 2003, Yang et al 2004]. However, it was reported that use of a CTLA-4 Ig fusion protein in ocular herpes infection converted $CD4^+$ $CD25^-$ T-cells into $CD4^+$ $CD25^+$ T-regs *in vitro* [Razmara et al 2008], thereby demonstrating the need for a better understanding of the relationship between T-regs and conventional T-cells. Future T-reg manipulation approaches may exploit mechanisms already utilized by certain pathogens in evading the immune system. In *L. major* infection, it was reported

that DCs induce CD103 integrin expression in T-regs, thus maintaining their presence at the site of infection [Suffia et al 2005]. In this same infection and some fungal infections, it was also shown that CCR5 is required for T-reg migration to the skin [Yurchenko et al 2006, Moreira et al 2008, and Kroetz et al 2010]. In transplantation studies, CCR4 was also reported to be important for T-reg migration and graft survival [Lee et al 2005, Yu et al 2011]. Ultimately, any strategy designed for T-reg manipulation must err on the side of caution since autoimmunity ensues in the absence of T-regs. A fine balance must be achieved when manipulating T-reg function *in vivo*, while at the same time maintaining a minimal risk for autoimmunity.

Importantly, all currently approved influenza vaccines work by eliciting an antibody response, and based on our findings T-reg enrichment does not effect the influenza (PR8) specific antibody response in mice. Thus, the manipulation of T-regs prior to vaccination may not be justified, at least as suggested in our animal model.

In the second part of this dissertation, I investigated whether antigen- specific $CD4^+$ T-helper cells and $Foxp3^+$ T-regulatory cell functions are altered by enriching membrane cholesterol. A major component of lipid rafts is cholesterol, which not only maintains membrane fluidity, but also rafts integrity and architecture. It is postulated that membrane cholesterol also influences the structural and functional stability of proteins in and outside of rafts. Thus, membrane cholesterol represents a potential target to modulate immune cell functions. This notion is further supported by the fact that therapeutic drugs designed to lower blood cholesterol like Lovastatin also reduce T-cell membrane cholesterol and alter cell signaling. Alternatively, therapeutic drugs designed to suppress immune cell

signaling such as glucocorticoids, displace crucial T-cell signaling machinery away from cholesterol-rich lipid rafts [Van Laethem et al 2001].

Our approach to enrich membrane cholesterol by *in vivo* intraperitoneal injection of squalene, a late cholesterol biosynthesis precursor, confirmed early studies demonstrating its ability to be converted into cholesterol [Eidinoff et al 1958, Maxwell et al 1958]. The use of *in vitro* squalene treatment was not a feasible alternative, since squalene is not immiscible in water or cell culture media. My preliminary results using various doses of squalene (25, 50, 75, and 180 µg) *in vivo* led me to conclude that a single i.p. injection of squalene at 180µg yielded the optimal membrane cholesterol enrichment in T-cells as determined by Filipin III stained cells in flow cytometry.

Analysis of membrane cholesterol content in various resting, lymphocyte subsets following *in vivo* squalene administration revealed differences between cell subsets in the accumulation of membrane cholesterol. Thus, CD4 T-cells and $CD4^{+}Foxp3^{+}$ T-reg cells, and CD8 T-cells showed the highest cholesterol accumulation (40-55% above baseline), whereas B-cells and dendritic cells showed only a modest increase (5-10% above baseline). One explanation for the observed difference may be that certain cell subsets at rest have a set threshold for membrane cholesterol accumulation, in doing so possibly regulating their activity in the absence of stimulation.

Next, I questioned whether *in vivo* squalene administration altered the expression of key regulatory enzymes in *de novo* cholesterol synthesis. Resting CD4 T-cells from squalene treated mice showed a slight up-regulation in mRNA expression of the rate controlling enzyme HMG-CoA reductase, as compared to untreated mice. Regulation of *de novo* cholesterol synthesis is tightly regulated at several levels. The intracellular

cholesterol sensor, sterol regulatory element binding protein (SREBP) that controls HMG-CoA reductase synthesis, resides in endoplasmic reticulum (ER). A drop in cholesterol levels leads to localization of SREBP to the golgi complex by the associated cleavage-activating integral protein (SCAP) for proteolytic cleavage events. Once released, SREBP translocates to the nucleus and binds to the sterol response element (SRE) of the HMG-CoA reductase gene. Alternatively, a rise in cholesterol levels blocks the proteolytic cleavage events and SREBP is degraded in the nucleus [Berg et al 2007]. Thus, it appears that the introduction of squalene by-passes this regulatory mechanism. One explanation may be that squalene not only enriches plasma membrane cholesterol but also membranes of intracellular organelles like the ER and golgi that could ultimately alter the structure and function of serine proteases involved in SREBP proteolytic cleavages. Consequently, the serine proteases may become more functionally active, thereby sustaining cholesterol synthesis. As expected, the mRNA expression of the gene involved in squalene cycliczation to form cholesterol, squalene epoxidase, was also up-regulated.

Interestingly, I consistently observed an increased number of resting CD4 splenic T-cells in the absence of T-cell stimulation following membrane cholesterol enrichment by squalene. This was in agreement with early studies showing that provision of cholesterol through high and low density lipoproteins sustains a continuous homeostatic proliferation of T lymphocytes [Cuthberth et al 1987[a], Cuthbert et al 1987[b], Cuthbert et al 1986]. Conversely, the cholesterol lowering drug Atorvastatin, an HMG CoA reductase inhibitor, led to a reduction in the number of T-cells in humans [Ganesan et al 2011]. The molecular mechanism(s) by which membrane cholesterol promotes lymphocyte

proliferation remains largely unknown. In this study I found that CD4 T-cells from squalene treated mice not only had increased membrane cholesterol, but also increased IL-2 secretion. Given that IL-2 is potent T-cell growth factor, it may explain why cell frequency was increased in membrane cholesterol-enriched, resting CD4 T-cells.

Cholesterol-rich lipid rafts may regulate T-cell function through the partitioning of protein receptors and their signaling molecules. We and others have shown that membrane cholesterol depletion alters the distribution and/or function of some T-cell receptors and their ability to signal [Matko et al 2002, Stoica-Nazarov et al 2008]. However, little is known about the effect of membrane cholesterol-enrichment on the spatiotemporal partitioning of protein receptors and subsequent tyrosine phosphorylation events necessary for efficient T-cell signaling.

Analysis of GM1 distribution, a constantly associated lipid raft marker, by CLSM revealed that resting CD4 T-cells from squalene treated mice had a richer distribution throughout the membrane, as compared to untreated mice. This finding further warranted the investigation of alterations in receptor subunits involved in T-cell growth (IL-2Rα), Th1/Th2 differentiation (IL-12Rβ2 and respectively IL-4Rα), as well as their phosphorylated signaling molecules (STAT-5, STAT-4, and respectively STAT-6).

Although overall protein synthesis in resting CD4 splenic T-cells remained quantitatively unchanged after enrichment of membrane cholesterol, fine alterations in tyrosine phosphorylation were detectable. In the absence of stimulation, increased recruitment of phosphorylated- STAT-4 to IL-12Rβ2, STAT-5 to IL-2Rα, and ZAP-70 to CD3 ζ-chain was detected, whereas phosphorylated STAT-6 recruitment was decreased in membrane cholesterol enriched CD4 T-cells relative to base levels. As discussed

earlier (see introduction), the TCR/CD3 ζ-chain, IL-2Rα and IL-4Rα subunits are generally located within rafts, unlike IL-12Rβ2 which mostly resides outside of rafts. Interestingly, the ability of CD28 receptor to recruit PI3K was not affected by membrane cholesterol enrichment in resting CD4 T-cells. CD28 signaling also occurs through the binding of adaptor proteins Grb2 or Gads to its proximal cytoplasmic motif, which was reported to promote IL-2 transcription independent of PI3K recruitment [Crooks et al 1995, Kim et al 1998, Sanchez-Lockhart et al 2004]. These results suggested that membrane cholesterol enrichment by squalene influences phosphorylation events favoring a Th1 phenotype, independent of CD4 T-cell stimulation. Also, CD3/CD28 stimulation enhanced mRNA transcription of the Th1 master transcription factor T-bet in membrane cholesterol-enriched CD4 T-cells. This Th1-induced phenotype was also confirmed by increased ability of membrane cholesterol-enriched CD4 T-cells to secrete increased levels of the Th1 signature cytokine IFN-γ and membrane cholesterol-enriched APCs to secrete increased IL-12, upon antigen-specific stimulation. Notably, analysis of membrane cholesterol-enriched CD4 T-cells in a mouse model for inducible T1D showed enhanced reactivity of antigen-specific, diabetogenic Th1 cells.

The spatiotemporal re-distribution of the IL-2Rβ2 subunit into rafts observed by CLSM may explain, in part, why enrichment in membrane cholesterol diverts CD4 T-cells toward a Th1 phenotype. Polarized receptor clustering or 'capping' of IL-2Rα may have also provided more efficient autocrine signaling in membrane cholesterol-enriched CD4 T-cells. This 'capping' phenomenon was also visualized for IL-4Rα; however it did not support enhanced IL-4 signaling through STAT6 phosphorylation. One explanation

may be that membrane cholesterol-enrichment interferes with the assembly or stability of the interaction between IL-4Rα and common γ-chain subunits.

It was of particular interest to determine whether membrane cholesterol enrichment altered antigen-specific $CD4^{+}Foxp3^{+}$ T-reg function, given the findings described above. Since membrane cholesterol content following *in vivo* squalene administration in T-regs was comparable to that of conventional CD4 T-cells, it was intriguing that it did not alter their ability to suppress T-effector cytokine secretion upon antigen-specific *in vitro* stimulation. Secretion of inhibitory molecules by T-regs is one mechanism of suppression which may remain unaffected by membrane cholesterol enrichment. It is not known whether receptors involved in cell-cell contact mediated suppression are redistributed following membrane cholesterol enrichment. It may be of interest to investigate whether the migratory ability of T-regs is altered by membrane cholesterol enrichment, since it was reported that hypercholesterolemia prevents the migration of T-regs to atherosclerotic lesions [Maganto-Garcia et al 2011].

Some HMG-CoA reductase inhibitors (statins) have been reported to reduce T-cell membrane cholesterol, alter T-cell signaling, and interfere with MHC Class II antigen presentation [Brumeanu et al 2006, Goldman et al 1996, Ghittoni et al 2006, Ghittoni et al 2005]. Interestingly, in certain autoimmune diseases characterized by aberrant T-cell activation and inflammation, statins were shown to have beneficial effects [Leung et al 2003, McCarey et al 2004, Van Denderan et al 2006, Vollmer et al 2006]. Given the importance of membrane cholesterol on T-cell activation and MHC Class II expression, it raises the issue whether individuals being treated with statins for high cholesterol have reduced vaccine efficacy, particularly altered B-cell antibody production. In 2007,

Packard and colleagues enrolled 123 healthy volunteers with an average age of 24 and immunized them with hepatitis A vaccine intramuscularly. At the same time, patients were given a 30 day supply of Atorvastatin (40 mg) or placebo. Their findings concluded that Atorvastatin had no effect on the virus-specific antibody production 1 month after vaccination and statin treatment, despite having significantly reduced total cholesterol compared to placebo. However, the authors do not pre-treat with Atorvastatin for one month prior to vaccination which may be a better indicator of whether statins effect vaccination since the maximum effect of statins is normally achieved at about 4-6 weeks, well after the development of virus-specific antibodies. In a separate study, 20 healthy individuals with similar baselines for anti-tetanus toxoid antibodies were treated with a short regime of Atorvastatin (10 days, 40 mg/patient) or placebo and on the fifth day administered a tetanus toxoid (TT) booster. They found that short-term Atorvastatin treatment significantly reduced total lymphocytes 6 days after booster but returned to baseline by day 15 [Lee et al 2006]. Interestingly, they showed increased anti-TT IgG1 antibodies compared to placebo 15 days after booster. It is known that antibodies generated against TT are mostly IgG1, but the finding that short term statin treatment increased anti-TT IgG1 antibodies compared to placebo conflicts with previous findings by Packard et al. The major differences between the two studies are the starting point of Atorvastatin treatment, duration of statin treatment, and type of viral vaccination (ie., hepatitis A vs. tetanus toxoid and initial vaccination vs. booster). Thus, it is difficult to interpret the effect on statins on vaccination, according to these studies. In my study, I found no significant alterations in membrane cholesterol content in B cells and dendritic cells following a single dose of squalene treatment (180 μg) in mice, suggesting that

these cells may have a different threshold for changes in membrane cholesterol as opposed to T-cells. It is possible that unlike T-cells, B cells are unaffected by statins which would agree with the findings by Packard et al, however this does not explain why short-term statin treatment would increase antibody production. A major caveat of the second study compared to the first study is the sample size (Lee study, 20 vs. Packard study, 123 participants). Overall, the effect of statins on vaccination in humans is still unclear.

A question that remains to be addressed is to what extent squalene enrichment of membrane cholesterol vs. squalene itself contributes to the sensitization of CD4 T-cells towards Th1 differentiation. It is well documented that certain hydrocarbon oils like incomplete Freud's adjuvant (IFA) and the mineral oil component pristine can induce inflammation, particularly when injected intraperitoneally in mice. However, much less is known about whether squalene acts in a similar mechanism. In our study, I did not observe any abnormalities by gross macroscopic examination of the peritoneum or the major organs within the abdominal cavity or of the liver or spleen by H&E histological analysis in mice treated with a single dose (180 μg) of squalene. However, mice treated with four doses (180 μg/dose) given in one week intervals had increased accumulation of cholesterol in the spleen and liver, in addition to increased serum HDL cholesterol fraction, thus the reason for choosing a single squalene dose for subsequent experiments. The increased fraction of HDL may be explained by the increase of overall cholesterol in squalene treated mice thereby promoting cellular cholesterol transfer to HDL. It has been previously reported by Satoh and colleagues that a large dose of squalene injected intraperitoneally (0.5 mL) resulted in increased levels of IL-12, IL-6, and TNF-α

secretion in the peritoneal lavage compared to PBS treated mice. At this dose, squalene was reported to be a much weaker inducer of IL-12 and IL-6 compared to pristine and IFA. Similarly, we found increased IL-12 production in APCs isolated from the spleen of mice treated with a single dose of squalene (180 μg) compared to untreated mice which enhanced IFN-γ production by CD4 T-cells following co-culturing with antigen-pulsed APCs. However, we did not observe a significant difference in IL-6 or IL-1α secretion. Based on the findings by Satoh and colleagues, squalene has the potential to be an inflammatory agent when injected intraperitoneally at higher doses. It remains to be addressed whether a single dose of squalene at 180 μg treatment in mice increases the inflammatory cytokines IL-12, IL-6, and TNF-α in the peritoneal cavity following i.p. injection.

Squalene has been used as an adjuvant for many vaccines; however the mechanism by which it exerts its immune modulatory properties is unclear. It is reported that the MF59 adjuvant (squalene in water emulsion) delays release of antigen, stimulates cytokine production, and enhances recruitment of dendritic cells at the injection site [Seubert et al 2008]. A pertinent question to ask is whether squalene can activate the immune response by binding to innate immune receptors. The innate immune response utilizes pattern recognition receptors generally expressed by APCs such as Toll-like receptors (TLR) and Nod-like receptors (NLR) in order to sense danger and generate an inflammatory response. In the context of vaccination, certain adjuvants like alum have been shown to activate the Nod-like receptor 3 (NLRP3) inflammasome complex. This inflammasome complex is composed of a sensor protein (NLRP3), the adapter protein ASC, and the inflammatory protease caspase-1. Upon cellular stress like infection, the

inflammasome complex mediates the production of mature IL-1β. This inflammatory cytokine is involved with fever, T-cell activation, and macrophage activation. A recent study using various knock out (KO) mice for the NLRP3 inflammasome complex reported that ASC KO mice produced significantly less virus-specific IgG antibodies after MF59 adjuvanted H5N1 intramuscular vaccination compared to wild type mice [Ellebedy et al 2011]. Interestingly in the same study, the NLRP3 KO or Caspase-1 KO mice did not effect virus-specific IgG or HAI titers. The authors conclude that ASC plays a critical role in the induction of an antigen-specific antibody response to MF59 adjuvanted H5N1 vaccine, independent of NLRP3 and Caspase-1. This finding was recently confirmed by Seubert and colleagues who also showed that MF59 adjuvanticity is independent of NLRP3 using NLRP3 KO mice vaccinated intraperitoneally with *Neisseria meningitides* antigens and that bone marrow-derived DCs treated with increasing doses of MF59 alone *in vitro* do not induce pro IL-1β processing [Seubert et al 2011]. Additionally, they show that TLRs are not activated by MF59 *in vitro* using a TLR reporter system, however MyD88 KO mice administered MF59 adjuvanted *Neisseria meningitidis* serotype B vaccination had significantly reduced levels of antigen-specific antibody production compared to wildtype. It remains to be addressed whether TLR activation occurs following MF59 *in* vivo and whether MyD88 is critical for influenza-specific antibody production. Together, these findings suggest that MF59 may act independently of inflammasome complex formation. The use of innate immune component knockout mice (ie., TLR KO, MyD88 KO, NALP KO, and RIG-I KO mice) treated with squalene or squalene adjuvanted influenza vaccines will provide a better understanding for the role of squalene as an innate inflammatory stimulus.

A potential immune molecule that squalene may bind is the MHC-I like protein CD1d, which is expressed by dendritic cells, B-cells, monocytes, and some thymocytes in mice. The CD1d molecule is generally responsible for presenting microbial lipids to CD1 restricted T-cells like the invariant natural killer T-cells (iNKT) which upon activation can secrete Th1 and Th2 cytokines to activate NK cells, DCs, and T-cells [Brigl and Brenner 2004]. Because the CD1 structure contains a hydrophobic channel it is able to bind hydrocarbon alkyl chains like glycolipids. Galli and colleagues found that mice immunized with H3N2 influenza virus adjuvanted with α-galactosylceramide (αGC), a glycolipid known to activate iNKT via CD1d presentation, lead to enhanced virus-specific IgG antibody titers compared to mice immunized with virus alone or adjuvanted with alum [Galli et al 2007]. They also compared the adjuvant effect of αGC with MF59 and found they both provided a similar degree of protection following H1N1 influenza challenge in mice. Although they do not further investigate the mechanisms of squalene on iNKT activation, they found that iNKTs activated by αGC elicited an enhanced anti-viral antibody response and promoted the generation of antigen-specific CD4 T-cells. Thus, it is possible that squalene adjuvanted vaccines work in the same manner, yet this remains to be addressed.

In our study, we found an increase in membrane lymphocyte cholesterol as early as 3 days following squalene treatment. The first 1-2 weeks following influenza vaccination is a critical time period for the development of protective anti-viral immune responses. According to the World Health Organization, squalene adjuvants have been reported to contain 10 mg of squalene per dose. This is a sufficient amount of squalene at the site of injection to potentially activate the innate immune responses in conjunction with viral

antigens, as well as squalene uptake by recruited lymphocytes to synthesize membrane cholesterol. Since squalene is an oil it provides a slow release of antigen, which may sustain stimulation leading to enhanced B-cell responses. Together, these mechanisms may contribute to how squalene works as an adjuvant.

There is a growing appreciation for how membrane cholesterol influences lymphocyte functions. In the current study, I show that *in vivo* squalene administration leads to membrane cholesterol-enrichment in peripheral lymphocytes. Consequently, CD4 T-cells are diverted toward a T-helper type 1 response. This was found to be in association with enhanced Th1 signaling and spatiotemporal redistribution of Th1 and Th2 associated cytokine receptors. Membrane cholesterol may represent a potential target to modulate immune cell functions in various conditions like autoimmunity, infection, vaccination, and allergic immune responses. Therefore, understanding the cellular and molecular changes associated with alterations in membrane cholesterol will help facilitate the design of such pharmacological agents.

Bibliography

Aandahl EM, Michaelsson J, Moretto WJ, et al. Human CD4+ CD25+ regulatory T cells control T-cell responses to human immunodeficiency virus and cytomegalovirus antigens. J Virol 2004;78:2454-9.

Arcaro A, Gregoire C, Boucheron N, et al. Essential role of CD8 palmitoylation in CD8 coreceptor function. J Immunol 2000;165:2068–76.

Afkarian M, Sedy JR, Yang J, et al. T-bet is a STAT1-induced regulator of IL-12R expression in naive CD4 T cells. Nat Immunol. 2002;3:549-557.

Andersson J, Tran DQ, Marko P, et al. CD4+ Foxp3+ regulatory T cells confer infectious tolerance in TGF-β dependent manner. J Exp Med 2008; 205:1975-81.

Baecher-Allan C, Wolf E, Hafler DA. MHC class II expression identifies functionally distinct human regulatory T cells. J Immunol 2006;176(8):4622-31.

Ban Y, Tozaki T, Tobe T, et al. The regulatory T cell gene FOXP3 and genetic susceptibility to thyroid autoimmunity: an association analysis in Caucasian and Japanese cohorts. J Autoimmun 2007; 28:201-7.

Barthlott T, Moncrieffe H, Veldhoen M, et al. CD25+ CD4+ T cells compete with naive CD4+ T cells for IL-2 and exploit it for the induction of IL-10 production. Int Immunol. 2005 Mar;17(3):279-88. Epub 2005 Jan 31.

Bennett CL, Christie J, Ramsdell F, et al. The immune dysregulation, polyendocrinopathy, enteropathy, X-linked syndrome (IPEX) is caused by mutations of FOXP3. Nature Genet 2001;27: 20-21.

Berg JM, Tymoczko JL, Stryer L. Biochemistry. Sixth Ed. New York: Freeman and Company, 2007. Pg.742.

Beyer M, Classen S, Endl E, et al. Comparative approach to define increased regulatory T cells in different cancer subtypes by combined assessment of CD127 and FOXP3. Clin Dev Immunol. 2011;2011:734036.

Bopp T, et al. Cyclic adenosine monophosphate is a key component of regulatory T cell-mediated suppression. J Exp Med 2007;204:1303–1310.

Borsellino G, Kleinewietfeld M, Di Mitri D, et al. Expression of ectonucleotidase CD39 by Foxp3+ Treg cells: hydrolysis of extracellular ATP and immune suppression. Blood 2007;110(4):1225-32.

Brigl M, Brenner MB. CD1: antigen presentation and T cell function. Annu Rev Immunol. 2004;22:817-90.

Brumeanu TD, Preda-Pais A, Stoica C, et al. Differential partitioning and trafficking of GM gangliosides and cholesterol-rich lipid rafts in thymic and splenic CD4 T-cells. Molec Immunol 2007;44:530-540.

Brumeanu TD, Goldstein R, Casares S. Down-regulation of autoreactive T-cells by HMG CoA reductase inhibitors. Clin Immunol 2006;119: 1-12.

Cabrera R, Tu Z, Xu Y, et al. An immunomodulatory role for CD4(+)CD25(+) regulatory T lymphocytes in hepatitis C virus infection. Hepatology 2004;40:1062-71.

Canda-Sanchez A, Salgado FJ, Perez-Diaz A, et al. Differential distribution of both IL-12Rbeta chains in the plasma membrane of human T cells. J Membr Biol 2009;227: 1-12.

Cantrell DA, Collins MK, Crumpton MJ. Autocrine regulation of T-lymphocyte proliferation: differential induction of IL-2 and IL-2 receptor. Immunology 1988;65: 343-349.

Cantrell D, Smith K. The interleukin-2 T-cell system: a new cell growth model. Science 1984;224: 1312.

Chen Y, Kuchroo VK, Inobe J, et al. Regulatory T cell clones induced by oral tolerance: suppression of autoimmunity encephalomyelitis. Science. 1994;265:1237-1240.

Chen W et al. Conversion of peripheral $CD4^{+}CD25^{-}$ naive T cells to $CD4^{+}CD25^{+}$ regulatory cells by TGF-beta induction of transcription factor Foxp3. J Exp Med 2003;198, 1875−1886.

Clark LB, Appleby MW, Brunkow ME, et al. Cellular and molecular characterization of the scurfy mouse mutant. J Immunol 1999;162(5):2546-54.

Coffman RL, Carty J. A T cell activity that enhances polyclonal IgE production and its inhibition by interferon-gamma. J Immunol. 1986 Feb 1;136(3):949-54.

Collison LW, Pillai MR, Chaturvedi V, et al. Regulatory T cell suppression is potentiated by target T cells in a cell contact, IL-35- and IL-10-dependent manner. J Immunol. 2009 May 15;182(10):6121-8.

Crooks ME, Littman DR, Carter RH, et al. CD28-mediated costimulation in the absence of phosphatidylinositol 3-kinase association and activation. Mol. Cell. Biol. 1995; 15: 6820 – 6828.

Crotty S. Follicular helper CD4 T cells (TFH). Annu Rev Immunol 2011. 29:621–63.

Cuthbert JA, Lipsky PE. Promotion of human T lymphocyte activation and proliferation by fatty acids in low density and high density lipoproteins. J Biol Chem 1986;261: 3620-3627.

Cuthbert JA, Lipsky PE.[a] Regulation of lymphocyte proliferation by cholesterol: the role of endogenous sterol metabolism and low density lipoprotein receptors. Int J Tissue 1987;React 9: 447-457.

Cuthbert JA, Lipsky PE.[b] Provision of cholesterol to lymphocytes by high density and low density lipoproteins. Requirement for low density lipoprotein receptors. J Biol Chem 1987;262: 7808-7818.

Eidinoff ML, Knoll JE, Marano BJ, et al. Cholesterol biosynthesis: studies related to the metabolic role of squalene. J Clin Invest 1958;37: 655-659.

Ellebedy AH, Lupfer C, Ghoneim HE, DeBeauchamp J, Kanneganti TD, Webby RJ. Inflammasome-independent role of the apoptosis-associated speck-like protein containing CARD (ASC) in the adjuvant effect of MF59. Proc Natl Acad Sci U S A. 2011 Feb 15;108(7):2927-32. Epub 2011 Jan 26.

Fallarino F, et al. Modulation of tryptophan catabolism by regulatory T cells. Nat Immunol 2003;4:1206–1212.

Fowell D, Mason D. Evidence that the T cell repertoire of normal rats contains cells with the potential to cause diabetes. Characterization of the CD4+ T cell subset that inhibits this autoimmune potential. J Exp Med 1993;177: 627–636.

Galli G, Pittoni P, Tonti E, et al. Invariant NKT cells sustain specific B cell responses and memory. Proc Natl Acad Sci U S A. 2007 Mar 6;104(10):3984-9. Epub 2007 Feb 27.

Ganesan A, Crum-Cianflone N, Higgins J, et al. High dose atorvastatin decreases cellular markers of immune activation without affecting HIV-1 RNA levels: results of a double-blind randomized placebo controlled clinical trial. J Infect Dis 2011; 203: 756-764

Giamarellos-Bourboulis EJ, Raftogiannis M, Antonopoulou A, et al. Effect of the Novel Influenza A (H1N1) Virus in the Human Immune System. PloS ONE 2009; 4(12):e8393.-2750.

Ghittoni R, Patrussi L, Pirozzi K, et al. Simvastatin inhibits T-cell activation by selectively impairing the function of Ras superfamily GTPases. FASEB J. 2005 Apr;19(6):605-7. Epub 2005 Jan 27.

Ghittoni R, Napolitani G, Benati D, et al. Simvastatin inhibits the MHC class II pathway of antigen presentation by impairing Ras superfamily GTPases. Eur J Immunol. 2006 Nov;36(11):2885-93.

Godfrey VL, Rouse BT, Wilkinson JE. Transplantation of T cell-mediated, lymphoreticular disease from the scurfy (sf) mouse. Am J Pathol 1994;145(2):281-6.

Godfrey VL, Wilkinson JE, Russell LB. X-linked lymphoreticular disease in the scurfy (sf) mutant mouse. Am J Pathol 1991;138(6):1379-87.

Goebel J, Forrest K, Morford L, et al. Differential localization of IL-2- and -15 receptor chains in membrane rafts of human T cells. J Leukoc Biol 2002; 72: 199-206.

Goldman F, Hohl RJ, Crabtree J, et al. Lovastatin inhibits T-cell antigen receptor signaling independent of its effects on ras. Blood 1996; 88: 4611-4619.

Gómez-Martín D, Díaz-Zamudio M, Romo-Tena J, et al. Follicular helper T cells poise immune responses to the development of autoimmune pathology. Autoimmun Rev. 2011 Apr;10(6):325-30.

Gondek DC, Lu LF, Quezada SA, et al. Cutting edge: contact-mediated suppression by CD4+CD25+ regulatory cells involves a granzyme B-dependent, perforin-independent mechanism. J Immunol 2005; 174:1783–1786.

Grossman WJ, et al. Differential expression of granzymes A and B in human cytotoxic lymphocyte subsets and T regulatory cells. Blood 2004;104:2840–2848.

Groux H, O'Garra A, Bigler M, et al. A $CD4^+$ T-cell subset inhibits antigen-specific T-cell responses and prevents colitis. Nature 1997;389:737-742.

Harrington LE, Hatton RD, Mangan PR, et al. Interleukin 17-producing CD4_ effector T cells develop via a lineage distinct from the T helper type 1 and 2 lineages. Nat Immunol 2005;6:1123-1132.

Hillyard DZ, Cameron AJ, McDonald KJ, et al. Simvastatin inhibits lymphocyte function in normal subjects and patients with cardiovascular disease. Atherosclerosis 2004;175:305–313.

Ho YK, Brown S, Bilheimer DW, Goldstein JL. Regulation of low density lipoprotein receptor activity in freshly isolated human lymphocytes. J Clin Invest 1976;58:1465-1474.

Hui-Chen H, PingAr Y, Wang J, et al. Interleukin 17-producing T helper cells amd interleukin 17 orchestrate autoreactive germinal center development in autoimmune BXD2 mice. Nat Immunol 2008;9(2):166-175.

Huber S, Schramm C, Lehr H, et al. Cutting edge: TGF-β signaling is required for the in vivo expansion and immunosuppressive capacity of regulatory CD4+CD25+ T cells. J Immunol 2004;173:6526-6531.

Hurwitz JL, Hackett CJ. Influenza-specific suppression: contribution of major viral proteins to the generation and function of T suppressor cells. J Immunol 1985; 135:2134-39.

Hwang ES, Szabo SJ, Schwartzberg PL, and Glimcher LH. T helper cell fate specified by kinase-mediated interaction of T-bet with GATA-3.Science 2005;307:430-433.

Iikuni N, Lourenco EV, Hahn BH, and La Cava A. Cutting Edge: Regulatory T cells directly suppress B cells in systemic lupus erythematosus. J. Immunol 2009;183:1518–1522.

Ivanov II, Zhou L, Littman DR. Transcriptional regulation of Th17 cell differentiation. Semin Immunol 2007; 19:409-417

Iwashiro M, Messer RJ, Peterson KE, et al. Immunosuppression by CD4+ regulatory T cells induced by chronic retroviral infection. Proc Natl Acad Sci USA 2001;98:9226-30.

Jang E, Cho WS, Cho ML, et al. Foxp3+ regulatory T cells control humoral autoimmunity by suppressing the development of long-lived plasma cells. J Immunol. 2011 Feb 1;186(3):1546-53. Epub 2011 Jan 5.

Jury EC, Isenberg DA, Mauri C and Ehrenstein MR. Atorvastatin restores Lck expression and lipid raft-associated signaling in T cells from patients with systemic lupus erythematosus. J Immunol 177;2006:7416–7422.

Kabouridis PS, Janzen J, Magee AL and Ley SC. Cholesterol depletion disrupts lipid rafts and modulates the activity of multiple signaling pathways in T lymphocytes. Eur J Immunol 2000;30:954–963.

Karube K, Ohshima K, Tsuchiya T, et al. Expression of FoxP3, a key molecule in CD4CD25 regulatory T cells, in adult T-cell leukaemia/lymphoma cells. Br J Haematol 2004;126:81-4.

Kaplan MH, Sun YL, Hoey T, Grusby MJ. Impaired IL-12 responses and enhanced development of Th2 cells in Stat4-deficient mice. Nature 1996;382: 174-177.

Kaplan MH, Schindler U, Smiley ST, Grusby MJ. Stat6 is required for mediating reponses to IL-4 and for development of Th2 cells. Immunity 1996;4:313-319.

Kearley J, Barker JE, Robinson DS, Lloyd CM. Resolution of airway inflammation and hyperactivity after in vivo transfer of CD4+CD25+ regulatory T cells is interleukin 10 dependent. J Exp Med 2005;202; 1539-1547.

Kim, H. H., M. Tharayil, and C. E. Rudd. Growth factor receptor-bound protein 2 SH2/SH3 domain binding to CD28 and its role in co-signaling. J. Biol. Chem. 1998;273: 296 –301.

Kinter AL, Hennessey M, Bell A, et al. CD25(+)CD4(+) regulatory T cells from the peripheral blood of asymptomatic HIV-infected individuals regulate CD4(+) and CD8(+) HIV-specific T cell immune responses in vitro and are associated with favorable clinical markers of disease status. J Exp Med 2004;200:331-43.

Kojima A, Prehn RT. Genetic susceptibility to post-thymectomy autoimmune diseases in mice. Immunogenetics 1981;14:15–27.

Komiyama Y. et al. IL-17 plays an important role in the development of experimental autoimmune encephalomyelitis. J. Immunol. 2006:177, 566–573.

Kroetz DN, Deepe GS, Jr. CCR5 dictates the equilibrium of proinflammatory IL-17+ and regulatory Foxp3+ T cells in fungal infection. J Immunol. 2010;184:5224–31.

Kubach J, Lutter P, Bopp T, et al. Human CD4+CD25+ regulatory T cells: proteome analysis identifies galectin-10 as a novel marker essential for their anergy and suppressive function. Blood 2007;110(5):1550-8.

Kusam S, Toney LM, Sato H, et al. Inhibition of Th2 differentiation and GATA-3 expression by BCL-6. J. Immunol. 2003;170, 2435–2441.

Lee BO, Rangel-Moreno J, Moyron-Quiroz JE, et al. CD4 T cell-independent antibody response promotes resolution of primary influenza infection and helps to prevent reinfection.J Immunol. 2005 Nov 1;175(9):5827-38.

Lee I, Wang L, Wells AD, et al. Recruitment of Foxp3+ T regulatory cells mediating allograft tolerance depends on the CCR4 chemokine receptor. J Exp Med. 2005 Apr 4;201(7):1037-44.

Lee PY, Scumpia PO, Byars JA, et al. Short-term atorvastatin treatment enhances specific antibody production following tetanus toxoid vaccination in healthy volunteers.Vaccine. 2006 May 8;24(19):4035-40. Epub 2006 Jan 9.

Lehoux JG, Kandalaft N, Belisle S, Bellabarba D. Characterization of 3-hydroxy-3-methylglutaryl coenzyme A reductase in human adrenal cortex. Endocrinology 1985; 117: 1462-1468.

Leung BP, Sattar N, Crilly A, et al. A novel anti-inflammatory role for simvastatin in inflammatory arthritis. J Immunol. 2003;170:1524-1530.

Levy-Lahad E, Wildin RS. Neonatal diabetes mellitus, enteropathy, thrombocytopenia, and endocrinopathy: further evidence for an X-linked lethal syndrome. J. Pediat 2001;138: 577-580.

Lim HW, Hillsamer P, Banham AH, Kim CH. Cutting edge: direct suppression of B cells by $CD4^+CD25^+$ regulatory T cells. J Immunol. 2005;175:4180–4183.

Lund JM, Hsing L, Pham TT, Rudensky AY. Coordination of early protective immunity to viral infection by regulatory T cells. Science 2008;320(5880):1220-24.

Lio CW, Hsieh CS. A two-step process for thymic regulatory T cell development. Immunity 2008; 28:100-11.

Loud AV, Bucher NL. The turnover of squalene in relation to the biosynthesis of cholesterol. J Biol Chem 1958;233: 37-41.

Lund JM, Alexopoulou L, Sato A, et al. Recognition of single-stranded RNA viruses by Toll-like receptor 7. Proc. Natl. Acad. Sci. USA 2004; 101: 5598 –5603.

MacDonald AJ, Duffy M, Brady MT, et al. CD4 T helper type 1 and regulatory T cells induced against the same epitopes on the core protein in hepatitis C virus-infected persons. J Infect Dis 2002; 185:720-7.

Maganto-Garcia E, Tarrio ML, Grabie N, et al. Dynamic changes in regulatory T cells are linked to levels of diet-induced hypercholesterolemia. Circulation 2011;124: 185-195.

Mangan PR, Harrington LE, O'Quinn DB, et al. Transforming growth factor-beta induces development of the T(H)17 lineage. Nature 2006;441:231-234.

Marshall-Clarke S, Tasker L, Buchatska O, et al. Influenza H2 haemagglutinin activates B cells via a MyD88-dependent pathway. Eur J Immunol 2006;36:1521-4141

Matko J, Szollosi J.[a] Landing of immune receptors and signal proteins on lipid rafts: a safe way to be spatio-temporally coordinated? Immunol Lett 2002; 82: 3-15.

Matko J, Bodnar A, Vereb G, et al.[b] GPI-microdomains (membrane rafts) and signaling of the multi-chain interleukin-2 receptor in human lymphoma/leukemia T cell lines. Eur J Biochem 2002; 269: 1199-1208.

Maxwell LE, Knoll JE, Marano BJ, et al. Cholesterol Biosynthesis. Studies related to the metabolic role of squalene. J Clin Invest 1958 May; 37(5):655–659.

Mbow ML, De Gregorio E, Valiante NM, Rappuoli R. New adjuvants for human vaccines. Curr Opin Immunol 2010; 22: 411-416.

McCarey DW, McInnes IB, Madhok R, et al. Trial of Atorvastatin in Rheumatoid Arthritis (TARA): double-blind, randomised placebo-controlled trial. Lancet. 2004;363:2015-2021

McIntyre TM, Klinman DR, Rothman P, et al. Transforming growth factor beta 1 selectivity stimulates immunoglobulin G2b secretion by lipopolysaccharide-activated murine B cells. J Exp Med. 1993 Apr 1;177(4):1031-7.

McKinstry KK, Strutt TM, Swain SL. Hallmarks of CD4 T cell immunity against influenza. J Intern Med. 2011 May;269(5):507-18

Mills KHG, McGuirk P. Antigen-specific regulatory T cells: their induction and role in infection. Seminars Immunol 2004;16:107-117.

Montixi C, Langlet C, Bernard AM, et al. Engagement of T cell receptor triggers its recruitment to low-density detergent-insoluble membrane domains. EMBO J 1998; 17: 5334-5348.

Moore KW, de Waal Malefyt R, Coffman RL, O'Garra A. Interleukin-10 and the interleukin-10 receptor. Annu Rev Immunol. 2001;19:683-765.

Moreira AP, et al. CCR5-dependent regulatory T cell migration mediates fungal survival and severe immunosuppression. J Immunol. 2008;180:3049–56.

Mukasa R, Balasubramani A, Lee YK, et al. Epigenetic instability of cytokine and transcription factor gene loci underlies plasticity of the T helper 17 cell lineage. Immunity. 2010 May 28;32(5):616-27. Epub 2010 May 13.

Murakoshi M, Nishino H, Tokuda H, et al. Inhibition by squalene of the tumor-promoting activity of 12-O-tetradecanoylphorbol-13-acetate in mouse-skin carcinogenesis. Int J Cancer 1992;52: 950-952

Nakae S, Nambu A, Sudo K & Iwakura Y. Suppression of immune induction of collagen-induced arthritis in IL-17–def,icient mice. J. Immunol. 2003;171, 6173–6177

Nishizuka Y, Sakakura T. Thymus and reproduction: sex-linked dysgenesia of the gonad after neonatal thymectomy in mice. Science 1969;166:753–755.

Nguyen DH, Espinoza JC, Taub DD. Cellular cholesterol enrichment impairs T cell activation and chemotaxis. Mech Ageing Dev 2004;125: 641-650.

Nurieva RI, Chung Y, Martinez GJ, et al. Bcl6 mediates the development of T follicular helper cells. Science 2009;325:1001–5

Oswald-Richter K, Grill SM, Shariat N, et al. HIV infection of naturally occurring and genetically reprogrammed human regulatory T-cells. PLoS Biol 2004;2:E198.

Owen CJ, Jennings CE, Imrie H, et al. Mutational analysis of the FOXP3 gene and evidence for genetic heterogeneity in the immunodysregulation, polyendocrinopathy, enteropathy syndrome. J Clin Endocrinol Metab. 2003 Dec;88(12):6034-9.

Packard RR, Schlegel S, Senouf D, Burger F, Sigaud P, Perneger T, Siegrist CA, Mach F. Atorvastatin treatment and vaccination efficacy. J Clin Pharmacol. 2007 Aug;47(8):1022-7. Epub 2007 Jun 4.

Pandiyan P, Zheng L, Ishihara S, et al. CD4+CD25+Foxp3+ regulatory T cells induce cytokine deprivation-mediated apoptosis of effector CD4+ T cells. Nat Immunol. 2007 Dec;8(12):1353-62.

Park H, Li Z, Yang XO, et al. A distinct lineage of CD4 T cells regulates tissue inflammation by producing interleukin 17. Nat Immunol 2005;6:1133-1141.

Parolini I, Topa S, Sorice M, et al. Phorbol ester- induced disruption of the CD4-Lck complex occurs within a detergent-resistant microdomain of the plasma membrane. J Biol Chem 1999;274:14176–87.

Passerini L, Di Nunzio S, Gregori S, et al. Functional type 1 regulatory T cells develop regardless of FOXP3 mutations in patients with IPEX syndrome. Eur J Immunol. 2011;41(4):1120–1131.

Penhale WJ, Farmer A, McKenna RP, Irvine WJ. Spontaneous thyroiditis in thymectomized and irradiated Wistar rats. Clin Exp Immunol 1973;15:225–236.

Penhale WJ, Stumbles PA, Huxtable CR, Sutherland RJ, Pethick DW. Induction of diabetes in PVG/c strain rats by manipulation of the immune system. Autoimmunity 1990;7:169–179.

Pralle A, Keller P, Florin EL, et al. Sphingolipid-cholesterol rafts diffuse as small entities in the plasma membrane of mammalian cells. J Cell Biol 2000;148:997–1008.

Prior IA, Muncke C, Parton RG. and Hancock, JF. Direct visualization of Ras proteins in spatially distinct cell surface microdomains. J. Cell Biol. 2003; 160, 165-170.

Rao R, Logan B, Forrest K, Roszman TL, Goebel J. Lipid rafts in cytokine signaling. Cytokine Growth Factor Rev 2004;15: 103-110.

Rao CV, Newmark HL, Reddy BS. Chemopreventive effect of squalene on colon cancer. Carcinogenesis 1998;19: 287-290.

Rouse BT and Sehrawat S. Immunity and immunopathology to viruses: what decided the outcome? Nat Rev Immunol 2010;10:514-526.

Rouse BT, Sarangi PP, Suvas S. Regulatory T cells in virus infections. Immunol Rev 2006;212:272-86.

Razmara M, Hilliard B, Ziarani AK, Chen YH, Tykocinski ML. CTLA-4 x Ig converts

naive CD4+CD25- T cells into CD4+CD25+ regulatory T cells. Int Immunol. 2008 Apr;20(4):471-83. Epub 2008 Feb 13.

Sakaguchi S, Takahashi T, and Nishizuka Y. Study on cellular events in post-thymectomy autoimmune oophoritis in mice. II. Requirement of Lyt-1 cells in normal female mice for the prevention of oophoritis. J Exp Med 1982;156: 1577–1586.

Sakaguchi S, Sakaguchi N, Asano M, Itoh M, Toda M. Immunological self-tolerance maintained by activated T cells expressing IL-2 receptor alpha-chains (CD25). Breakdown of a single mechanism of self-tolerance causes various autoimmune diseases. J Immunol 1995;155:1151-1164.

Sakaguchi S. Naturally arising Foxp3-expressing CD25+CD4+ regulatory T cells in immunological tolerance to self and non-self. Nat Immunol 2005; 6:345-52.

Sakaguchi S, Miyara M, Costantino CM, Hafler DA. FOXP3+ regulatory T cells in the human immune system. Nat Rev Immunol. 2010 Jul;10(7):490-500. Epub 2010 Jun 18.

Sanchez-Lockhart M, Marin E, Graf B, et al. Cutting edge: CD28-mediated transcriptional and posttranscriptional regulation of IL-2 expression are controlled through different signaling pathways. J Immunol. 2004 Dec 15;173(12):7120-4.

Saraiva M, O'Garra A. Nat Rev Immunol. The regulation of IL-10 production by immune cells.2010 Mar;10(3):170-81. Epub 2010 Feb 15.

Schapiro JM, Segev Y, Rannon L, Alkan M, Rager-Zisman B. Natural killer (NK) cell response after vaccination of volunteers with killed influenza vaccine. J Med Virol. 1990 Mar;30(3):196-200.

Seddiki N, Santner-Nanan B, Tangye SG, Alexander SI, Solomon M, Lee S, Nanan R, Fazekas de Saint Groth B. Persistence of naive CD45RA^{+} regulatory T cells in adult life. Blood 2006;107:2830–2838.

Serra P, et al. CD40 ligation releases immature dendritic cells from the control of regulatory CD4+CD25+ T cells. Immunity 2003;19:877–889.

Seubert A, Monaci E, Pizza M, O'Hagan DT, Wack A. The adjuvants aluminum hydroxide and MF59 induce monocyte and granulocyte chemoattractants and enhance monocyte differentiation toward dendritic cells. J Immunol 2008;180:5402–5412

Seubert A, Calabro S, Santini L, et al. Adjuvanticity of the oil-in-water emulsion MF59 is independent of Nlrp3 inflammasome but requires the adaptor protein MyD88. Proc Natl Acad Sci U S A. 2011 Jul 5;108(27):11169-74. Epub 2011 Jun 20.

Simons K and Toomre D. Lipid rafts and signal transduction. Nat. Rev. Mol. Cell Biol. 2000; 1, 31-39.

Smith RH, Ziola B. Cyclophosphamide and dimethyl dioctadecyl ammonium bromide immunopotentiate the delayed-type hypersensitivity response to inactivated enveloped viruses. Immunology 1986; 58(2):245-50.

Snapper CM, Paul WE. B cell stimulatory factor-1 (interleukin 4) prepares resting murine B cells to secrete IgG1 upon subsequent stimulation with bacterial lipopolysaccharide. J Immunol. 1987 Jul 1;139(1):10-7.

Sonderegger, I. et al. Neutralization of IL-17 by active vaccination inhibits IL-23–dependent autoimmune myocarditis. Eur. J. Immunol. 2006;36, 2849–2856.

Stevens TJ, and Arkin, IT. Do more complex organisms have a greater proportion of membrane proteins in their genomes? Proteins 2000;39, 417–420.

Suffia I, Reckling SK, Salay G, Belkaid Y. A role for CD103 in the retention of CD4+ CD25+ Treg and control of Leishmania major infection. J Immunol. 2005;174:5444–55.

Sugimoto K, Ikeda F, Stadanlick J, Nunes FA, Alter HJ, Chang KM. Suppression of HCV-specific T cells without differential hierarchy demonstrated ex vivo in persistent HCV infection. Hepatology 2003;38:1437-48.

Sun J, Madan R, Karp CL, Braciale TJ. Effector T cells control lung inflammation during acute influenza virus infection by producing IL-10. Nat Med 2009; 15:277-84.

Suvas S, Azkur AK, Kim BS, et al. CD4+CD25+ regulatory T cells control the severity of viral immunoinflammatory lesions. J Immunol 2004;172:4123-32.

Szabo SJ, Dighe AS, Gubler U, Murphy KM. Regulation of the interleukin (IL)-12R beta 2 subunit expression in developing T helper 1 (Th1) and Th2 cells. J Exp Med 1997;185:817-824.

Szabo SJ, Kim ST, Costa GL, et al. A novel transcription factor, T-bet, directs Th1 lineage commitment. Cell 2000;100:655–669.

Szabo SJ, Sullivan BM, Stemmann C, et al. Distinct effects of T-bet in TH1lineage commitment and IFN-gamma production in CD4 and CD8 T cells. Science 2002;295:338–342.

Tani-ichi S, Maruyama K, Kondo N, Nagafuku M, Kabayama K, et al. Structure and function of lipid rafts in human activated T cells. Int Immunol 2005;17: 749-758.

Thomas S, Kumar RS, Brumeanu TD. Role of lipid rafts in T cells. Arch Immunol Ther Exp (Warsz) 2004;52: 215-224.

Thornton AM, Shevach EM. Suppressor effector function of CD4+CD25+ immunoregulatory T cells is antigen nonspecific. J Immunol 2000; 164:183-90.

Tilvis RS, Miettinen TA. Dietary squalene increases tissue sterols and fecal bile acids in the rat. Lipids 1983;18: 32-36.

Usui T, Preiss JC, Kanno Y, et al. T-bet regulates Th1 responses through essential effects on GATA-3 function rather than on IFNG gene acetylation and transcription. J Exp Med 2006;203:755-766.

Vahlenkamp TW., Tompkins MB, Tompkins WAF. The role of CD4+CD25+ regulatory T cells in viral infections. Veterinary Immunol.Immunopathol. 2005;108:219-225.

Van Denderen JC, Peters M, Halm VV, et al. Statin therapy might be beneficial for treating patients with ankylosing spondylitis. Ann Rheum Dis. 2006;65:695-696

Van Duuren BL, Goldschmidt BM. Cocarcinogenic and tumor-promoting agents in tobacco carcinogenesis. J Natl Cancer Inst 1976;56: 1237-1242.

Veldhoen M, Hocking RJ, et al. TGFbeta in the context of an inflammatory cytokine milieu supports de novo differentiation of IL-17-producing T cells.Immunity. 2006 Feb;24(2):179-89.

Verhoeye FR, Descamps O, Husson B, et al. An improved method for detection of low density lipoprotein receptor defects in human T lymphocytes. J Lipid Res 1996; 37: 1377-1384.

Viola A, Schroeder S, Sakakibara Y, Lanzavecchia A. T lymphocyte costimulation mediated by reorganization of membrane microdomains. Science 1999;283: 680-682.

Vinton C, Klatt NR, Harris LD, et al. CD4-like immunological function by CD4- T cells in multiple natural hosts of simian immunodeficiency virus. J Virol. 2011 Sep;85(17):8702-8. Epub 2011 Jun 29.

Vollmer T, Key L, Durkalski V, et al. Oral simvastatin treatment in relapsing-remitting multiple sclerosis. Lancet. 2004;363: 1607-1608

Walker MR, Carson BD, Nepom GT, et al. De novo generation of antigen-specific CD4+CD25+ regulatory T cells from human CD4+CD25- cells. Proc Natl Acad Sci U S A 2005; 102:4103-8.

Weiss L, Donkova-Petrini V, Caccavelli L, et al. Human immunodeficiency virus-driven expansion of CD4+CD25+ regulatory T cells, which suppress HIV-specific CD4 T-cell responses in HIV-infected patients. Blood 2004;104:3249-56.

Wildin RS, Ramsdell F, Peake J, et al. X-linked neonatal diabetes mellitus, enteropathy and endocrinopathy syndrome is the human equivalent of mouse scurfy. Nature Genet 2001;27: 18-20.

Wilson NJ, Boniface K, Chan JR, et al. Development, cytokine profile and function of human interleukin 17-producing helper T cells. Nat Immunol 2007;8:950-957.

Wu C, Wang X, Gadina M, et al. IL-12 receptor beta 2 (IL-12R beta 2)-deficient mice are defective in IL-12-mediated signaling despite the presence of high affinity IL-12 binding sites. J Immunol 2000;165(11):6221-8.

Xavier R, Brennan T, Li Q, McCormack C and Seed B, Membrane compartmentation is required for efficient T cell activation. Immunity 1998;8:356–360.

Yamano Y, Takenouchi N, Li HC, et al. Virus-induced dysfunction of CD4+CD25+ T cells in patients with HTLV-I-associated neuroimmunological disease. J Clin Invest 2005;115:1361-8.

Yu D, Rao S, Tsai LM, et al. The transcriptional repressor Bcl-6 directs T follicular helper cell lineage commitment. Immunity 2009;31:457–68
Yu K, Chen Z, Khatri I, Gorczynski RM. CCR4 dependent migration of Foxp3+ Treg cells to skin grafts and draining lymph nodes is implicated in enhanced graft survival in CD200tg recipients. Immunol Lett. 2011 Dec 30;141(1):116-22.

Yurchenko E, Tritt M, Hay V, et al. CCR5-dependent homing of naturally occurring CD4+ regulatory T cells to sites of Leishmania major infection favors pathogen persistence. J Exp Biol Med. 2006;203:2451–60.

Zacharias DA, Violin JD, Newton AC, Tsien RY. Partitioning of lipid-modified monomeric GFPs into membrane microdomains of live cells. Science 2002;296:913–916.

Zarek PE, et al. A2A receptor signaling promotes peripheral tolerance by inducing T-cell anergy and the generation of adaptive regulatory T cells. Blood 2008;111:251–259.

Zhao DM, Thornton AM, DiPaolo RJ, Shevach EM. Activated $CD4^{+}CD25^{+}$ T cells selectively kill B lymphocytes. Blood 2006;107:3925–3932.

Zhou X, Bailey-Bucktrout S, Jeker LT, et al. Instability of the transcription factor Foxp3 leads to the generation of pathogenic memory T cells in vivo. Nat Immunol 2009;10(9):1000-1007.

Zhu J, Davidson TS, Wei G, et al. Down-regulation of Gfi-1 expression by TGF-beta is important for differentiation of Th17 and CD103+ inducible regulatory T cells. J Exp Med. 2009 Feb 16;206(2):329-41. Epub 2009 Feb 2.

Appendix

Statement of Author Contribution

The author was personally involved in the planning and execution of all experiments described in this dissertation, and played a crucial role in the writing of both manuscripts presented here. The author has presented different stages of this work as both oral and poster presentations in a number of scientific meetings, in addition to co-authoring papers unrelated to this dissertation. This dissertation serves as partial fulfillment of the dissertation requirements for the Molecular and Cell Biology Program at the Uniformed Services University, Bethesda, MD, 20814.